Welcome from the School of Engineering & Design

It is my pleasure to welcome you to ReSCon'11, the Fourth SED Research Student Conference. This annual conference, which is now a regular feature of the School activities, aims at giving our research students an opportunity to practice their oral and written presentation skills, by presenting their research findings to their colleagues, academic members of staff and industrial collaborators. This year's event will consist of three days of technical presentations, along with a poster session and a social event.

The abstracts contained in this book focus on a particular aspect of the students' research, selected to appeal to a diverse audience rather than attempting to describe their entire doctoral project. They have all been peer-reviewed by fellow research students. We would encourage all participants to ask questions and provide comments on the oral and poster presentations, to maximise the feedback given to the students.

The ResCon Committee, composed entirely of research students, has invested considerable time and effort to ensure the success of the event. They deserve our appreciation in organising every aspect of the conference. The School is also grateful to Dr Joanne Cole for her academic support and to the SED Research Office, particularly Mrs Carole Carr and Miss Rebecca Byrne, whose administrative support was crucial in making this event successful.

I trust you will enjoy the conference and will find these three days interesting and informative.

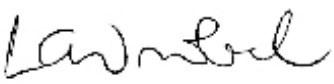

Professor Luiz C. Wrobel
Deputy Head of School (Research)
School of Engineering and Design
Brunel University, UK

Welcome from the ResCon'11 Committee

Dear Participant,

It is our great pleasure to welcome you to the 4th Annual Research Students Conference, ResCon'11.

This year's conference boasts three days of oral and poster presentations which all showcase the high quality and diversity of the research being conducted within the School of Engineering and Design and its affiliates. In addition the conference also includes an informal social event following Monday's proceedings and we hope you will take this opportunity to meet with fellow students and staff.

We would like to express our grateful thanks to the supervisory panel; Prof. Luiz Wrobel and Dr. Jo Cole, whose experience and expertise in research has proved an invaluable asset to this year's committee. Also, we would like to thank Carole Carr, the Research Office Manager and Becca Byrne, the Research Administrator whose hard work and guidance has been the foundation for the ResCon success. A special thanks to all the academic staff who have donated their time and support to judge the presentations and posters. Finally, we would like to thank the School of Engineering and Design and the Graduate School for donating prize money.

Thank you for attending the 4th Annual Research Students Conference. We hope you thoroughly enjoy the three days and we look forward to welcoming you.

ResCon'11 Committee

Contents

ResCon'11 Committee

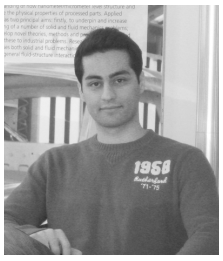

Mohammadreza Anbari Attar: Chair

I graduated from the University of Manchester in 2007 with a Master of Science in Laser Photonics. After a year working in industry, I joined the Brunel Centre for Advanced Power train and Fuels Research, where I've started my PhD research project on Laser Diagnostic Techniques for Combustion. ResCon has already established as an excellent multidisciplinary research conference here at Brunel. As a chair of the committee, I will help my colleagues to make a successful conference and to promote it further.

Thian Hong, Ng : Vice-chair

My name is Thian Hong, Ng originated from Malaysia. I joined Brunel in 2010 as a PhD student working on material chemistry research. This has further allowed me to work as an active member in the British Bioalcohol Project – HOOCH and I am truly enjoying it. As a Vice-Chair for ResCon'11, my role is to give my full support to the Chair and act in the chair's absence. We have a group of enthusiastic committee members from multi-disciplinary backgrounds. With the full effort from all of us and the advisory panel, I am sure we can make ResCon'11 a most successful and enjoyable one.

Odette Valentine: Conference Programme, Advertising & Graphic Design

I came to Brunel in October 2010 to commence a PhD in wearable technology funded by the RCUK Digital Economy Horizon programme. I have degrees in Natural Sciences from Cambridge University and Fashion Design Technology from the London College of Fashion, UAL; most recently completing an MA. In addition I have industry experience in marketing and knowledge transfer having worked at the National Physical Laboratory, and aim to use some of my experience of organising and marketing technical events to help with the organisation of ResCon'11. I also hope to encourage participation from research students within the design disciplines and promote collaboration across the whole of SED.

Shariq Mahmood Khan: Webmaster

I graduated from NED University of Engineering & Technology, Karachi – Pakistan in 2007 with a Master of Computer Science & Information Technology. I came to Brunel in October 2010 to commence a PhD in Vehicular Ad hoc Networks under the supervision of Dr.Qiang Ni at the Wireless Networks & Communication Centre. I joined ResCon'11 to gain experience in working with a team of people from completely different backgrounds. As webmaster, I hope to ensure the conference website is updated with latest conference information. Further, I hope to ensure ResCon continues to represent Brunel students as well as to open doors in the future as an international conference.

Hussein Janna: Abstract Co-ordinator / Presentation Co-ordinator

I am a PhD student who joined Brunel in 2007, having a previous background in Civil and Environmental Engineering. I am working on understanding the effectiveness of advanced treatment techniques in eliminating emerging contaminants such as pharmaceutical compounds and personal care products from wastewaters. In order to expand my knowledge, raise my profile and gain a valuable experience, I have become involved in organizing ResCon'11. My duty as a member of the committee is to help participating students to improve their skills by advising on their presentation. I hope ResCon 11 will be dynamic and highly successful conference.

ResCon'11 Committee

Inmaculada Andres: Abstract Co-ordinator / Presentation Co-ordinator

I graduated from the University of Greenwich in 2009 with a Master by Research Project of Chemistry and started a PhD at Brunel, in the Wolfson Centre for material processing, the following October. My work in this group is mainly concerned with the synthesis and characterization of new complexes for application in organic light emitting diodes (OLEDs). As a team member for ResCon'11 team my roles are to ensure that all the presentations are well-organised and promote the research talent at Brunel University to get the highest expectations in this region.

Shahzad Ahmed Memon: Abstract Co-ordinator / Graphics

I started my PhD from May 2008 in Centre for Electronics System Research (CESR). My PhD research is about the development of novel methods for liveness detection in fingerprint biometrics. ResCon'11 will provide the platform to all research students to present the themes and outcomes of their research and an excellent chance to discuss it with other research students and staff. It is my second time to be involved as a member of the ResCon organizing committee and hope this would be again a valuable and memorable event for all of SED research students.

Mahmoud Arman: Registration Co-ordinator

I joined Brunel in October 2008 to work towards my PhD studies in Electronics Engineering, specializing in power electronics. My work includes a novel filter design which can be adopted in many applications. Recently, I joined Research Student Conference (ResCon '11) organizing committee to gain experience by working with junior and senior researchers from other fields of research. As conference registration coordinator, I have to ensure that all related work is well organized and going smoothly with other committee members. I do hope that my contribution in ResCon '11 will promote and assist in the success of this year's well established event.

Olayinka Oladiran: Registration Co-ordinator

I joined Brunel University in April 2010 for a PhD programme in Civil Engineering. Having a previous background in Construction Management, I decided to delve into the experimental order of things; hence my research work is based on "Innovative ways of analysing Shrinkage Cracking in concrete fibres; A focus on experimental methods and numerical modeling. "I find it of great interest to become a member of the ResCon'11 committee. Taking a post in the registration team will boost my familiarity with colleagues as well as enhance my knowledge base. Ultimately, I intend to contribute my quota to the entire team and the upcoming conference in the process.

Saba Al-Rubaye: Poster Co-ordinator

I joined Brunel in 2010 for a PhD in Electrical and Communication Engineering. I became involved in the research student conference to gain valuable experience by working with colleagues from different research backgrounds. For ResCon'11, I expect to meet and exceed the aims and objectives of the conference. As poster co-ordinator, my role is to make sure that the poster sessions are well-planned, and include all the top-quality research at Brunel.

ResCon'11 Advisory Panel
Academic Staff

Prof. Luiz Wrobel: Deputy Head of School (Research)

Dr. Jo Cole: Lecturer Particle Physics

Carole Carr: Research Office Manager

Rebecca Byrne: Research Administrator

ResCon'10
Previous prize winners

Congratulations to last year's prize winners

Oral Presentation

1st	Michael Bromfield
2nd	Irma Aleknaviciute
3rd	Alexander Plant

Extended Abstract

1st	Farnaz Nickpour
Joint 2nd	Mark Dowson; Yulia Anopa

Poster

1st	Matthew Littlefield
2nd	Thomas Walker
3rd	Kodikara Manjula Silva

Programme

ResCon11 Day 1 - 20 June			
Registration 8.30 - 8.50			
Welcome/Opening Speech	9.00 - 9.10	Prof. Chris Jenks, Vice Chancellor	
Welcome/Opening Speech	9.10 - 9.20	Prof. Geoff Rodgers, Pro-Vice Chancellor (Research)	
Session 1 Chair intro	9.20 - 9.25	Prof. Peter Hobson, Deputy Head of School (UG)	
Session 1 Energy & Power	9.25 - 10.45	Nazia Nusrat	Development of novel state estimation algorithms for active distribution network
		Phillip Ashton	Opportunities to exploit phasor measurement units (PMUs) and synchrophasor measurements on the UK transmission network
		Siva Panchadcharam	Evaluation of throughput and latency performance for MV/LV communications infrastructure
		James Allan	The potential of hybrid PVT systems throughout Europe
Break	10.45 - 11.10	Tea/Coffee	
Session 2 Chair intro	11.10 - 11.15	Dr. Dan Pickford, Lecturer, Institute for the Environment	
Session 2 Sustainability /renewable resources	11.15 - 12.35	Bupa Apagu Ankidawa	Determination of the suitability of hand drillings in lowland areas of Adamawa State, Nigeria
		Lei Zhao	Novel bio-composites based on whole utilisation of wheat straw
		Thian Hong Ng	Cereal straw pre-treatment for bio-fuel application: comparison between extrusion and conventional steam explosion
		Sitthi Duangphet	Poly(3-hydroxybutyrate-co-3-hydroxyvalerate) and poly(butylene adipate-co-terephthalate) blends: crystallization behaviour and thermal degradation
Break	12.35 - 14.05	Lunch / Poster session	
Session 3 Chair intro	14.05 - 14.10	Prof. Robert Withnall, Wolfson Centre for Materials Processing	
Session 3 Materials properties, performance and testing	14.10 - 15.30	Edward Boughton	Screen printed carbon nanotube field emission devices
		Myles Worsley	Novel routes to hollow inorganic microspheres with nanoshells
		Olayinka Oladiran	Preliminary investigation on restrained shrinkage cracking of concrete with circular & elliptical ring specimens
		Xiao Yan	A study on the upconverting properties of terbium and erbium codoped yttrium oxysulfide nanocrystals
Break	15.30 - 15.55	Tea/Coffee	
Session 4 KEYNOTE SESSION	15.55 -16.30	KEYNOTE presentation 'Lunacy - the Mother of Invention?' Prof. John Fyson, Wolfson Centre for Materials Processing What makes an inventor? Should we all think 'out of the box'? In an engaging presentation referencing the original Lunar Society and the early industrial revolution; Prof. Fyson demonstrates that by getting groups of people with diverse interests in one place today, great innovations can follow.	
Social event 16.30 -20.30			

ResCon11 Day 2 - 21 June			
Registration 8.50 - 9.10			
Welcome/Opening Speech	9.10 - 9.20	Prof. Savvas Tassou, Head of School	
Session 5 Chair intro	9.20 - 9.25	Prof. David Harrison, Head of Design and Manufacture Research Group	
Session 5 Design processes/ Design for useability	9.25 - 10.45	Jian Ruan	A constraint-based DRM Matrix for design collaboration
		Bader Alfawwaz	Usability of eGovernment Websites in Jordan
		Mohammed Al-Masarweh	An assessment of sighted guide performance by using different screen resolution for Brunel remote guidance System
		Odette Valentine	Soft-wear: identifying meaningful design spaces for wearable technology
Break	10.45 - 11.10	Tea/Coffee	
Session 6 Chair intro	11.10 - 11.15	Dr. Jo Cole, Lecturer in Particle Physics	
Session 6 Innovation management & enterprise	11.15 - 12.15	Abdulrhman Albesher	Systems of Innovation in Saudi Arabia: Assessment of the innovation capabilities for enterprises based on the development of intelligent cities
		Mohammad Alnawayseh	Electronic grocery shopping logistics in developing countries, Jordan as a case study: Home delivery reference framework
		Yolanda Silvera	Key performance indicators within food supply chains- focusing on on-time delivery- How does this affect the supplier relationships?
Break	12.15 - 13.45	Lunch /Poster session	
Session 7 Chair intro	13.45 -13.50	Prof. Abdul Sadka, Head of Electronic and Computer Engineering	
Session 7 Communications systems/ Networks	13.50 - 15.10	Hadi Noureddine	Energy efficient routing using multiple heterogeneous-radios in mobile ad-hoc networks
		Nazar Radhi	Estimation primary user localization using cognitive radio networks
		Sofian Hamad	A novel efficient flooding algorithm based on node position for mobile ad hoc network
		Seyedreza Abdollahi	An integrated transportation system for baseband data, digital and analogue radio signal over fibre network
Break	15.10 -15.35	Tea/Coffee	
Session 8 Chair intro	15.35 -15.40	Prof. Jack Silver, Executive Director Wolfson Centre for Materials processing	
Session 8 Imaging /Detection/Displays	15.35 -16.55	Alexander Reip	Improving the detection of latent fingerprints using phosphor nanopowders
		Immaculada Andres	Copper based materials for a new generation of displays
		Kazimali Khaki	Face recognition with weightless neural networks using the MIT database
		Magdalena Nowak	Novel grain refiner for Al-Si alloys

ResCon11 Day 3 - 22 June			
Registration 8.50 - 9.10			
Welcome/Opening Speech	9.10-9.20	Prof. Luiz Wrobel - Deputy Head of School (Research)	
Session 9 Chair intro	9.20 - 9.25	Prof. Kai Cheng, Head of AMEE - Advanced Manufacturing & Enterprise Engineering	
Session 9 Modelling, simulation and particles	9.25 - 11.05	Mhd Saeed Sharif	Positron emission tomography volume analysis based on ANN
		Nikolai Issakov	Computational design and tuning of graphene bilayer grown on the 4H-SiC substrate
		Matthew Littlefield	Initial Results of a CAD import into G4MICE
		William P. Martin	Measurement of the top-antitop quark production cross section at CMS with 36 pb-1 of data in the electron+jets channel with b-tagging
		Shahzad Memon	Liveness in fingerprint images by active pore detection Technique
Break	11.05 - 11.20	Tea/Coffee	
Session 10 Chair intro	11.20 - 11.25	Dr. Cristinel Mares, Lecturer - MSc Course Director (Aerospace Engineering)	
Session 10 Applied mechanics	11.25 - 12.45	Mutinda Musuva	Wavelet-based finite element method for static and vibration analysis
		Boris Kubrak	Direct numerical simulation of oxygen transfer at the air-water interface in a convective flow environment and comparison to experiments
		Irma Aleknaviciute	Plasma assisted pyrolysis of gaseous hydrocarbons to produce COx free hydrogen
		Mohammadreza Anbari Attar	In-cylinder gas temperature measurement with two-line planar laser induced fluorescence
Conference closing remarks	12.45- 12.50	Prof. Luiz Wrobel - Deputy Head of School (Research)	
Break	12.50 - 14.00	Lunch /Poster session	
Poster judging session	14.00 - 16.00	**All poster competition entrants to be present along with judges**: Prof. Luiz Wrobel, Deputy Head of School (Research) Dr. Jo Cole, Lecturer in Particle Physics Dr. Kate Hone, Director Graduate School Prof. Robert Withnall, Wolfson Centre for Materials Processing Prof. Z Fan, Director BCAST Prof. Peter Hobson, Deputy Head of School (UG) Dr. Senthila Pathmananthan, Graduate School Dr. Sara Silve, Lecturer in Design Dr. David Smith, Lecturer Centre for Sensors and Instrumentation Professor Akram Khan, Chair in Particle Physics & e-Science Dr. Thanos Megaritis, Reader, MSc Course Director (Auto & Motorsport) Industrial Training Tutor Dr. Lionel Ganippa, Senior Lecturer, Course Director of Foundations of Engineering	

Extended Abstracts

Development of novel state estimation algorithms for active distribution network

N. NUSRAT* (nazia.nusrat@brunel.ac.uk), M.R. IRVING (malcolm.irving@brunel.ac.uk),

G.A. TAYLOR (gareth.taylor@brunel.ac.uk)

Brunel Institute of Power Systems, Brunel University

EXTENDED ABSTRACT

Abstract: The increasing penetration of Distributed Generation and emerging smart metering technologies are transforming the distribution networks from passive to active conditions. In such active networks, extensive monitoring and remote control technologies are essential. Therefore, a State Estimation (SE) tool is the core component in future distribution management systems. Extensive research is ongoing with regard to the development of novel Distribution System State Estimation (DSSE) tools for improved network monitoring and control. The novel DSSE tool is required to be scalable to fit into small to large size networks, operable with limited real time measurements and able to execute the computation of large volumes of data in a limited time. This paper proposes and develops a novel scalable DSSE tool that satisfies the requirements for present and future distribution network infrastructure and management systems. The proposed DSSE tool applies an emerging meta-heuristic optimization mechanism known as Differential Evolution Algorithm (DEA). A detailed investigation is performed with various case studies related to expected scenarios of future distribution networks.

I. INTRODUCTION

The state estimation tool takes the network measurement information, together with a parameterized network model and estimates the real-time state of the distribution system. The estimator outputs can then be fed into the main control functions and asset management software. As a matter of fact, the power system state estimator is capable to produce acceptable result when there is high redundancy of real measurements. However, most of the Medium Voltage (MV) and Low Voltage (LV) region of the networks are poorly monitored and the availability of required real time measurements is not practical due the massive size of the system and the associated costs. Also, the various data origins such as real, pseudo and virtual measurements lead to new challenges with regard to the degree of trust to different types of measurements. The algorithms and procedures for distribution system state estimation should be capable to endure heavy computational burden arising from the massive size of MV-LV networks. A vital and desirable property for the DSSE tool is scalability to fit into variable sizes of distribution networks in different locations. All these together make the development of an efficient SE tool strongly challenging[1]. In this research we have aimed to develop a novel scalable DSSE tool capable to confront these challenges efficiently. The emerging technology of High Performance Computation (HPC) technology and high speed communication infrastructure will bring widespread benefits to the application of proposed DSSE tool.

II. PROPOSED NOVEL DSSE TOOL

We have chosen a robust evolutionary optimization method, known as the Differential Evolution Algorithm (DEA) as the estimation tool where Weighted Least Square minimization criteria have been utilized. DEA is a derivative free direct search algorithm[2] that does not build any concrete matrix. The DEA based DSSE tool is therefore free from matrix ill conditioning problems and operable even if any part of the networks is unobservable. Beside these advantages, the major drawbacks could be the communication bottleneck and heavy computation expenses.

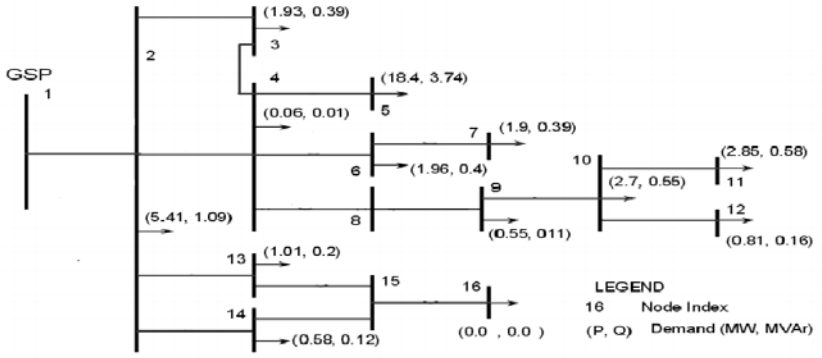

Figure 1(a) The 16 Bus Networks

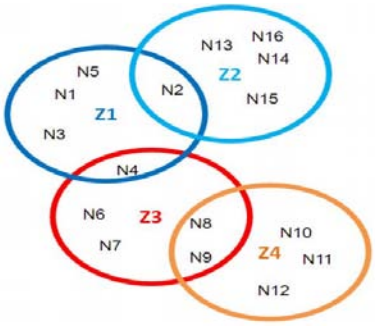

Figure 1(b). The sub-zones

These issues can be effectually resolved by applying parallel computation tool supported by HPC and novel ICT solution. The proposed method divides the network into small zones that we refer as sub-zones. Sub-zones can be consisted of five to ten nodes and each sub-zone is overlapped with the neighbouring zones by one or two nodes. Each sub-zone performs its local estimation almost independently. There will be exchange of information among sub-zones in form of 'artificial measurements'. We refer the estimations of voltage magnitude and phase angle of the overlapped nodes, executed by the neighbouring sub-zones as the 'artificial measurements' for a local estimator. The local estimator considers the artificial measurement as an additional measurement with a low degree of trust. In the proposed algorithm, the exchange of information occurs a several times in order to provide co-ordination among sub-zonal estimation. A 16 bus system in Fig. 1(a) is case studied and the network division is shown in Fig. 1(b) in form of circular diagrams. There are fours sub-zones (Z1-Z4) consisting of five nodes (N1-N16) each. The algorithm's flowchart is presented in Fig. 2(a). In Fig. 2(b) an outcome of applying this scalable DSSE tool is presented. We have taken a set of measurement for the 16 bus networks and the measurement errors vary up to 55% percent. The measurement is consisted of one real time voltage, two real time real/reactive power injection and thirty pseudo real/reactive power injection measurements. The estimator is run five times to check the consistency and we receive consistent voltage estimation for all five runs. The voltage estimation error is less that 0.2% in all cases.

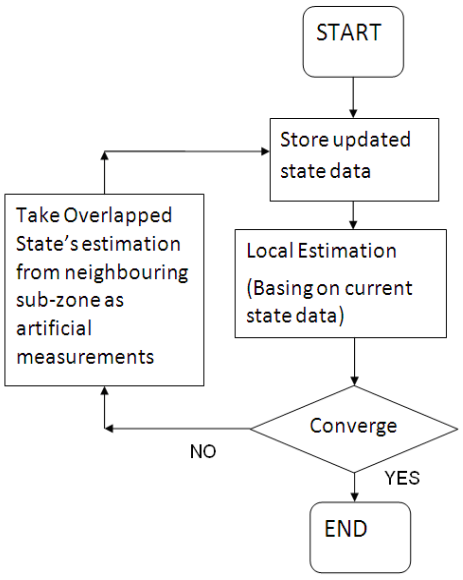

Figure 2(a) Flow Chart

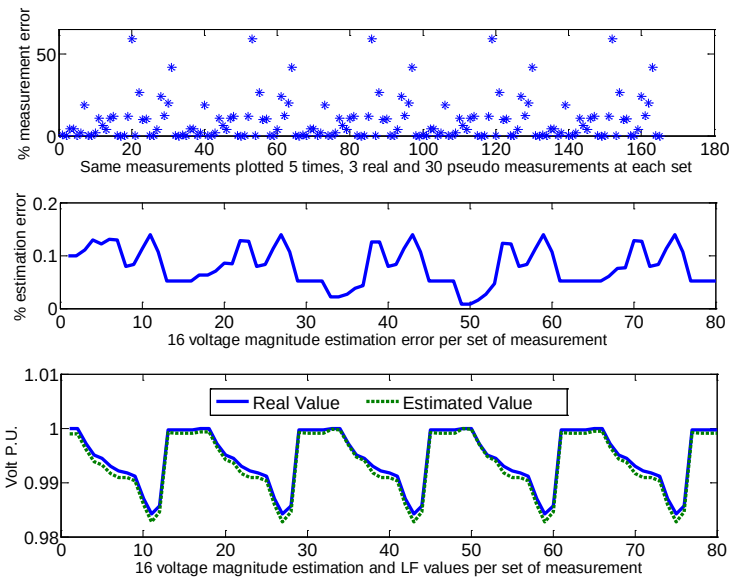

Figure 2(b). Measurement error distribution and voltage estimation for a set of measurement running five times

References

1. Taylor, G., M. Irving, N. Nusrat, R. Liao, and S. Panchandaram. “Developing Novel Information And Communications Technology Based Solutions For Smart Distribution Network Operation” UPEC2010, 2010.
2. Price, K., R. Storn, and J. Lampinen. Differential Evolution: A Practical Approach to Global Optimization, Ch. 1-5. Springer-Verlag, 2005.

Acknowledgements

The authors would like to acknowledge the FP7-ICT-ENERGY-2009-1 Novel ICT solutions for Smart Electricity Distribution Networks programme for the funding of this research.

Key words: Distribution System State Estimation, Differential Evolution Algorithm, Scalable, sub-zone.

Opportunities to exploit Phasor Measurement Units (PMUs) and synchrophasor measurements on the UK transmission network

Phil M. ASHTON*[1, 2] (phil.ashton@uk.ngrid.com); Gareth A. TAYLOR[1] (gareth.taylor@brunel.ac.uk)
Alex M. CARTER[2] (alex.carter@uk.ngrid.com)
[1] Network Operations, National Grid, St Catherine's Lodge, Sindlesham, RG41 5BN, UK
[2] Brunel Institute of Power Systems, Brunel University, Uxbridge, Middlesex, UB8 3PH, UK

EXTENDED ABSTRACT

Abstract

As a result of CO_2 reduction legislation at both EU and government level, the GB electricity grid operator National Grid is tasked with connecting up to 30GW of wind generation to the existing transmission system by 2020. The inherent variability in this method of generation will require the System Operator to maximise the use of existing transmission corridors, running lines closer to their thermal limits. In addition, transmission technologies currently unfamiliar to National Grid such as series compensation, intra-network HVDC and an increase in the number of HVDC interconnections will also be implemented to help integrate the additional generation. It is understood that the networks will need to become more flexible in order to maintain security of supply; to achieve this, improvements of overall system monitoring will also be required. Phasor Measurement Units (PMUs) and synchronised phasor measurements have become the 'measurement technique of choice for electric power systems' [1] and to this extent are viewed as a key tool in monitoring oscillations within the GB power system. PMUs are being deployed, initially as an extension to Dynamic System Monitoring (DSM) and with this paper we discuss the challenges involved with implementing a Wide Area Monitoring System (WAMS) solution. In addition a number of additional roles and applications that that the PMU system could exploit in order to improve control of the network are also proposed.

DSM and SCADA systems

National Grid is required by Grid Code CC6.1 to ensure the Transmission System is operated within certain technical, design, and operational criteria which define allowable frequency variations and voltage variations, waveform quality and voltage fluctuations. In order to meet this obligation National Grid must be able to monitor and record these measurements at appropriate locations. [2] Typically DSM solutions have been achieved through a mixture of fault recorders and data loggers which sit outside standard substation SCADA systems as described in figure 1.

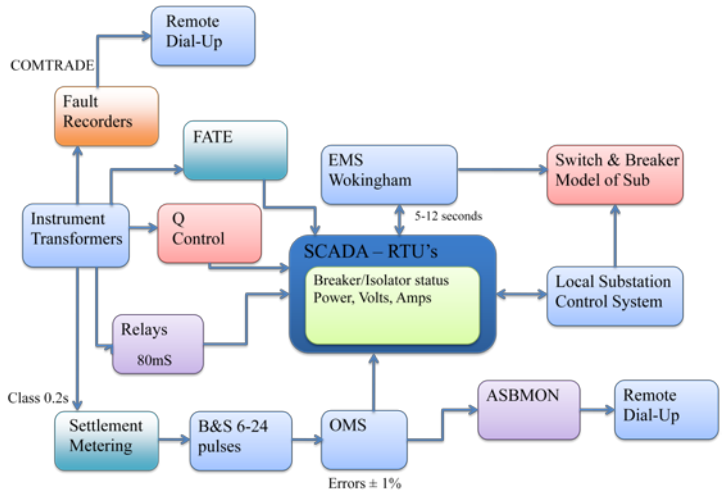

Figure 1: Substation SCADA systems

It is suggested that a more conventional way of integrating a WAMS solution would be by PMUs adopting additional system monitoring roles. The benefits of this integration would be realised through reduced capital and support costs and consistency in the accuracy and availability of data that will be critical to the operation of the transmission system of the future. This will be investigated in terms of both centralised and localised applications and how this could require different levels of integration and different resolutions of data.

The operational frequency at present is monitored through the Frequency And Time Error (FATE) system; around 10 sites monitor the local frequency and this information is sent back to the control room, where one of these readings represents the system frequency. This is normally taken from the electrical centre of the network, which should be an area of stability and less susceptible to the deviations that occur on the outskirts of the network. As the frequency information is not time synchronised direct comparisons can not be made between different areas of the network. Online comparisons could add significant capacity to the system to identify emerging power system conditions and play an important role in overall situational awareness [3].

Investigation into the feasibility for PMUs to adopt other traditional SCADA roles should also be considered, such as operational metering and the Ancillary Service Business Monitoring Service (ASBMON). Relays can already be considered as a first level of Wide Area Measurement Protection And Control (WAMPAC) but full integration with the rest of the systems could allow a number of unique protection applications that would employ an angle-based logic.

Phasor Measurement Units, PMUs.

The PMU was developed through logical progression of the Symmetrical Components Distance Relay (SCDR) [4], which used a relaying algorithm based on the measurement of positive-sequence, negative-sequence and zero-sequence voltages and currents at the transmission line terminal. It was soon recognised that the positive-sequence measurements are of great value in their own right as they constitute the state vector of a power system and are of fundamental importance in all power systems analysis [5]. The earliest modern applications involving direct measurements of phase angle differences was reported in several papers in the early 1980's [6, 7, 8] .

Today they are becoming the tool of choice for monitoring power system dynamics and in the future it is suggested that the PMU may take over the role of many existing pieces of equipment. In the meantime a large amount of investigation is required into the correct implementation of PMUs and WAMS within the existing control systems at National Grid. The additional control and monitoring systems are bound by there own standards and many communicate through differing protocols to different systems. This paper will present a detailed overview of current progress and future plans regarding opportunities to exploit PMU deployment across National Grid.

References.

[1] A.G. Phadke and J.S. Thorp – Synchronized Phasor Measurements and Their Applications, Power Electronics and Power Systems, Springer 2008.
[2] National Grid – The Grid Code: CC.6.6 System Monitoring
http://www.nationalgrid.com/uk/Electricity/Codes/gridcode/
[3] Yingchen Zhang, Penn Markham, Tao Xia,Lang Chen, Yanzhu Ye, Zhongyu Wu, Zhiyong Yuan, Lei Wang, Jason Bank, Jon Burgett, Richard W. Conners and
Yilu Liu. Wide-Area Frequency Monitoring Network (FNET) Architecture and Applications
IEEE TRANSACTIONS ON SMART GRID, VOL. 1, NO. 2, SEPTEMBER 2010
[4] A.G. Phadke, M. Ibrahim, T. Hlibka IEEE Transactions on Power Apparatus and Systems,Vol.PAS-W, 110.2, March/Apr Fundamental Basis for Distance Relaying with Symmetrical Components.

[5] Phadke, A.G., Thorp, J.S, and Adamiak, M. G., “A new measurement technique for tracking voltage phasors, local system frequency and rate of change of frequency”, IEEE Transactions on PAS. Vol. 102, No. 5, May 1983, pp 1025-1038.
[6] Missout, G. and Girard, P., “Measurement of bus voltage angle between Montreal and Sept-Iles”, IEEE Transactions on PAS. Vol. 99, No. 2, March/April 1980, pp 536-539.
[7] Missout, G., Beland, J., and Bedard, G., “Dynamic measurment of the absolute voltage angle on long transmission lines”, IEEE Transactions on PAS. Vol. 100, No. 11, November 1981, pp 4428-4434.
[8] Bonanomi,P., “Phase angle measurement with synchronized clocks – principles and applications”, IEEE Transactions on PAS. Vol. 100, No. 11, November 1981, pp 5036-5043.

Keywords: PMU, WAMS, WAMPAC, Transmission System Monitoring and Control

Evaluation of throughput and latency performance for mv/lv communications infrastructure

S. PANCHADCHARAM*[1], Q. NI[1], G. A. TAYLOR[1], M. R. IRVING[1], L. LEWIN-EYTAN[2], K. SHAGIN[2],

[1]*Brunel institute of Power Systems (BIPS)*

[2]*IBM Haifa Research Lab, Israel*

EXTENDED ABSTRACT

Abstract

Conventional power grid infrastructure is undergoing evolutionary changes with regard to the emerging smart grid concepts. Distribution Network Operators (DNOs) will experience considerable infrastructure changes in order to accomplish the massive task of developing novel, low-cost and scalable communication technologies required to exploit smart meters. Interoperable communication solutions enable the control and observability of Medium Voltage and Low Voltage (MV/LV) network devices and hence improve overall network management and control at the distribution level.

This paper presents the evaluation of throughput and latency performance for MV/LV communication links using the OPNET simulator. Various communication technologies, GPRS/UMTS and bus-link, have been tested. To validate the proposed simulation techniques, the results are compared against experimental tests performed by IBM Haifa. The comparison of results prove that the simulation models match relatively well with the practical experiments. Hence the simulation techniques can be used to analyse the deployment of extensive communications infrastructure in advance of field trials. The simulation techniques can also be integrated within a novel Distribution Management System (DMS) test-bed to support the communication aspect of DMS functionalities before and during the field trial phase. A novel power line communications (PLC) model is proposed and implemented within the simulation tool OPNET that will contribute towards further performance analysis of communication technologies for smart grids.

Introduction

Integration of scalable ICT infrastructures with Smart Grids is a major challenge[1]. Two way communications are essential and critical at many points due to the timely and critical communication of information from end user to a distribution network control center or vice versa. Current communication systems do not often support the need for two way communication for medium voltage (MV) and low voltage (LV) level network environments. Distribution network control centers in many countries have often deployed communication technologies without considering future Smart Grid requirements to support much greater amounts of MV/LV devices that will generate much larger amounts of data. The challenge of extensively communicating and storing large amounts of data using existing communication infrastructure and storage devices requires novel, secure and low-cost technological solutions.

Approach

Figure 1 describes the network configuration for a simple network used by IBM Haifa for the GPRS/UMTS and PLC testing to evaluate the communication link performance based on throughput and latency characteristics[2]. This is the full 4-level hierarchical structure representing nodes in each level and each node can be realised as a local concentrator on a LV network or gateways between several LAN to reflect a whole WAN configuration. Initial laboratory testing of these nodes was performed in an office environment at IBM in order to evaluate the performance of UDP and TCP transport protocols over GPRS/UMTS and PLC and resulted in the expected output and the same network has been simulated using the OPNET simulator as shown in Figure 2.

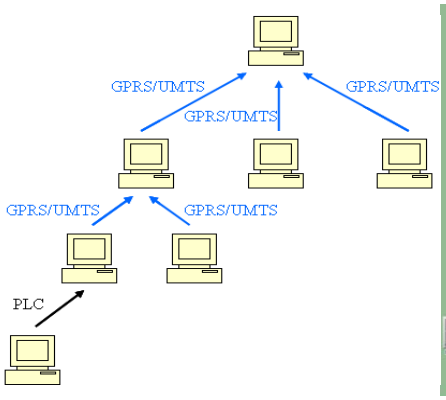

Figure 1: 4-Level hierarchical topology (IBM Haifa)

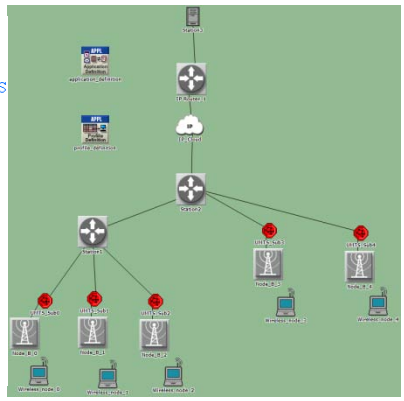

Figure 2: 4-Level hierarchical topology (OPNET)

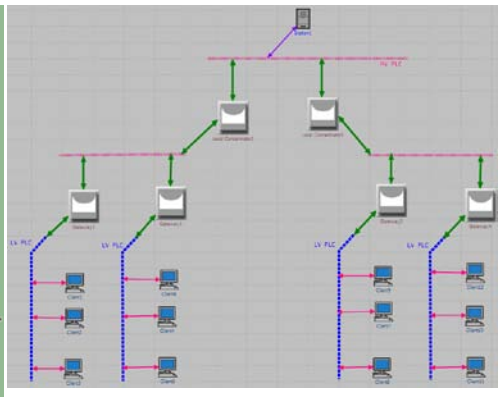

Figure 3: Typical LV network set-up in OPNET

Figure 3 demonstrates the set-up of a typical LV network with several nodes and the performance of the bus-link communication has been studied to evaluate the scalability criteria of required ICT solutions.

Mobile communication technologies have evolved with time and different standards, 2G (GSM), 2.5G (GPRS), 3G (UMTS), etc. have emerged to support the growing demand for modern mobile applications. Significant improvement in data rates from GPRS (56 Kbps) to UMTS (384 Kbps) enabled the latter to be efficient for the modern smart phone to support bandwidth intensive applications (audio, video, etc.) on the move. Potential deployment of these technologies has also been considered in the smart grid environment and testing is ongoing to analyze their performance in terms of throughput and latency under extreme network conditions. As part of the initial research in the HiPerDNO project[1] a performance evaluation of GPRS versus UMTS for both UDP and TCP transport layer protocols was performed, demonstrating the differences between UDP and TCP in both technologies, as well as investigating the relationship between latency and throughput performance in each technology. These initial experimental tests have been further investigated using the OPNET simulator for similar scenarios and the results match relatively well.

Further research and simulation development will enable the testing of different communication technologies with regard to scalability in order to plan future field trials conveniently and cost-effectively. A comparative study of throughput and latency performance for different data rates against various protocols for UK scenario is ongoing. Once PLC has been fully modelled in OPNET, further studies will be performed to realise the implementation and improvement of communication technologies including a high speed messaging layer infrastructure that is being developed by IBM[1,2].

References

[1] Taylor, G.A.; Irving, M.R.; Nusrat, N.; Liao, R.; Panchadcharam, S.;, ”Developing novel information and communications technology based solutions for smart distribution network operation”, 45th International conference, UPEC, 2010

[2] B. Carmeli, G. Gershinsky, A. Harpaz, N. Naaman, H. Nelken, J. Satran, P. Vortman, “High Throughput Reliable Message Dissemination”, SAC 04 Proceedings of the 2004 ACM symposium on Applied Computing, 2004

Key words: **Distribution networks, DNO, Communications Infrastructure, OPNET, GPRS/UMTS, PLC, UDP/TCP**

The potential of hybrid PVT systems throughout Europe

James ALLAN
BDSP Partnership & Brunel University, School of Engineering and Design

EXTENDED ABSTRACT

Introduction

The photovoltaic (PV) industry is the fastest growing renewable energy industry. Its growth has been fuelled by the introduction of Feed-In-Tariffs (FITs) around the world. In comparison with other technologies, PV has a low energy generation density and utility scale plants require a large amount of space. In countries such as the UK this requirement may compete with arable farmland that is essential for food production. As a result it makes sense to integrate PV systems into retrofit or new build construction projects.

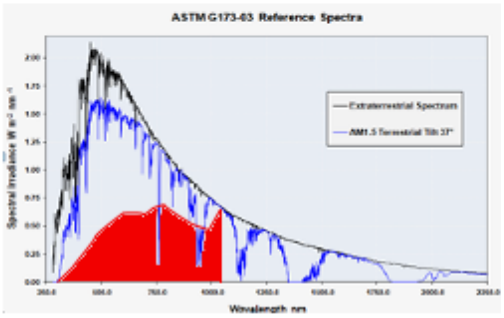

Figure 1: The utilisation of the solar spectrum

One of the difficulties with BIPV is that there is often limited space for a sizeable PV output. To make best use of the available space, an enhancement of efficiency is required to generate more energy per unit area. Conventional PV systems only make use of a small percentage of the solar spectrum and whatever can't be used is wasted as heat. If it is possible to recover and use this waste heat, the overall efficiency of the system can be increased.

The most common PV-Thermal (PVT) systems either use water or air based collectors. Past studies have shown that PVT is more efficient than having two separate systems[1] and extensive work has been carried out to improve heat transfer properties[2]. Despite this, there has been little carried out to show how the performance differs under varying climatic conditions and how the system can be optimised to account for these variations.

This study investigates how performance varies across the different climates of Europe with the aim of deriving a series of suggestions that could help optimise system design and encourage the uptake of PVT in the future.

Design/Methodology/Approach

The hybrid system was modelled using Transys. The collector was sized at 5 m^2 with an optimal flow rate, of 5L/hour/m^2 of collector, as determined by Kalogirou[3]. The parameters used to define the system are shown in Table 1.

Collector Area	$5m^2$
Collector Fin Efficiency Factor	0.96
PV Cell Efficiency	0.15
Fluid Thermal Capacitance	4.19kJ/kg.K
Collector Plate Absorptance	0.92
Collector Loss Coefficient[3]	$6W/m^2.K$
Temperature Coefficient of Solar Cell Efficiency	0.005/K
Packing Factor	1

Table 1: Parameters used to describe the PVT system in TRNSYS.

Findings/Results

Results have shown that a PVT hybrid system has the potential to supply over 90% of the domestic hot water demand in a hot European country such as Spain and nearly 60% in a more temperate climate such as the UK. The use of hybrid systems can increase the efficiency of conventional PV systems from 12% to 34% in the London and to 32% in Madrid.

Conclusion / Discussion

Heating is responsible for a considerable part of the energy demand of a domestic property. It is therefore essential to first establish the individual load profiles across Europe when optimising such systems. Even though there is a reduced efficiency for the electrical and thermal generation compared with conventional systems, the fact that it is more efficient to use a hybrid system than to have two separate systems illustrates that there is still scope for improvement. If the properties of such systems begin to mimic those of the conventional systems then it is likely that vast improvements in efficiency will be seen.

This research aims to look at optimising the design of PV thermal systems by; generating accurate demand profiles which can be intelligently matched with renewable supply, integrating hybrid systems to form multifunctional building components, optimising the properties of systems for different climates and improving existing simulation models so that hybrid systems can be integrated into the design process.

References

1. Zondag, H.A., De Vries, D.W., Van Helden, W.G.J., Van Zolingen, R.J.C. & Van Steenhoven, A.A. (2003) "The yield of different combined PV-thermal collector designs", *Solar Energy*, vol. 74, no. 3, pp. 253-269.
2. Charalambous, P.G., Maidment, G.G., Kalogirou, S.A. & Yiakoumetti, K. (2007) "Photovoltaic thermal (PV/T) collectors: A review", *Applied Thermal Engineering*, vol. 27, no. 2-3, pp. 275-286.
3. Kalogirou, S.A. (2001) "Use of TRNSYS for modelling and simulation of a hybrid pv-thermal solar system for Cyprus", *Renewable Energy*, vol. 23, no. 2, pp. 247-260.

Keywords: PV, Solar Thermal, Hybrid Systems, Heat Transfer

Determination of the suitability of hand drillings in lowland areas of Adamawa State, Nigeria

Buba Apagu ANKIDAWA*[1], Suzanne LEROY[1], Philip COLLINS[2]

[1]Institute for the Environment, Brunel University, Uxbridge, London, UK

[2]Department of Civil Engineering, School of Engineering and Design, Brunel University, Uxbridge, London, UK

EXTENDED ABSTRACT

Introduction

Manually drilling is a practical solution for well less than 40 meters deep in alluvial sediments, loose material such as clay and sand and soft weathered rock formations such as soft sand stone and lime-stone (Labas et al., 2010). Water bore drilling encompasses a variety of techniques which include simple hand auguring to the use of conventional, truck mounted, and hydraulic drilling rigs; Hydraulic rigs require more operational maintenance expertise and more expensive component parts. Poor access routes to potential drill sites can prevent such large rigs reaching remote rural areas (Sutton, 2007).

In developing country like Nigeria water is obtainable from hand drilling borehole installed on alluvium formations, which are mostly found along the river flood plains. In Adamawa State, for example, alluvium formations are found along River Benue flood plains, where most of the farmers practice irrigation during the dry season. It would not be economical to use machine drilling rigs for such formation, rather simple and affordable hand drilling techniques should be adopted in the area in order to boost agricultural production in the state. The application of hand drilling is limited to areas with soft unconsolidated geological formations such as alluvium deposits, sufficiently shallow water tables and high permeability aquifers - many suitable areas of loose sediments, Quaternary alluvial deposits exist along River Benue flood plain and shallow water table in Adamawa State.

Groundwater is an important source of water supply both for domestic and irrigation purposes; because it can be readily tapped by well within the community it serves. For this reason it is important to obtain a thorough regional and localized geological assessment of borehole hand drilling potential in the lowland areas of the state to ensure a productive borehole with a safe aquifer yield.

The aim of this research is to assess the suitability of the low cost hand drilling techniques as the best method of accessing groundwater on the alluvium formations along the flood plain of River Benue valley, Yola local government area of Adamawa State, Nigeria.

The scope of this research covers assessment of the suitability of hand drilling techniques on the Quaternary alluvium formations on the flood plains of River Benue, within Yola town, Adamawa State, Nigeria.

The research will involve collecting secondary data such as hydrogeology data of the study area and primary data such as a characterisation of the sediment in the floodplain by sedimentology on auger samples (Fig 1) and as watertable depth estimation by resistivity survey by using ABEM Terrameter Equipment.

The results from the above survey analysis will be used in the selection of a suitable hand drilling technique that will suit the alluvium formations along the flood plain of River Benue, of the study area. If necessary, a selected existing design will be modified and adapted to the specific requirements of the River Benue valley.

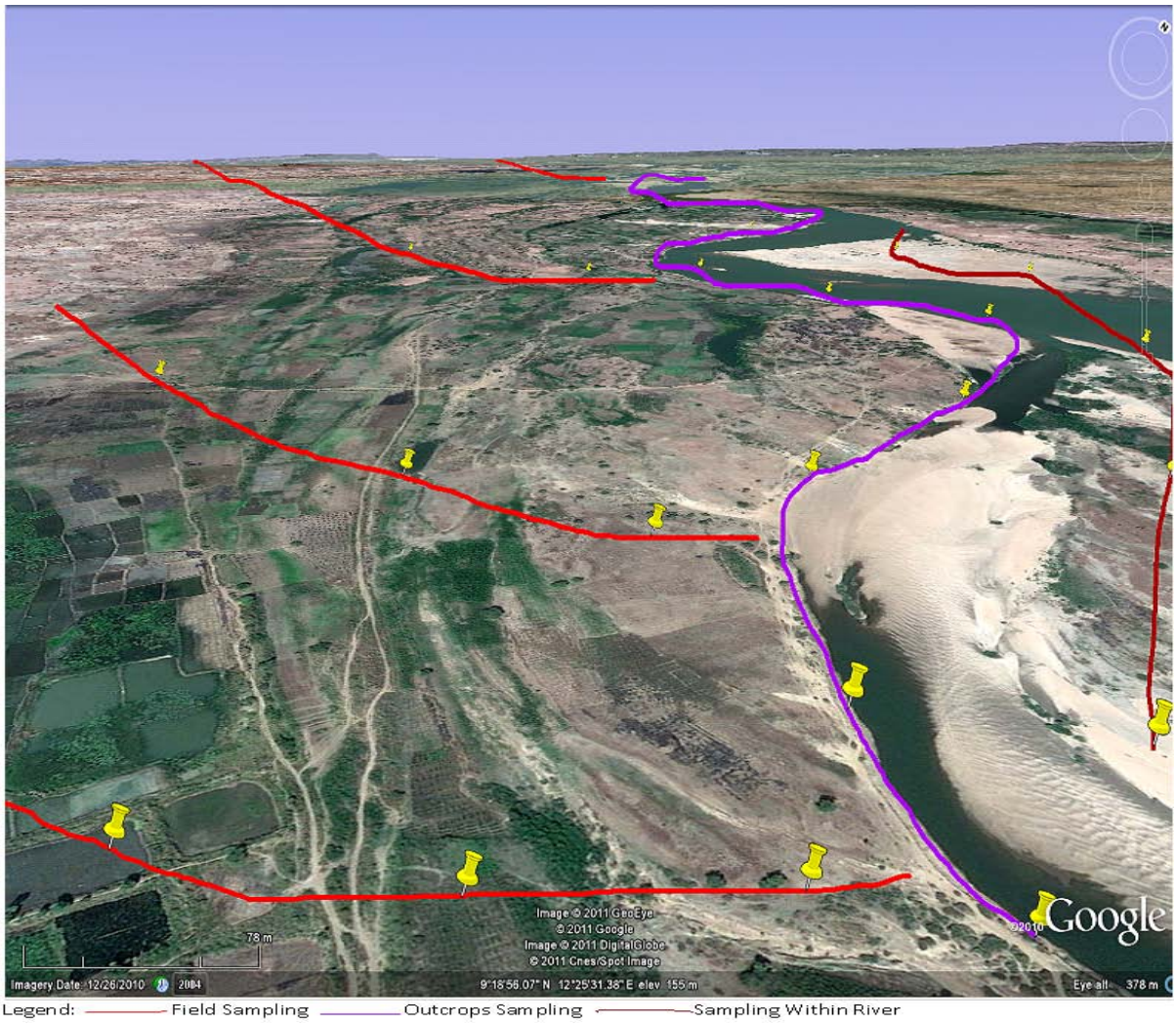

Fig 1: Map Showing Sampling Location Points in the Study Area

References

(1)Google Earth (2011) "Google Earth Image". *US Dept. of State Geographer. MapLink/Tele Atlas Europa Technologies*.

(2)Labas, J., Vuik, R., Van der Wal, A. & Naugle, J. (2010) "Augering Technical Training Handbook on Affordable manual wells drilling". *Published by the PRACTICA Foundation*, 2010. Available online at www.practicafoundation.nl. Pp. 1 – 78. Last accessed on 15th December, 2010.

(3)Suttan, I. (2007) "An Assessment of Hand drilling potential in Upland and Lowland, Dambo Environment of Malawi". *Unpublished M.Sc, Thesis, school of Applied science, water management. Cranfield University*. Pp. 1 – 140.

Keywords: Hand Drilling, Alluvial Aquifers, River Benue valley, Sediment, ABEM Terrameter.

Novel bio-composites based on whole utilisation of wheat straw

Lei ZHAO, Wendy XIA, Jim SONG, Karnik TARVERDI, Wenhui SONG*

Research in Biodegradable Materials, Department of Mechanical Engineering & Wolfson Centre for Materials Processing, Brunel University, UK

EXTENDED ABSTRACT

Introduction

This research aims to develop a portfolio of bio-composites based on whole utilisation of renewable wheat straw for industrial applications. The concept is based on a previous work on a novel twin-strew extrusion technology for processing of feedstock in wheat straw reinforced bio-composites. It demonstrated that straw raw material could be restructurised into a feedstock with cellulose fibre finely dispersed in the non-cellulose matrix, which can be utilised as a bonding phase without having to be removed as in conventional processes to extract the cellulose. [1]The whole straw can thus be utilised to avoid waste of materials and the negative impacts to environment associated with the extraction process. Through this collaborative research, the consortium is to address the scientific and technical problems in materials formulation/processing, product design/manufacturing, enhancement of functionality/ performance as well as economical/environmental assessment so as to develop a series of cost-effective bio-composites and products, which satisfy diverse technical and environmental performance requirements in the industrial sectors across packaging, horticulture, building/construction and shooting sports.

Methodology

1) Raw wheat straw was prepared in two ways. The first way of is simply fractionated by mechanical granulating or ball milling. The second way is the deep preparation with straw treated by NaOH and processed through extrusion.

2) The two kind of straw with different treatment level were all applied to combine with different binder or matrix into different designed formulations. Extrusion was the main processing method producing the products. Tube products were produced directly from the extruder. For products with complicate and board shape, the master batch prepared through extrusion was then formed into shape by compression moulding or injection moulding. Figure 1 briefly illustrates the main processing route of straw bio-composites.

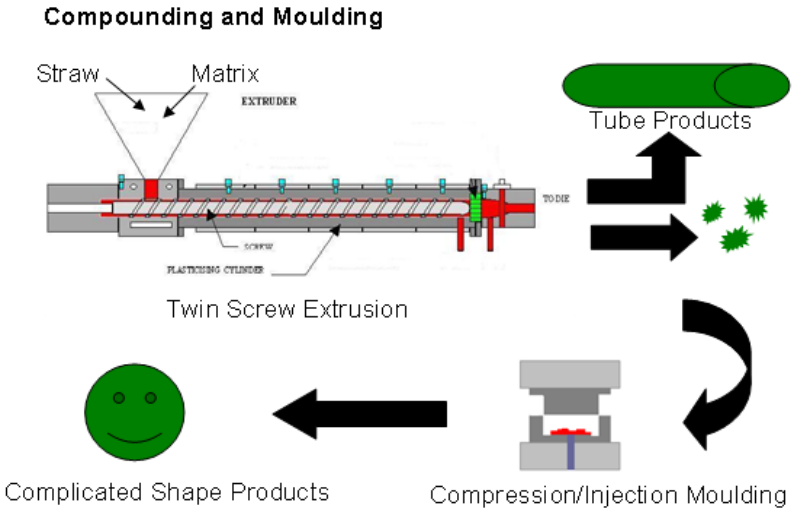

Fig 1 processing route of the straw bio-composites

3) Tensile, tear, 3-point bending, impact tests were employed to detect the mechanical properties of the product samples. Light microscopy, SEM, FTIR mapping were used to examine the morphology of microstructures and bonding mechanisms. TGA and DSC were involved to explore the thermal behaviors of biopolymers and bio-composites.

Results and Findings

The key results achieved in the research are as follow:

1) Wheat straw can be processed into varieties of forms according to the applications. It can be highly processed through combined chemical treatment and mechanical force to become self-reinforced composite with good flow ability. It can be moderately processed through mild treatment and mechanical force to improve its compatibility with other bio-polymers as good filler.

2) The applications of wheat straw prove to be versatile. There are 4 systems of straw based composites developed in this project:

a).100% straw system b).Straw-starch system c).Straw-starch-clay system

d).Straw-biopolymer system

A relationship of processing---property was established for each system which provides key understanding to both processing parameters and end product property. The mechanical properties of composites from above systems range from flexible to rigid, from tough to brittle. The dimensions of products range from 1mm thick of sheet to 16mm of boards.

3) A 100% wheat straw product without added adhesives can be produced through compression moulding in industrial scale. Its mechanical properties are comparable to existing commercial straw boards with added bonding agent.

4) Wheat straw-wheat flour composite has excellent mechanical properties and has great potential applications as 100% natural products.

5) A balanced property of bio-pigeon was achieved through novel processing and formulation by using straw-flour-clay system.

6) Biopolymers, like biolice and bioflex, with straw content of 25-30 wt. % by weight can be produced through existing extrusion/injection technology. The products can match property requirements of gun wads and mulch mats.

Conclusion and Further work

The idea of bio-composites based on whole utilisation of wheat straw is successfully realised in this project. The designed end-products can prove the feasibility of industrious production of straw based composites.

Products with higher straw content (more than 40 wt. %) were not yet produced in this project, but great potential exists based on good flow ability of highly processed straw. If a novel technology developed which can cope with natural polymer, products with 100% straw will become reality.

References

1. STI LINK project (2003-2006), “Novel processing of cereal straws for fiber packaging materials”, DEFRA ref No. LK0818.

Keywords: Straw, bio-composites, extrusion

Cereal straw pre-treatment for bio-fuel application: comparison between extrusion and conventional steam explosion

Thian Hong NG*, Jim SONG, Karnik TARVERDI

Wolfson Centre for Material Processing,
thian.ng@brunel.ac.uk, jim.song@brunel.ac.uk

EXTENDED ABSTRACT

Introduction

Global bio-fuel production has been increased rapidly over the last decade driven by the fossil fuel crisis. Concerns about the long-term sustainability of the liquid bio-fuel, in term of competition of feedstock in supply of foods have been raised with regard to the first-generation bio-fuels, which are produced primarily from food crops such as grain, sugar cane and vegetable oils. This has driven the development of the second-generation bio-alcohol derived mainly from lignocellulosic biomass feedstock such as cereal straw. There is abundant supply of cereal straw in UK. Approximately 5-6 million tonnes of wheat straw are produced in the UK annually but only 1% is currently traded.

Pre-treatment of lignocellulosic biomass is a crucial step as it has direct impact on the subsequent yield of enzymatic hydrolysis to produce glucose and alcohol fermentation processes in the production of bio-fuel. Several physical [1-3], chemical [4, 5] and biological [6, 7] pre-treatments have been developed to improve the digestibility of biomass, but the need to reduce the energy inputs for the treatment, and processing costs in general, has generated consensus around the use of simple thermo-chemical pre-treatments [8]. A batch process, such as steam explosion is most commonly used method for lignocellulosic pre-treatment. However, steam explosion process was reported with limitation of carbohydrate degradation and oxidation of lignin, which would result in potential fermentation inhibitors [2]. Issues of inhibitor formation will have direct impact on final yield recovery of bio-alcohol.

Extrusion technology was recently reported with good potential for pre-treatment of lignocelluloses biomass [2, 3, 9, 10]. Extruder has ability to provide high shear, rapid heat transfer, effective and rapid mixing and feasibility to combine with other pre-treatment – all in a continuous process. Extrusion at low barrel temperature has potential to minimise the limitations reported in steam explosion. This study aims to further obtain a good understanding of twin-screw extrusion pre-treatment of cereal straw by a systematic comparison between extrusion and conventional steam explosion. Pre-treated straw were characterised with a portfolio of analytical technique and correlated to the yield of glucose after enzymatic hydrolysis in order to identify the effectiveness of pre-treatment process.

Methodology

Raw wheat straw (RWS) was pre-treated using a five-barrel Betol twin screw co-rotating extruder and a conventional steam explosion reactor, respectively. Detail of pre-treatment conditions and sample variation were summarised in Table 1. Two low temperature extrusions with one of it has chemical (NaOH) included during pre-treatment were selected for the comparison. While for steam explosion, trial was conducted in both medium and severe condition, respectively. High temperature and pressure were applied for steam explosion pre-treatment. Raw wheat straw was included as control.

Analytical technique was used to characterise the pre-treated straw under different condition. Scanning electron microscope (SEM) was used for visual assessment of the morphology. Fourier transform infra-red (FTIR) was used for investigating the physio-chemical change in plant component. Thermal gravimetric analysis (TGA) was used for investigating the thermal degradation behaviour in relation to the changes took place during pre-treatments. Yield of glucose in enzymatic hydrolysis was given based on a digestion at 10% straw concentration in buffered medium for 16 hours.

Sample	Pre-treatment Condition
RWS	Wheat straw as received without pre-treatment
EX01	Extruded @ 100rpm, 50^0C, Straw:H_2O 1:2
EX02	Extruded @ 100rpm, 50^0C + 4% NaOH (alkaline), Straw:H_2O 1:2
SE01	Steam exploded @ 10mins, 190^0C, 11.6 Bars
SE02	Steam exploded @ 10mins, 220^0C, 22.2 Bars (severe steam explosion)

Table 1: Sample Details

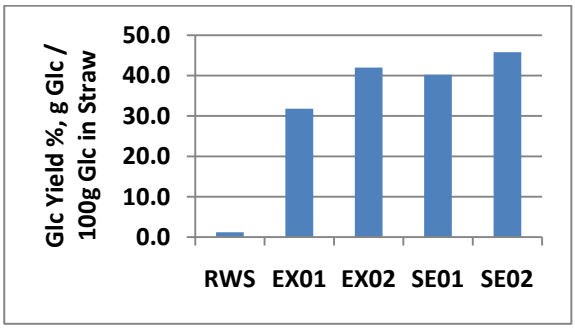

Figure 1 : Yield of glucose recovery after enzymatic hydrolysis

Key findings

After the pre-treatment, there is at least 30 times increased of the glucose recovery in straw. Steam exploded straw with severe pre-treatment condition - SE02 was reported with highest glucose yield at 45.8g of glucose / 100g glucose in straw (showed in Figure 1). Good yield was supported by characterisation findings from SEM, FTIR and TGA. Under low temperature extrusion with chemical supplemented, pre-treated straw shows a comparable result to steam explosion.

Challenges & Limitation

Low temperature extrusion alone yields with 14% glucose lower in comparison to highest yield from stream explosion. In order to achieve equivalence or even better pre-treatment efficiency, optimisation on extrusion capability is required. This has to be done without further depend on chemical impact due to cost and environmental considerations. Temperature factor will potentially helps to increase the degree of fractionation for extrusion. However, high pre-treatment temperature (>200°C) will tempted to generate inhibitor, which is not preferred in the fermentation process.

Conclusion and Motivation of future works

Development of extrusion as pre-treatment method is worth for further study. Room for optimisation under thermal-mechanical factor such as screw profile and temperature of extrusion would be helpful to increase the effectiveness of fractionation. Post process washing can be used as a separation method to recover by-product generated from pre-treatment and use for other bio-refinery application while improving the yield of enzymatic hydrolysis.

Pre-treatment condition can be significantly contributes to the final processing cost as well as impact on carbon footprint. Advance comparison between extrusion and steam explosion in term of total energy demand would be worth to be further explore since the operating temperature for extrusion is much lower than the steam explosion process. Low temperature pre-treatment has great potential to reduce operation cost and can minimise the inhibitors generation during the pre-treatment process.

References

[1] N. Mosier, R. Hendrickson, N. Ho, M. Sedlak and M. R. Ladisch, "Optimization of pH controlled liquid hot water pretreatment of corn stover," *Bioresour. Technol.*, vol. 96, pp. 1986-1993, 12, 2005.

[2] C. Karunanithy and K. Muthukumarappan, "Optimization of switchgrass and extruder parameters for enzymatic hydrolysis using response surface methodology," *Industrial Crops and Products*, vol. In Press, Corrected Proof, .

[3] S. -. Lee, Y. Teramoto and T. Endo, "Enhancement of enzymatic accessibility by fibrillation of woody biomass using batch-type kneader with twin-screw elements," *Bioresour. Technol.*, vol. 101, pp. 769-774, 2010.
[4] F. Sun and H. Chen, "Comparison of atmospheric aqueous glycerol and steam explosion pretreatments of wheat straw for enhanced enzymatic hydrolysis," *Journal of Chemical Technology and Biotechnology*, vol. 83, pp. 707-714, 2008.
[5] A. M. J. Kootstra, H. H. Beeftink, E. L. Scott and J. P. M. Sanders, "Comparison of dilute mineral and organic acid pretreatment for enzymatic hydrolysis of wheat straw," *Biochem. Eng. J.*, vol. 46, pp. 126-131, 2009.
[6] J. S. Bak, M. D. Kim, I. -. Choi and K. H. Kim, "Biological pretreatment of rice straw by fermenting with Dichomitus squalens," *New Biotechnology*, vol. 27, pp. 424-434, 2010.
[7] F. Ma, N. Yang, C. Xu, H. Yu, J. Wu and X. Zhang, "Combination of biological pretreatment with mild acid pretreatment for enzymatic hydrolysis and ethanol production from water hyacinth," *Bioresour. Technol.*, vol. 101, pp. 9600-9604, 12, 2010.
[8] L. D. Gomez, C. Steele-King and S. McQueen-Mason, "Sustainable liquid biofuels from biomass: the writing's on the walls," *New Phytol.*, vol. 178, pp. 473-485, 06, 2008.
[9] C. Karunanithy and K. Muthukumarappan, "Combined effect of alkali soaking and extrusion conditions on fermentable sugar yields from switchgrass and prairie cord grass," in 2009, pp. 5165-5193.
[10] S. -. Lee, Y. Teramoto and T. Endo, "Enzymatic saccharification of woody biomass micro/nanofibrillated by continuous extrusion process I - Effect of additives with cellulose affinity," *Bioresour. Technol.*, vol. 100, pp. 275-279, 2009.

Keywords : wheat straw, bio-fuel, pre-treatment, extrusion, steam explosion

Poly(3-hydroxybutyrate-co-3-hydroxyvalerate) and poly (butylene adipate-co-terephthalate) blends: crystallization behaviour and thermal degradation

*Sitthi DUANGPHET, Damian SZEGDA, Jim SONG * and Karnik TARVERDI*
Wolfson Centre for Materials Processing, Brunel University, Uxbridge, Middlesex, UB8 3PH, UK
(*Corresponding author: jim.song@brunel.ac.uk)

EXTENDED ABSTRACT

Introduction

Constant increase of petrochemical based plastic waste in the environment has motivated the research on biodegradable polymers. Poly(3-hydroxybutyrate-co-3-hydroxyvalerate) (PHBV) is one of the most promising substitute polymers for high-barrier food packaging applications. However, the application of PHBV is restricted because of material cost and inferior thermal stability properties [1]. Blending PHBV with polymers such as poly(butylene adipate-*co*-terephthalate) (PBAT) is a useful and economical method to improve its properties [2].

This study is being undertaken to investigate the effect of PBAT on thermal stability and crystallization behavior on PHBV with conventional polymer processing equipment.

Methodology

For minimisation of thermal degradation, PHBV/PBAT blends were prepared in a Thermo Fisher Polylab twin screw extruder using a negative temperature profile as presented below, with a 150 x 2mm sheet extrusion die attachment.

Barrel	1	2	3	4	5	6	7	8	9	10	Sheet die
Temp °C	120	175	175	170	165	160	155	150	145	140	135

The compounds were extruded using screw speed of 90 rpm, and collected as sheets after passing through water cooled three roll stacks.

Differential scanning calorimetry (DSC) measurements (mass 9.5±0.5mg) was performed using TA instrument Q2000 differential scanning calorimeter under nitrogen atmosphere. The isothermal crystallization temperatures from 120 to 150 ºC were employed. The thermal degradations of the blends (mass 10.5±0.5mg) were analysed by thermal gravimetric analysis (TGA) technique in the temperature range from 40 to 600 ºC using TA instrument Q500 under nitrogen flow rate of 10 cm^3/min.

Findings/Results

The DSC curves, obtained from PHBV/PBAT blends, unblended PHBV and unblended PBAT, on the second cooling scans at a cooling rate of 10°/min are presented in Figure 1.

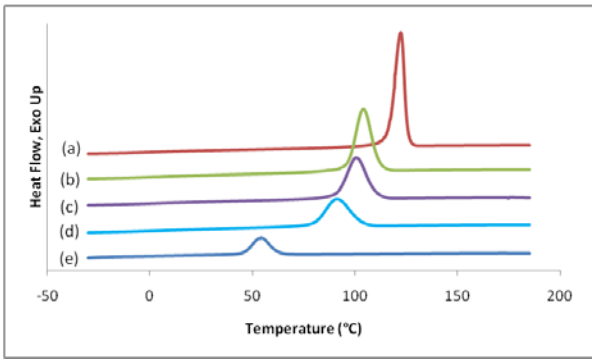

Figure 1. DSC second cooling curves of PHBV/PBAT blends at a cooling rate of 10ºC min^{-1} showing the shift of cold crystallization temperature (Tcc): a) 100/0; b) 85/15; c) 70/30, d) 50/50 and e) 0/100

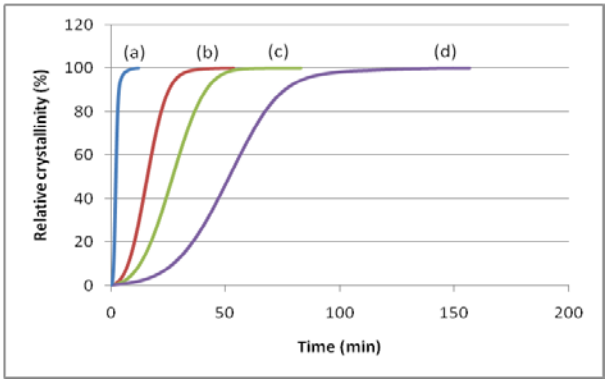

Figure 2. The development of relative crystallinity with crystallization time of PHBV/PBAT blends at 130ºC: a) 100/0; b) 85/15; c) 70/30 and d) 50/50.

For all blend ratios, only single crystallization peaks can be observed. The indirect measurement of the crystallization rate could be correlated to the melt crystallization temperatures (Tmc) and cold crystallization temperatures (Tcc) [3]. Generally, a lower Tmc indicates slower crystallization, whereas a lower Tcc indicates faster crystallization. This behaviour suggests that the process of crystallization of PHBV is retarded with the presence of PBAT. The retarding of crystallization rate is also confirmed by isothermal crystallization study as shown in Figure 2.
The results clearly show that the rates crystallization of the polymer blends are slower with the inclusion of increasing amounts of PBAT.
The nonisothermal thermogravimetric (TG) and the corresponding derivative thermogravimatric (DTG) (Figure 3.) present the thermal degradation of PHBV/PBAT blends.

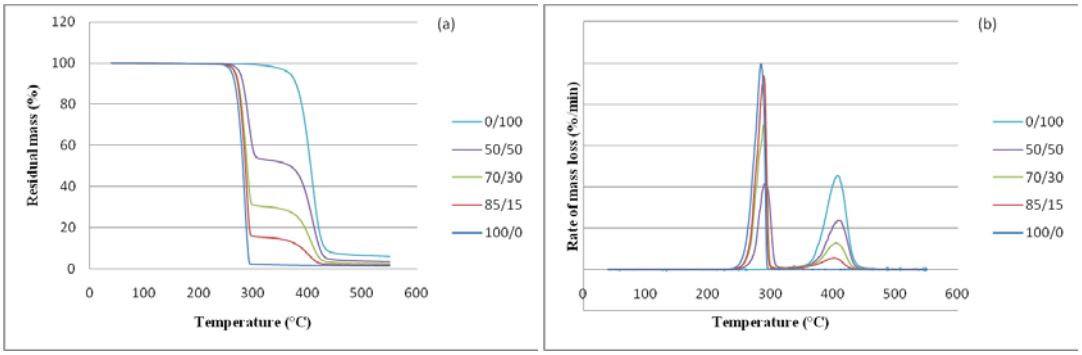

Figure. 3. TG curves (a) and DTG curves (b) of PHBV/PBAT blends at heating rates 10 ºC/min.

From these figures it is evident that the weight loss of pure PHBV and PBAT occurs in a one-step process. Whilst, the thermal decomposition of PHBV/PBAT blends consists of mainly two separate decomposition steps with two maximum rate peaks. This result confirms the immiscibility of the blend between PHBV and PBAT.
The results show that the weight loss of pure PHBV emerges at lower temperature, while weigh loss of PHBV blends can be postponed to higher temperature with the increase ratio of PBAT. DTG curves show the temperatures at the maximum rate of decomposition in PHBV/PBAT blends. The highest rate of PHBV decomposition is obtained when PBAT is not present while the blend PHBV/PBAT 50/50 displays the slowest rate of PHBV decomposition. This means that increasing the content of PBAT in the blend reduces the rate of PHBV decomposition.

Conclusion

Based on the data obtained it can be concluded that biodegradable PBAT improves thermal stability of PHBV, nevertheless it delays the rate of crystallization.

References

[1] M. Erceg,T. Kovacic, and I. Karic, “Dynamic thermogravimetric degradation of poly(3-hydroxybutyrate)/aliphatic-aromatic copoyester blends,” *Polym. Degrad. Stab.*, vol. 90, pp. 86-94, 2005.
[2] A. Javadi, A.J. Kramschuster, S. Pilla, J. lee, S. Gong and L.S. Turng, “Processing and characterization of microcellular PHBV/PBAT blends,” *Polym, Eng, Sci.*, vol. 50, pp. 1440-1448, 2010.
[3] W. Kai, Y. He and Y. Inoue, “Fast crystallization of poly(3-hydroxybutyrate) and poly(3-hydroxybutyrate-*co*-3-hydroxyvalerate) with talc and boron nitride as nucleating agents,” *Polym. Int.*, vol. 54, pp. 780-789, 2005.

Keywords: PHBV/PBAT blends, Crystallization, Thermal degradation

Screen printed carbon nanotube field emission devices.

Edward BOUGHTON[1,2]*, Wenhui SONG[1], Benjamin JONES[2], Robert BULPETT[2], Sabina ORLOWSKA[3], Geoff SHEEHY[3], Michael WAITE[3], Mike MILLER [3]

1. The Wolfson Centre for Materials Processing
2. Experimental Techniques Centre
3. TMD Technologies Ltd., Hayes, Middlesex, UK

EXTENDED ABSTRACT

Introduction

Electron sources have applications in x-ray scanners, displays and microwave amplifiers. Currently, these technologies use thermionic electron emission, in which a filament of a low work function material is heated to high temperature to give electrons enough energy to overcome the potential barrier and escape the material. An accelerating voltage draws off the electron beam. By contrast, field electron emission is a process by which electrons are able to escape without additional thermal energy. Field emission ordinarily occurs only at very high electric fields. However, a sharp tip concentrates electric field lines, meaning the local field strength may be several orders of magnitude higher [1]. Field emission can therefore occur from a sharp tip at lower applied fields. The extent to which the required field is lowered is measured by the field enhancement factor, β, and is proportional to the aspect ratio of the tip [2]. Carbon nanotubes (CNTs) are 1-dimensional tubes composed of graphene sheets of hexagonally-arranged carbon atoms [3]. This study aims to exploit the high aspect ratio, small size and ballistic conductivity of multiwalled carbon nanotubes (MWNTs) to fabricate a field emission electron source with low turn-on field, a large number of individual emission sites and high current density by a screen-printing method.

Methodology

Sample	A	B	C
Production	Arc Discharge	Chemical Vapour Deposition(CVD)	Chemical Vapour Deposition (CVD)
Length	200-300nm	~300□m	>10□m
Avg. Diameter	8.4nm	100nm	7nm
Purity	Low	90%	88%
Aspect Ratio	24 - 36	3000	1429

Table 1: CNT species

Three CNT samples were selected (table 1). In each case, the CNTs were suspended in solvent by ultrasonication for 30 minutes. An inorganic binder material was added at this stage. The addition of further agents to control rheological properties results in a thick, black ink. A DEK-240 screen-printer is used to apply a thin, uniform layer of the ink to a gold-coated glass microscope slide, forming a circular emitter with area 1cm^2. Baking at 450°C in air improves adhesion of the CNTs to the substrate and drives of undesired ink components.

Testing is performed in high vacuum (typically ~1 x 10^{-6} mbar) using a purpose-built apparatus allowing the emitter to be held at a fixed distance of 200μm from a flat, metallic anode. A high voltage DC power supply is used to apply a potential of up to -8kV to the emitter. An integrated microammeter is used to record the resulting emission current as the potential is varied.

Results

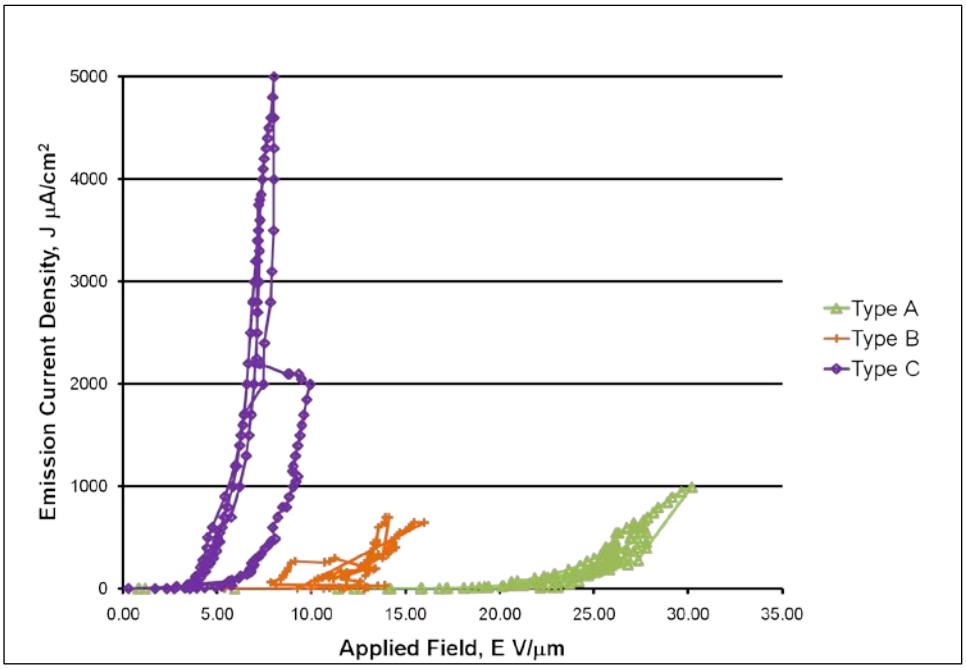

Fig. 1: FE performance of printed emitters

Fig. 1 shows electron emission current as a function of applied electric field for each of the three CNT species. Type C exhibits superior performance, having turn-on field of 3.5 $V\mu m^{-1}$ and maximum emission current of $5mAcm^{-2}$. β was found to be 1920 for this emitter.

Discussion

Analysis with scanning electron microscopy shows that the type B CNTs lie flat on the surface of the substrate, meaning their high aspect ratio is not exploited. This is attributed to their relatively large size. The small size and low purity of the type A material means there are few, if any, protruding CNTs making good contact with the substrate. The performance of the type C material is attributed to the small size of the CNTs allowing them to protrude, and the purity. Before application in a real-world device, the emitter's uniformity must be assessed by replacing the anode with a phosphor screen, allowing the number and distribution of emission sites to be observed. The emitter should also be tested in pulsed-mode operation, as required by x-ray applications. Higher currents should be achievable in this regime, as a lower duty cycle requires less thermal energy to be dissipated.

References

1. A. Buldum and J.P. Lu, Physical Review Letters 91, 23 (2003)
2. W.A. de Heer, A. Chatelain and D. Ugarte, Science 270, 1179 (1995).
3. J.D. Carey, R.C. Smith and S.R.P. Silva, J. Mater. Sci: Mater. Electron. 17 (2006)

Keywords: carbon nanotubes, field electron emission.

Novel routes to hollow inorganic microspheres with nanoshells

Myles P. WORSLEY* and Paul A. SERMON

Wolfson Centre for Materials Processing, Brunel University, Uxbridge, Middx., UB8 3PH

EXTENDED ABSTRACT

Introduction

There is a need for hollow microspheres in medicine [1], drug delivery [2], pigments [3] and photocatalysts [4,5]. Their composition is a critical factor in these applications and determines their properties. They can be constructed from many different materials and by various strategies.

One method used in the preparation of hollow microspheres involves polystyrene (PS) spherical templates [6-8]. This route can be used to synthesise hollow metal oxide spheres such as ZnO that could have electrochemical applications. Quite often these routes require multiple stages to achieve the end product, for instance the production of ZnO hollow spheres first involves the synthesis of PS microspheres by dispersion polymerisation. The resulting PS microspheres can then be used as templates in the ZnO reaction mixture. PS cores are removed by annealing at 600°C. In a similar manner, hollow mesoporous microspheres SiO_2 can also be produced using a sol-gel process with tetraethylorthosilicate (TEOS) in the presence of a template. [9,10]. In this case the PS microspheres are again used and added to the initial TEOS reaction mixture.

Templates are not a necessary requirement for the formation of this morphology, for example, Co_3O_4 spheres have been produced through a wet-chemical approach [11]. In this example, the first step was autoclaving of the precursors at 180°C for 12h, followed by washing and drying with solvent to remove the excess reagents and by-products. To achieve the hollow microspheres the product was annealed at 500°C. A similar route has also been used to prepare CuO spheres for gas sensing applications [12].

Hollow polymer microspheres are also common and relate more to the biological application that their inorganic counterparts. One of the routes to which these are produced involves synthesising core-shell microspheres and then removing the core. For instance, hollow poly(N-isopropylacrylamide) (PNIPAAm) microspheres were prepared by a two-stage distillation precipitation polymerization [13]. The poly(methacrylic acid) (PMAA) core was then subsequently removed through dialysis (over a 2 week period). Alternatively, another example is the use of an oil in water emulsion template to prepare monodisperse poly(hydroxyethyl methacrylate–methyl methacrylate) (poly(HEMA–MMA)) microspheres by interface polymerisation [14].

Thus there is flexibility in the many routes for the production of hollow microspheres. For instance, they can even be synthesised out of pure carbon microspheres (prepared by chemical vapour deposition) through oxidation in air at >450°C [15].

Development and Benefits of a Novel Route

In this study, a novel bottom-up nanotechnology route has been explored for TiO_2 (see scanning electron micrograph in Figure 1), SiO_2, Al_2O_3, ZrO_2, tricalcium phosphate and $CaCO_3$ microspheres with nanoshells. These appear to have good potential. Comparisons are made with biomimetic materials (e.g. from pollen templates).

Some of the main considerations for this technology include its novelty and unique properties. The route used here gives production control over microsphere diameter, shell thickness and composition of a wide range of designer nanomaterials. This control and flexibility is one of several advantages that the current method has over existing technology. Other advantages of this technology include a low temperature preparation route and a reduced number of steps required to reach the end product. The current acquired data has shown that this potential is obtainable.

Potential of the Research

It is envisaged that these microspheres will be able to be used a multitude of applications as described in the previous paragraphs. It is hoped that the ability to control aspects of morphology and composition will enable the technology to compete effectively against current known materials and methods.

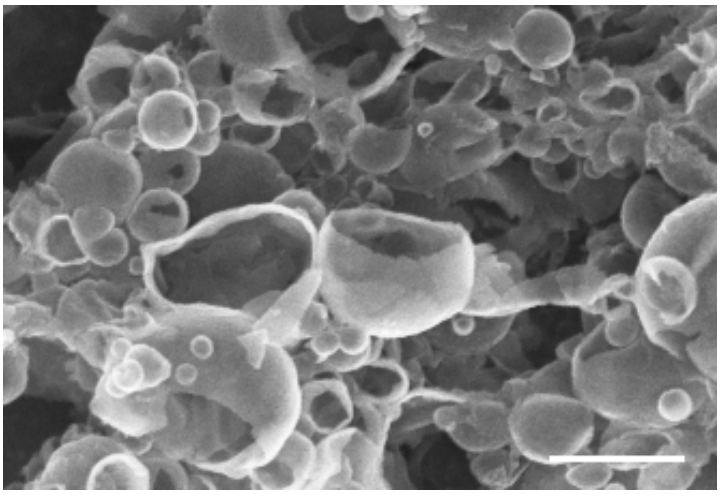

Figure 1: SEM micrograph of TiO_2 hollow microspheres. Scale bar=1µm.

References

[1] Hong, S. J. et al. *Acta Biomaterialia*, 5, 1725 (2009);
[2] Shuyi, L. et al *Nanomedicine: Nanotechnology, Biology and Medicine*, 6, 127 (2010);
[3] Luo, X. and Zhang L. *J. Chromatography A*, 1217, 5922 (2010);
[4] Ye, M. et al *J. Hazardous Materials*, 184, 612 (2010);
[5] Junqi, L. *Applied Surface Science*, 257, 5879 (2011);
[6] Yang, Y. et al. *Materials Chemistry and Physics*, 92, 164 (2005);
[7] Yang, Y. et al *J. Solid State Chemistry*, 179, 470 (2006);
[8] Chen, Z. et al *Colloids and Surfaces A* 355, 45 (2010);
[9] Wang, S. et al. *Microporous and Mesoporous Materials*, 139, 1 (2011);
[10] Zhang, C. et al *Particuology*, 8, 447 (2010);
[11] Tao, F. et al J. Solid State Chemistry, 182, 1055 (2009);
[12] Zhang, Y. et al *Sensors and Actuators B* 128, 293 (2007);
[13] Li, G. et al. *Polymer* 49, 3436, (2008);
[14] Zhang, H. et al. *J. Colloid and Interface Science*, 336, 235, (2009);
[15] Yang, Y et al. *New Carbon Materials*, 25, 431 (2010).

Keywords: hollow microspheres, metal oxides, preparation

Preliminary investigation on restrained shrinkage cracking of concrete with circular and elliptical ring specimens.

Olayinka OLADIRAN*, Xiangming ZHOU
olayinka.oladiran@brunel.ac.uk
School of Engineering and Design, Brunel University, Uxbridge, Middlesex, United Kingdom UB8 3PH,

EXTENDED ABSTRACT

This paper presents a study on assessing restrained shrinkage cracking of concrete with and without shrinkage-reducing admixtures (SRA) using both the conventional circular and the modified elliptical ring specimens. The results showed that the addition of SRA significantly reduced free shrinkage and increased the initial cracking time in ring tests and slightly reduced the compressive and tensile strength of concrete. Compared with circular ring specimens, elliptical ring specimens did not always crack earlier as expected but the cracking did seem to concentrate at certain locations along the circumference of the elliptical ring if under the same drying condition.

Introduction

In order for concrete structures to be serviceable, it is vital that cracking must be controlled. For instance, in most modern concrete design codes, the width of cracking has been limited to a certain value. Concrete shrinks when it is subjected to a drying environment particularly at early ages. The extent of shrinkage depends on many factors, including the properties of concrete, temperature and relative humidity of the environment, the age when concrete is subjected to drying environment, and the size of the structure [1]. If concrete is restrained from shrinking freely to a certain extent, tensile stresses will develop and concrete may crack in view of the fact that concrete has a low tensile strength especially at early ages. The extent of shrinkage is indeed the driving force for early-ages cracking of concrete, but whether cracking will occur or not is also dependent on the restraint in the structure and the stress relaxation, which may be particularly high in early-age concrete [2]. The circular ring test has been more widely used as a quality control test for assessing the shrinkage cracking potential of concrete mixtures. It is economical, simple to perform and does not pose difficulties in providing sufficient end restraint [3]. However, the circular ring test has low degree of restraint, resulting in a fairly long time before the first visible cracking is observed [2] [4]. Under worst conditions, a visible crack may not even be generated if the restraining core is not stiff enough [2]. Besides, initial cracking may appear anywhere along the circumference of a circular ring specimen, making it difficult to be located. To overcome the problems from traditional circular ring tests, He et al [5] proposed a modified ring test by using elliptical shaped specimens to increase stress intensity in concrete to promote crack generation and propagation in concrete. Because of this, characterising cracking sensitivity of concrete can be achieved in a short period so that the new elliptical ring test is appropriate for faster and large amount of materials evaluation. The elliptical ring geometry will help generate new ways of analysing the sensitivity of early-age cracking in concrete; it will generate cracks that will concentrate at certain positions. This test method potentially reduces the resources required for cracking detection. The ring geometry and thickness were varied in this investigation. It is however fully anticipated that the approach presented in this study can be extended for general use in quantifying the cracking potential of concrete under drying as well as under certain degree of restraint. It also describes recent experimental efforts to better understand the role of SRA on early-age cracking of concrete.

Results

Both circular and elliptical concrete ring specimens with the same nominal thickness were tested in pair subjected to the same drying environment for assessing the effects of SRA, ring geometry and degree of restraint on the ages of first major cracking of concrete in ring specimens under restrained shrinkage.

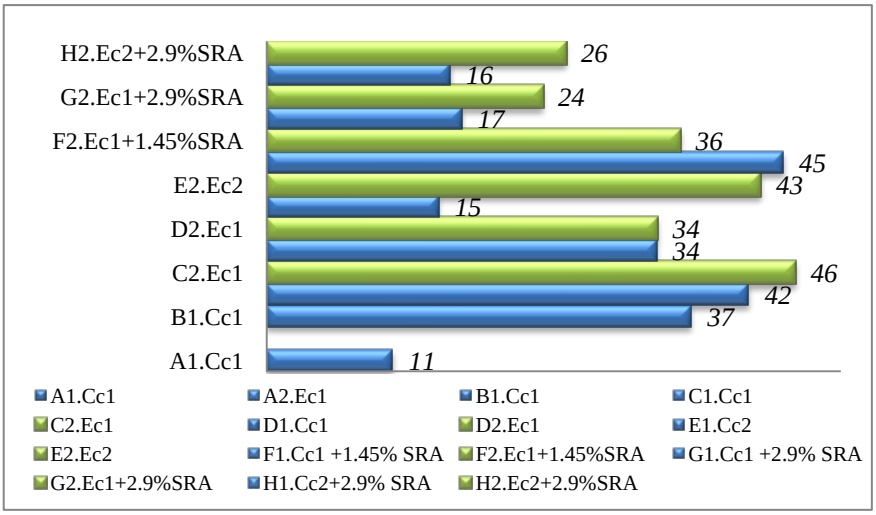

Age of specimens at first crack

*A1, A2 to H1, H2 = Specimen name: * C_c1 C_c2 = Circular rings with 35 & 12.5mm steel ring thickness
* E_c1 E_c2 = Elliptical rings with 35 &12.5mm steel ring thickness;*A1A2 – E1-E2 = Plain concrete;
* F1-F2 – H1H2 = Concrete with SRA

Conclusions

The addition of SRA slightly reduced the compressive and splitting tensile strengths of concrete at early ages. The effects varied depending on the age of concrete and the amount of SRA used. SRA significantly reduced the free shrinkage of concrete. The addition of SRA by replacing the same volume of mix water did not change the workability of concrete. The positions where initial cracks appeared suggests that with a greater ring sensitivity, stiffness and restraint, crack propagation will appear at an earlier age and at similar positions. Though it is expected that elliptical ring specimens crack earlier than circular ring specimens, this did not always happen in the restrained ring tests conducted in this research. However, the experimental results suggest that the position of cracking depended on the drying condition more than the geometries of ring specimens.

References

[1]M. Grzybowski, and S.P. Shah (1989), “A Model to Predict Cracking in Fibre Reinforced Concrete Due to Restrained Shrinkage,” Mag. Concr. Res., 41(1), pp 125-135.
[2]A. Bentur, and K. Kovler (2003), “Evaluation of Early Age Cracking Characteristics in Cementitious Systems,” Mater. Struct., 36(3), pp 183-190.
[3]A .Hossain, Jason Weiss, (2006) The role of specimen geometry and boundary conditions on stress development and cracking in the restrained ring test ; Cement and Concrete Research 36 189-199.
[4]J-H Moon, F. Rajabipour, B. Pease, and J.W. Weiss (2006), “Quantifying the Influence of Specimen Geometry on the Results of the Restrained Ring Test,” J. ASTM Int., 3(8), pp 1-14.
[5]Z. He, X.M. Zhou, and Z.J. Li (2004), “New Experimental Method for Studying Early-Age Cracking of Cement-Based Materials,” ACI Mater. J., 101(1), pp 50-56.

A study on the upconverting properties of terbium and erbium codoped yttrium oxysulfide nanocrystals

Xiao YAN*, Jack SILVER, Wenhui SONG, Robert WITHNALL

Wolfson Centre for Materials Processng

xiao.yan@brunel.ac.uk

EXTENDED ABSTRACT

Introduction

Upconverting phosphors have obtained great attention since initial interest in the 1950s. An upconverting phosphor is one which takes multiple photons of lower energy and converts them to one photon of higher energy (this is an anti-Stokes process). Possible applications of upconverting phosphors include upconverting lasers, photovoltaic cells biological labelling and 3-D displays. There has been considerable research on Lanthanide-doped nanocrystals for their efficient upconverting properties. Our former studies on Yb^{3+} and Er^{3+} ions co-doped Yttrium oxide has been suggested that ytterbium and erbium co-doped yttrium oxide (Y_2O_3:Er^{3+},Yb^{3+}) indicates that Y_2O_3:Er^{3+},Yb^{3+} nanocrystals can give out intense blue, blue-green and yellow upconverting emission bands under 632.8 nm red laser excitation although the presence of Yb^{3+} ions is detrimental when upconversion emission is excited by red laser light. In this paper, upconverting properties of terbium and erbium co-doped yttrium oxysulfide (Y_2O_2S: Tb^{3+}, Er^{3+}) nanoparticles with a define morphology are investigated. Up to our best knowing, there has been no similar work on this before.

Methodology

Rare earth oxides (RE_2O_3) were used as starting materials. RE_2O_3 (RE=Y, Tb and Er) powders were dissolved with diluted nitric acid and then carefully adjusted to aqueous solution with a PH value between 3.0 and 5.0. in a typical process, 25 ml $Y(NO_3)_3$ (0.5 M) was mixed with 12.6 ml $Tb(NO_3)_3$ (0.01 M) and 0.63 ml $Er(NO_3)_3$ (0.01M) solutions before diluted to 500 ml with deionised water. The solution was then heated to 100 ˚C. Then 30 g urea was added. The solution was kept at 100 ˚C with continuous stirring for 1 h since turbidity was observed. The precipitates mentioned above were filtered and washed twice using deionised water. The precipitates were dried at 60 ˚C in an oven, and soft white powders resulted. To convert the powders to oxysulfide, they were mixed evenly with sodium carbonate (Na_2CO_3) and sulphur (S) at a mole ratio of 1:1.5:2 covered with a mixture of Yttrium oxide (Y_2O_3), Na_2CO_3 and S (1:1.5:2 in mole) then fired at 900 ˚C for 1 h.
The obtained Y_2O_2S: Tb^{3+}, Er^{3+} powders were characterised with scanning electron microscope (SEM), X-ray Diffraction (XRD) to determine the morphology. Photoluminescence properties were examined and recorded with Horiba Jobin Yvon Labram HR raman spectrometer incorporated with a 632.8 nm red laser.

Results and discussions

It can be seen clearly from SEM micrographs of fired particles that particles are roughly spherical and although large particles can be observed most particles have a diameter less than 200 nm. The XRD pattern obtained from typical fired samples is identical to that of hexagonal Y_2O_2S: (Tb, Er) crystals.

Luminescence spectroscopy was used to investigate the upconverting properties of Y_2O_2S: (Tb, Er) materials. An emission spectrum of $Y_{1.989}O_2S$: ($Tb_{0.01}$, $Er_{0.001}$) particles is shown below. All of the emission manifolds correspond to transitions to the Er^{3+} ground state ($^4I_{15/2}$) from the following excited-state levels $^4F_{7/2}$, $^2H_{11/2}$ and $^4S_{3/2}$

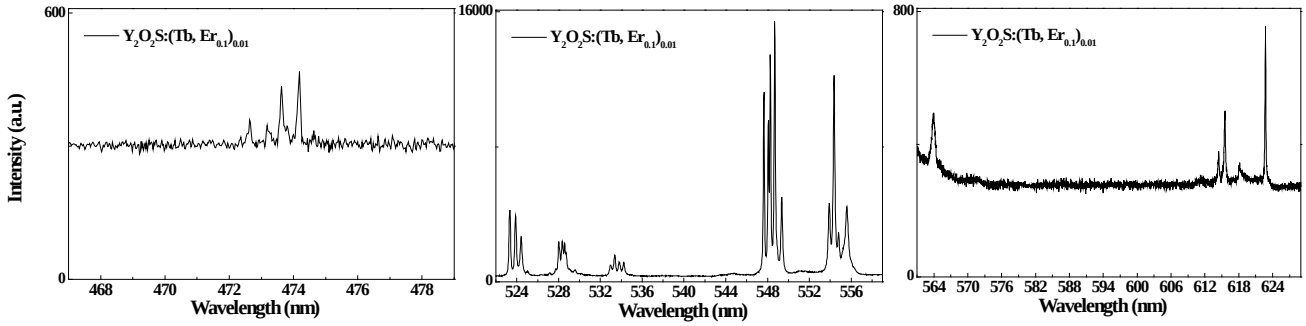

Figure 1. Upconverting emissions of $Y_{1.989}O_2S$: ($Tb_{0.01}$, $Er_{0.001}$) with 632.8 nm

In the upconvertion spectra of Y_2O_2S: (Tb, Er) particles, anti-stokes emissions in the range 520 to 560 nm, assigned to $^4S_{3/2} \rightarrow {}^4I_{15/2}$, are dominative. Overlay of normalised anti-stokes emission spectra of Y_2O_2S: (Tb, Er) particles in the range 520 to 560 nm is shown in Figure 3. The emission peaks of $Y_{1.9895}O_2S$: ($Tb_{0.01}$, $Er_{0.0005}$) particles have the lowest intensity. The intensity of emissions increases with concentration of Er^{3+} ions.

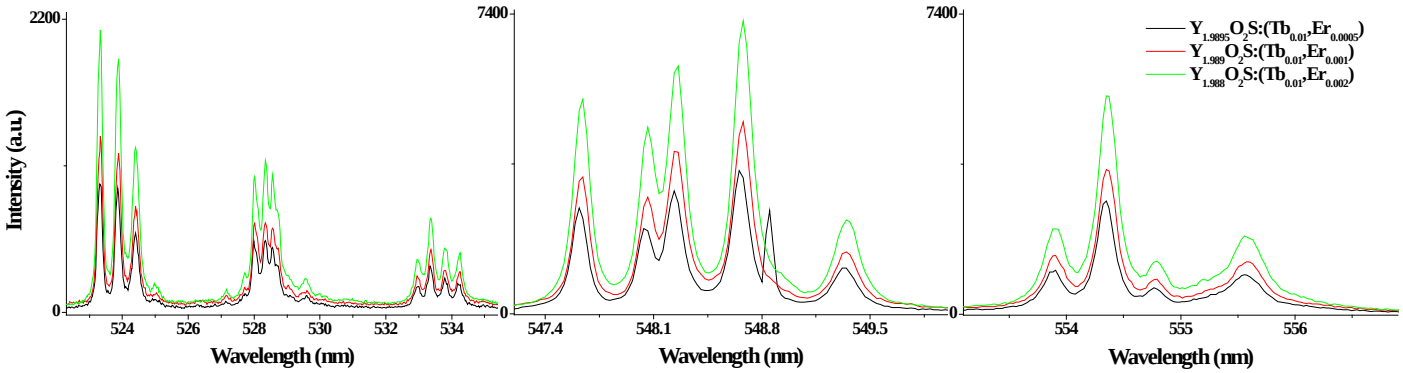

Figure 2. Overlay of normalized upconverting spectra of Y_2O_2S:(Tb, Er) nanocrystals under 632.8 nm laser

Conclusion

Y_2O_2S: (Tb, Er) nanocrystals can be obtained with urea precipitation method. It can exhibit blue, blue-green, green-yellow upconverting emissions when excited with 632.8 nm red laser. The intensity of emission bands increase with the concentration of Er^{3+} ions.

Reference

[1] Silver, J.; Martinez-Rubio, M. I.; Ireland, T. G.; Fern, G. R.; Withnall, R. *J. Phys. Chem.* B, 2001, 105, 948.

[2] Silver, J.; Withnall, R.; Marsh, P. J.; Lipman, A.; Ireland, T. G.; Fern, G. R., SID Symposium Digest of Technical Papers, 36 (2005) 594.

Keywords: upconverting, Y_2O_2S, upconversion spectrum

A constraint-based DRM matrix for design collaboration

Jian RUAN
School of Engineering and Design, Brunel University

EXTENDED ABSTRACT

The author proposed an approach, called constraint-based design risk management (DRM) with a conceptual framework on the basis of collaborative design features, risk management process and theory of constraints (TOC). This paper extended research on how to map, measure and migrate collaborative design risk by exploring crucial design constraints, and then identified design risk variables in light of specified risk criteria. Design constraints are quantitative parameter that infrequently impacts main design process and decisions. The combination of design constraints and risk criteria can be accessible and applicable by designers and mangers. Moreover, an enhanced computation method based on Bayesian theorem has been advanced to support the DRM matrix to measure collaborative design risk in a more efficient manner. In addition, a simulation prototype has been developed for case study evaluation.

Introduction

The global design collaboration based on multi-disciplinary and distributed environment is becoming a mainstream to new product development (NPD). However, during the process of collaborative design, risk is rarely mentioned. In particular, due to the complexity of design process and lack of efficient design decision-making, there has been some design collaboration failure across multiple companies. Some design projects cannot deliver the benefits as companies have expected through the collaboration. Moreover, a number of stakeholders, managers and designers expressed their disappointment at not seeing the projected savings in cost and time and critically discredit the value of design collaboration. Many studies in academia and commercial cases have suggested that risk assessment can be applied as an effective means in the field of design industry. Nevertheless, few of them conducted risk management research associated with design constraints under a collaborative environment from both theoretical and practical perspectives. In current risk practice, many risk practitioners simply report key risks to their management teams and no further analysis, which might subsequently give rise to confusion with excessive discussions. Consequently, to prevent the failure of design collaboration and conduct a satisfactory risk assessment, it is important to perform risk management in a heuristic process with an upstream perspective.

As theory of constraints (TOC) can be used to emphasises the cross-functional collaborative design processes from a chain perspective of tasks, functions, processes, roles and resources, a constraint perspective provides a useful way from which researchers and practitioners that can anticipate and resolve a variety of design problems. However, there is an uncertainty in the first phase of DRM, which is the identifying of main design constraints among different design spaces, where most of constraints are critical to the success of NPD.

Typically, these sorts of design constraints can be regarded as the source of weakest link or risk variable, which might greatly impact the performance of overall results. Thus, considering that only a few constraints that have significant and immediate influence on the whole system, it is essential to identify and evaluate these constraints in order to support designers and managers for mapping, measuring and migrating design risk variables in an accurate and efficient manner.

Design/Methodology/Approach

Literature Survey, Industry semi-structure interview, Simulation and Case studies

Findings

A constraint-based DRM matrix is developed on the basis of evaluated design constraints and risk criteria which provide a structured and proactive approach to map and measure design risk variables in an accurate and efficient manner. The development of the matrix caters for collaborative design projects by taking into consideration the accumulative design constraints as a result of risk variables within the level of tasks-dependency, role-interaction and resources-integration, which facilitates the design collaboration at an operational level. Moreover, an enhanced computation method based on Bayesian theorem has been advanced to support the DRM matrix to measure collaborative design risk in a more efficient manner. In addition, a simulation prototype has been developed for case study evaluation.

References

Ahmed. A., Kayis, B. and Sataporn, A. (2007), A review of techniques for risk management in projects, Benchmarking: An International Journal, Vol. 14 No. 1

Goonetillake, J.S., Carnduff, T.W. and Gray,W.A.,(2001), 'Integrity constraint management for design object versions in a concurrent engineering design environment', Database Engineering & Applications, International Symposium. Vol. pp.255 – 261.

Joan-Arinyo,R., Soto-Riera, A., and Vila-Marta,S. (2006), Constraint-Based Techniques to Support Collaborative Design, Journal of Computing and Information Science in Engineering, Volume 6, Issue 2, pp,139-149

Kayis, B., Zhou, M., Savci, S., Khoo, Y.B., Kusumo, R., Ahmed, A. and Rispler, A. (2004), "Development of an intelligent risk management system for minimizing problems in new product development", Proceedings of International Concurrent Engineering Conference, China

Mabin, V.J. and Balderstone, S.J. (2003), "The performance of the theory of constraints methodology: analysis and discussion of successful TOC applications", International Journal of Operations & Production Management, Vol. 23 No. 6, pp. 568-95.

Markeset,T., Kumar,U (2003) "Integration of RAMS and risk analysis in product design and development work processes: A case study", Journal of Quality in Maintenance Engineering, Vol. 9 Iss: 4, pp.393 – 410

Rong, Z.J, Li, P.G, Shao, X.Y. and Chen, K.S. (2006), 'Constraint-based Collaborative Design', IEEE Proceedings of the 10th International Conference on Computer Supported Cooperative Work in Design.

Keywords: design constraints, collaboration, risk management.

Usability of eGovernment websites in Jordan

Bader Methqal ALFAWWAZ*, Dr. Vanja GARAJ
School of Engineering and Design, Brunel University, London, UK

bader.alfawwaz@brunel.ac.uk

EXTENDED ABSTRACT

Introduction

eGovernment is defined as utilizing the Internet and the world-wide-web for delivering government information and services to citizens [1] while web usability is a clarity, simplicity, and consistency in the website design in order to allow users to perform their tasks easily [2].

Despite the remarkable increase of eGovernment services, governments have faced some challenges in making their websites usable [3]. [4] and [5] stated that usability has become one of the main problems influencing the adoption and development of eGovernment; and the failure to achieve acceptable levels of usability for eGovernment services threatens not only the eGovernment initiatives, but also the relationship between the government and citizens in general.

This issue is significant in developing countries such as Jordan, where the digital divide is wider [6], further inhibiting the eGovernment project. The purpose of this paper is to identify the status of the usability of eGovernment websites in Jordan from the managers' perspective. The research focused on the views of professionals in charge of managing eGovernment project in Jordan.

Methodology

The research involved a sample of 37 managers, in various capacities, and all were responsible in managing eGovernment project in Jordan.

The study applied the questionnaire technique. The questionnaire was originally designed in English and it was then translated into Arabic, the mother tongue of the participants in order to achieve the full understanding of the questions. All the participants were visited personally**.** On completion of all the participants, the questions have coded to enter the data into SPSS software. The analysis of the data obtained from the response to the questionnaire is presented below.

Results and Discussion

Good usability of any system is the main goal of interface designers, and the website must be satisfactory and have an excellent appearance as well as the experience of any user must be enjoyable. [7]; [8] and [9]. With reference to the results of the interfaces of the current eGovernment websites in Jordan; this is relatively not achieved because over half of respondents have experienced average and below average satisfaction. This is maybe because eGovernment websites in Jordan were developed by the IT government departments' teams, and the rest were developed by different certified IT companies in Jordan, and each one has a different layout and architecture as stated by [10].

Not involving the end-users or considering their feedback about the design is considered as challenge in this research. The results have revealed that the majority of respondents did not pay attention to the end-user requirements before establishing the eGovernment websites or even after launching the system for further developments. [4] mentioned that the participation of users during the design process increases their feeling of not being ignored, and encourages the adoption of any new system.

This is mean that there is no clear method adopted to consider user feedback and experience of the system as well as the existing system does not satisfy users' needs and is not considered sufficient. This is in agreement with [10] and [11], who pointed out that during the construction and design of Jordanian eGovernment websites, the expectations and needs of end-users have been ignored, and no account taken of what they want from the existing system.

This is in agreement with [10] and [11], who pointed out that during the construction and design of Jordanian eGovernment websites, the expectations and needs of end-users have been ignored, and no account taken of what they want from the existing system.

The biggest challenge of making a website usable to the end-users from the managers' point of views was investigated. Lack of awareness of usability was the major challenge, followed by the lack of involvement of the end-users in the initial state of design.

Lack of usability awareness remains one of the biggest challenges to making a website usable for end-users. This strongly suggests a very limited understanding of usability and its importance for the success of the websites. This lack of usability awareness costs the users both time and effort, with a detrimental impact on productivity, which could ultimately decide the success or failure of the system.

Conclusion

The outcome of the study has revealed that there are still no clear guidelines or standards regards usability. Moreover, when the websites were designed, attention to the end-users' requirement was not established before implementing the eGovernment websites, nor has it been established after the launch of the system as part of further development.

Despite all the investment from the Jordanian government in the eGovernment project, the absence of clear guidelines to govern eGovernment project initiation and operation might inhibit many difficulties to take off.

Jordanian governmental websites have not accommodated usability standards, and there is no awareness of needs and expectations and that will not be achieved unless they prioritise the usability dimension and address users' needs. It is important at this stage that the Jordanian eGovernment should address the current problems to ensure the provision of usable eGovernment websites in Jordan.

References

1. UNPAN, United Nations Public Administration Network. (2002). Benchmarking E-government: A Global Perspective. Assessing the Progress of the UN Member States, The United Nations.
2. Cappel, J., & Huang, Z. (2007). A usability analysis of company websites. The Journal of Computer Information Systems, 48 (1), 117-123.
3. Soufi. B, & Maguire, M. (2007). Achieving Usability Within the E-Government Web Sites Illustrated by a Case Study Evaluation. Human Interface and the Management of Information. Interacting in Information Environments, Springer, 777–784.
4. Stanziola, E., Minuto Espil, M., Landoni, L., & Montoya, S. (2006). Hidden Negative Social Effects of Poor eGovernment Services Design. (Eds.): EGOV 2006, LNCS 4084, Springer-Verlag Berlin Heidelberg, 150–161
5. Casaló, L., Flavián, C., & Guinaliú, M. (2005). The role of accessibility and commitment in the development of an e-government strategy. eGovernment Workshop '05 (eGOV05). September 13, 2005, Brunel University, West London, UK.
6. Elsheikh, Y., Cullen, A., & Hobbs, D. (2007). Towards e-government in the Middle East: A Jordanian Study. IADIS International Conference, ISBN: 978-972-8924-44-7.
7. O'Cass, A., & Fenech, T. (2003). Web retailing adoption: Exploring the nature of Internet users Web retailing behaviour. Journal of Retailing and Consumer Services, 10 (2), 81–94.
8. Van Welie, M., van der Veer, G. C., & Enlivens, A. (1999). Breaking down Usability. Proceedings of Interact '99, Edinburgh, Scotland.
9. Wei, X., & Zhao, J. (2005). Citizens' requirement analysis in Chinese e-Government. Proceedings of the 7th international conference on Electronic commerce. ACM Press, New York, 113, 525 – 428.
10. Mofleh, S. (2008). Managing e-government projects: the gap between supply and demand. PhD thesis, Bristol University, UK.
11. Mohammad, H., Almarabeh, T. & Abu Ali, A. (2009). E-government in Jordan. European Journal of Scientific Research, 35 (2), 188-197.

An assessment of sighted guide performance by using different screen resolution for Brunel remote guidance System

Mohammed AL-MASARWEH *, Vanja GARAJ and Wamadeva BALACHANDRAN
Department of Electronic and Computer Engineering
*Mohammed.Al-Masarweh@brunel.ac.uk

EXTENDED ABSTRACT

Introduction: In recent years, several systems have been proposed to help Visually Impaired Users (VIUs) to navigate through familiar and unfamiliar environments and thus enhance their mobility. These systems are meant to provide the users with an additional degree of freedom by allowing them to travel on foot safely and independently [1]. One of these systems is the Brunel Remote Guidance System (BRGS) (Figure 1) designed by navigation research team within the Centre for Electronic Systems Research at Brunel University (CECR). The system is based on integrating state of the art technologies, including satellite navigation (Global Positioning System (GPS)), wireless broadband, digital mapping (Global Information Systems (GIS)), databases, and real-time video streaming. The BRGS was successfully tested for assisting in navigating VIUs [2].

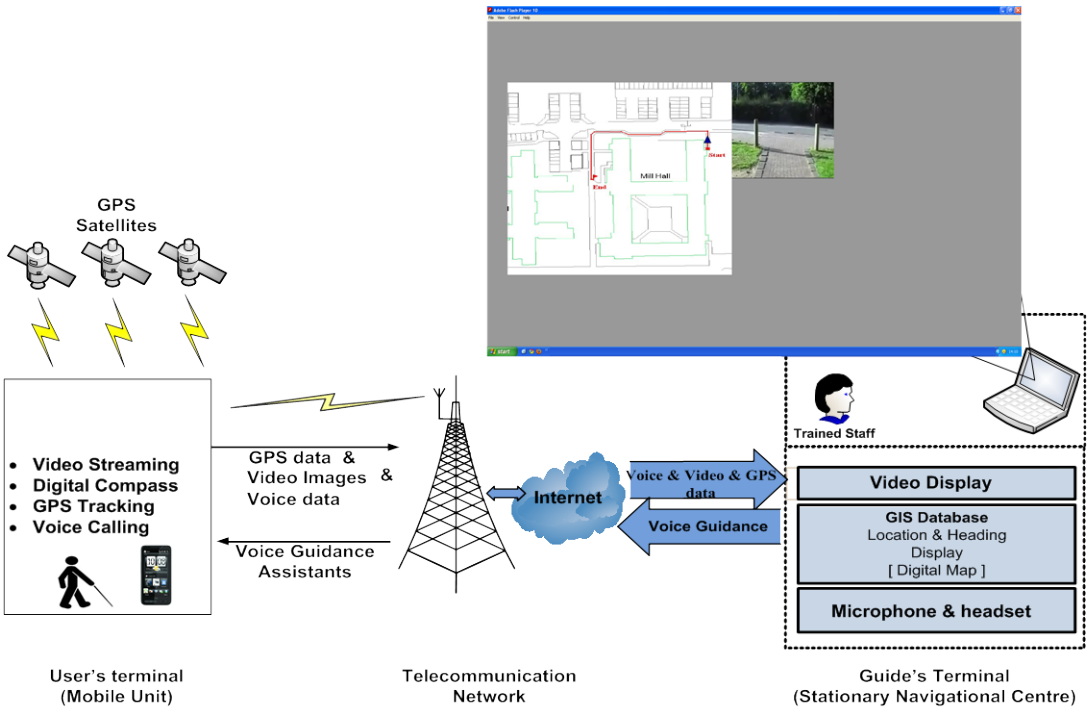

Figure 1: Brunel Remote Guidance System Prototype

BRGS consists of two main terminals: Guide and user terminals. The guide terminal contains a Sighted Guide (SG) person, who needs to assist the VIUs remotely, and a stationary PC. The user terminal includes VIUs and a mobile unit. These terminals have been connected by a wireless network (e.g. 3.5G). This wireless link is used to transmit; the voice communication, GPS location and video image. The video and the digital map are displayed into two-window screens on the guide terminal as shown in Figure 2. The digital map enables the SG to track the VIUs during the journey in order to reach the destination. The video image allows the SG to assist the VIUs by describing the environment ahead. The video image is streamed from the user terminal camera.

This paper presents a study that was undertaken to examine the effects of the map and the video screen resolutions on the performance of the SG in the guide terminal. The performance test was based on three performance factors; Wrong Turns Detection (WTD), Obstacles Detection (OD), and Response Time of Obstacles Detection (RTOD).

Methodology: In this study, a computer based simulation was developed from a typical video image and digital map on a LCD screen that the SG might view whilst assisting VIUs during their journey. The video was included different types of obstacles that similar to what the VIUs might face in real journey and the digital map was included the position of the VIUs. The study involved 80 sighted participants divided into four groups (G1, G2, G3 and G4) with 20 participants in each group. Each simulation was involved two window displays on a LCD monitor, one window display for the video image and the other for the digital map. The participants were asked to detect and report the obstacles into two types (Primary and Secondary obstacles) and to detect the wrong turns. The simulation was presented in four different combinations varying the standard resolutions of 352 x 288 pixels (CIF- Common Intermediate Format) and 704 x 576 pixels (4CIF- Four Common Intermediate Format). This combination of the digital map display and the video image display was given to each group as follow: G1 (4CIF x 4CIF), G2 (4CIF x CIF), G3 (CIF x 4CIF), G4 (CIF x CIF). The simulations were programmed to save the results in the log file in order to save as a PDF file format. This PDF files were analysed to evaluate the participant's performance as follows:

- WTD: it was measured by counting the number of times that VIUs derailed from pre-defined experimental turns. Furthermore, by calculating the distance between the beginning of wrong turn and the recognised point when the participant realizes that the VIU is out of the correct route. Figure 2 is shown the sequence of image captured for the wrong turn.

1. 2.

Figure 2: a sequence of image for the wrong turn

- OD: it was measured by counting the number of obstacles that participants correctly detected into two types' primary obstacle and secondary obstacle and compared with the overall obstacle during the journey. The Signal Detection Theory (SDT) was used to analyse the data [3].
- RTOD: it was measured based on the performance level for every group by classifying the response time of the participant in detecting the obstacles into two areas; the suitable and the unsuitable response time area, when the simulation gives more point for the detection within the suitable area. The percentage of the performance was calculated depending on the summation of the points for each group
-

Result: ANOVA [4] analysis was carried out in order to determine if the size of the screen resolution affects the participant's performance of the WTD, OD and RTOD tasks. The analysis was used to compare the mean of the three performance factors between the four groups as shown in Figure 2. The best performance is the highest mean value. The results of the ANOVA analysis are presented in table 1. Once ANOVA test was done, Post Hoc test [4] has taken a place in order to compare the group's results with each other to find out the optimum setup for this project. The Post Hoc results are shown in table 2.

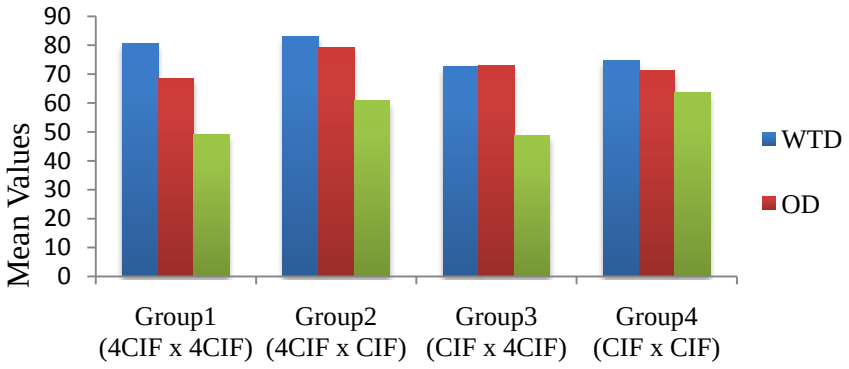

Figure 2: The mean values of performance factors

Category		F	Sig.
WTD	$F_{3,76}(\alpha = 0.05) = 6.295$	6.295	0.001
OD	$F_{3,76}(\alpha = 0.05) = 3.067$	3.067	0.033
RTOD	$F_{3,76}(\alpha = 0.05) = 4.747$	4.747	0.004

Table 1: ANOVA Analysis Results

Category	Main Group		Other groups	Sig.
WTD	G2	Vs.	G1	0.813
			G3	0.002
			G4	0.016
OD	G2	Vs.	G1	0.024
			G2	0.342
			G3	0.133
RTOD	G4	Vs.	G1	0.027
			G3	0.952
			G4	0.021

Table 2: Post Hoc Analysis Results

Conclusion: In this study, the SG performance has been evaluated by using different screen resolutions based on the three performance factors. ANOVA test has displayed that the statistical analysis results of the three performance factors between the participants groups is significant. The main outcome from the analysis and description of the result for this study is:

- The screen resolution has an effect on the performance of the sighted guide, which affects the overall performance of BRGS. The optimum setup for the screen resolutions for the guide terminal is G2's setup, which is a big map screen (4CIF [704p x 576p]) and small video screen (CIF [352p x 288p]).

References

[1] Z. Hunaiti, V. Garaj and W. Balachandran, "An assessment of the video image quality required in a remote vision guidance system for visually impaired pedestrians," *J. Telemed. Telecare,* vol. 12, pp. 400, 2006.

[2] V. Garaj, Z. Hunaiti and W. Balachandran, "Using remote vision: the effects of video image frame rate on visual object recognition performance," *Systems, Man and Cybernetics, Part A: Systems and Humans, IEEE Transactions on,* vol. 40, pp. 698-707, 2010.

[3] D. McNicol, *A Primer of Signal Detection Theory.* Lawrence Erlbaum, 2004.

[4] A. Field, *Discovering Statistics using SPSS for Windows: Advanced Techniques for Beginners (Introducing Statistical Methods Series).* Sage Publications, Thousand Oaks, California, 2005.

Keywords: Remote Guidance, GPS, GIS, Navigation, Visually Impaired Users, Screen Resolution, Detection, User Interface

Soft-wear: identifying meaningful design spaces for wearable technology

Odette VALENTINE, Priti VEJA, Sharon BAURLEY*
School of Engineering & Design

EXTENDED ABSTRACT

Introduction

Wearable technology (also commonly referred to as Smart Clothing) encompasses a gamut of products that variously integrate electrical components, smart materials or computational devices into garments or accessories traditionally worn or carried upon the human body (as opposed to merely portable or hand-held devices). Wearable technology has been heralded as the 'convergent future of the electronics and clothing industries'[1] and an enabler of truly ubiquitous computing and hyper-connectivity.

Wearable technology promises the intimacy and social familiarity of clothing combined with the information access, transmission and density provided by mobile communications and micro processing. Where personal freedom of choice and the rights of the individual (whether genuine or illusionary) is a fundamental driving force in many societies today, the potential for producing and delivering highly personalised services and experiences and providing channels of expression via a wearable product seems highly desirable.

However the transition from fantasy to reality for wearable technologies has lagged the development of the underlying technologies and to-date failed to generate anything more than 'niche solutions and novelty items'[3]. This has in part been attributed to the multi-disciplinary nature of the products concerned and the vast operational differences between the clothing and electronics/computing/mobile communications industries – in terms of product development, manufacture and product lifecycles. However the real root of the problem has been a technology push as opposed to a user pull driving product development. Despite the user /individual being the central component of a wearable system – the user has not been at the centre of the design process for wearable technology.

The overall theme of the research is a uniquely, design-led, practice based exploration of the new relationships required between the designer and the user/consumer that will catalyse the development of wearable technology products that resonate with consumers equally on both functional and aesthetic levels and deliver meaningful benefits on an everyday basis. It will encompass the design (in conjunction with users via digital technologies) and production of novel modular garment platforms demonstrating a high level of integration of electronic textile sensors, circuits and actuators.

Approach

The initial research approach has been to identify needs/product spaces where design (specifically fashion design) can play a significant role increasing mainstream consumer acceptance of the form factors suggested by the limits of the technology, by adapting existing and creating new affordances of clothing. Underlying this approach is the belief that fashion objects can create cultural value alongside functional value for such products.

Clothes and other body adornments can be read as signs –e.g. indicating the sex or social class of the wearer but the signifier (the physical form of the garment) has no "inherent meaning."[5] However, recent considerations of fashion, particularly as material culture [4] have gone some way in reclaiming agency for fashion objects, putting them on a par with the social relations they were previously only thought to represent. As such fashion can be considered as "the outcome of a precarious marriage between the processes of creative authorship, technological production and cultural dissemination."[2]

This is not to say however that many fashion objects are consumed (or rejected) for anything other than largely their symbolic value (as opposed to utility value). The symbolic value is defined at that moment and ephemeral. We consume these symbolic values in an attempt to furnish our identity, but our postmodern identities today are not based on class identity as espoused by Veblen, Simmel and Bourdieu, but on personal identity.[6]

Considering fashion as a potential cultural conduit for the acceptance of wearable technology has led to a more holistic approach to defining the design spaces for product development. Instead of asking "what can we do with the technology" the question has to be "why would we want to do it?" By considering what advantages are offered by an on-body system and taking a user need orientated approach it is possible to avoid recreating a taxonomy based upon classification of specific pre-identified applications.
The initial survey has thus not only considered academic publications but commercial and non-commercial products and artefacts, e-textile proponents and communities outside of the academic realm involved in new design transactions around electronic textiles and wearable technology.

Findings/Results
A design framework has been developed from identifying the potential inputs, processing and desirable effects and functions of an on-body system. The focus has been on these latter outputs, and initial pathways to product applications have been formulated in the four areas of: communication, body performance, mental stimulation and safety/protection.

In addition it became apparent that new digital ecologies are evolving for human computer interaction which will facilitate the acceptance and desires for wearable technologies. These ecologies are being driven by the way in which individuals: connect, engage, interact and increasingly depend upon digital communications tools.

Conclusion / Discussion
The development of the framework has suggested that designing for context is as important as designing for function. It has also highlighted the ongoing role of the enthusiast (the DIY /hacker/amateur) in the development of wearable technologies and how this role draws upon traditional popular practices in both home electronics and home dressmaking. Development of the framework has also underlined the need of understanding acceptance factors for the user (e.g. control, trust, expectations, regulations, dependency) and as well as the product (e.g. sustainability, accessibility, usability, desirability).

References
[1] Ariyatum, B.(2005) *New conceptual model for design development of smart clothing*, Brunel University.
[2] Breward,C. (2003) *Fashion*, Oxford University Press pp15
[3] Dunne, L.(2010) "Smart Clothing in Practice: Key Design Barriers to Commercialization", *Fashion Practice: The Journal of Design, Creative Process & the Fashion Industry*, vol. 2, no. 1, pp.41–66.
[4] Miller, D. (2005) "Introduction" in *Clothing as Material Culture*, eds. S. Kuchler & D. Miller New York: Berg, pp1-19
[5] Steele, V. (1989), "Appearance and Identity" in *Men and Women: Dressing the Part*, eds. C. Brush Kidwell & V. Steele Washington: Smithsonian Institute Press, pp. 6-21
[6] Svendsen, L. (2006) *Fashion: A Philosophy*, Oxford: Reaktion Books Ltd

Keywords: wearable technology, fashion design, user centred, design framework, digital communications

Systems of Innovation in Saudi Arabia: Assessment of the innovation capabilities for enterprises based on the development of intelligent cities.

Abdulrhman ALBESHER

Brunel University

EXTENDED ABSTRACT

Introduction

With the dramatic shift toward knowledge-based economy as a nation competitive advantage, the financial and competitive pressures on firms to improve innovation capabilities are increasing. Therefore, it is crucial to understand the environment and the forces that affect the innovation performance. There is an acknowledgement on the crucial impact of innovation performance on the nation competitive advantage. Moreover, there are attempts to study and even model the relationship between the firms' performance and their macro-environment. For instance the work of Porter [1] on the clusters theory and the Diamond model, The work of Edquist [2] that studied the impact of the innovation processes on the economy performance and other works such as Storper [3], Pyke and Sengen-berger [4], Schumpeter [5], Lundvall [6], Piore and Sabel [7], Amin and Thrift [8], Dutta and Segev [9], Cooke [10] and Nelson, R. [11].

Innovation Systems studies focus on the understanding of how to best align the innovation environment with the requirements of the innovation network toward better innovation performance. Since the later is dynamic the former will require a sustainable development and an effective assessment criterion. As a result the innovation system (sectorial, regional or national) comprises three dimensions the innovation process, the elements of the innovation network and the environment that integrate the innovation system. These three dimensions have evolved vividly with the advancement of ICT and as a result of the globalization. For instance the shift of the perspective of the innovation process from a liner innovation system to systematic innovation system, the emerge of the virtual innovation network and the initiative to trigger the community interaction with the innovation environment utilising the edge technology of the ICT technology as in the concept of intelligent cities suggested by Komninos [12]. The Intelligent city is a new concept emerged as an attempt to improve nation's competitive advantage. The development of intelligent cities or what is also named knowledge cities as noted by Francisco [13] is based on several theories as shown in Fig.1.

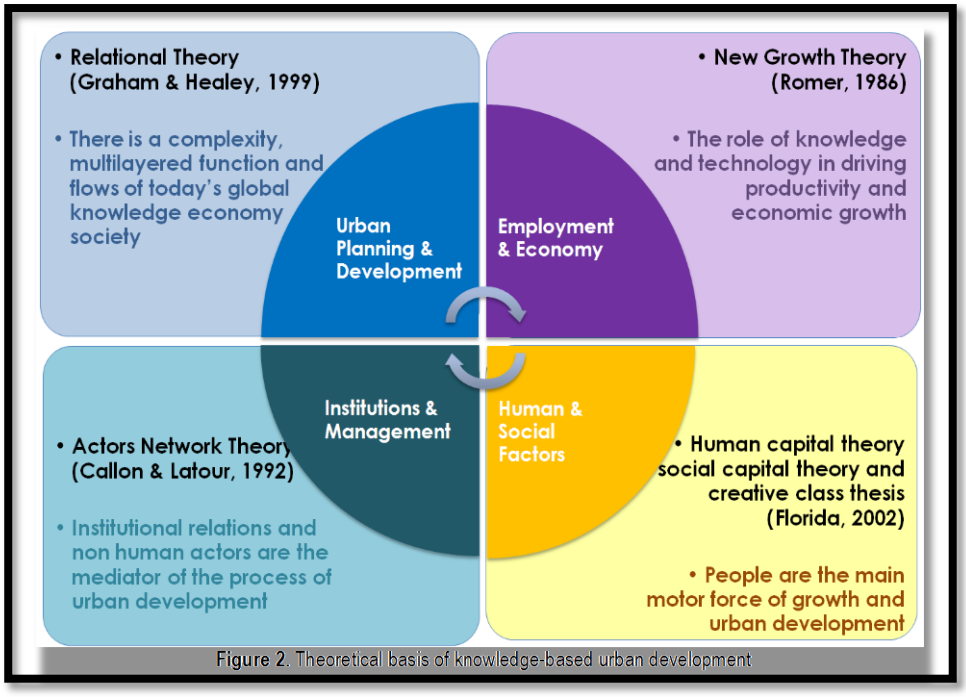

Figure 1: The theoretical bases for knowledge-based urban development

Source: Yigitcanlar, T. [14]

There are few attempts to propose a strategic framework for the development of intelligent cities. However the study of such development from at the firm level is limited.

Design/Methodology/Approach

This research attempt to contribute by proposing a research framework to better understand national competitive advantage based on the innovation capability. This will be used to research the innovation environment; the cluster architecture; innovation networks and entrepreneurship at the firm level. Saudi Arabia has committed to develop four intelligent cities from scratch based on a cutting-edge technology of ICT. Therefore the research will attempt to assess innovation systems in Saudi Arabia and the key factors that influence the momentum of the innovation performance including ICT and globalisation. The factors characterising the development level of the knowledge-based economy will be identified from a literature review that is drawn from the fields of innovation management; innovation systems, knowledge management, development of intelligent cities.

The assessment will consider four levels of the innovation systems comprising national; regional; cluster and firm level to assess their competitiveness capability. Since the ICT plays a critical role in the innovation systems as well as the development of intelligent cities. The IT and telecommunications industry provision for businesses will also be assessed in terms of service provision and performance. The study will compare the needs and service deployment for large firms and SMEs (small and medium enterprises).

Findings/Results

Expected in the middle of the 2012

Conclusion / Discussion

Expected in the end of the 2012

References:

1.Porter, M. (1990) The Competitive Advantage of Nations. Free Press, New York.
2.Edquist, C. (Ed.), 1997. Systems of Innovation: Technologies, Institutions and Organizations. Pinter, London.
3.Storper, M. (1992) The limits to globalization: technology dis- tricts and international trade. Economic Geography 68, 60–93.
4.Pyke, F. and Sengenberger, W. eds (1992) Industrial District and Local Economic Regeneration. Institute for Labour Studies, Geneva.
5.Schumpeter, J.A. (1942) Capitalism, Socialism, and Democracy. Harper, New York.
6.Lundvall, B.-A. (1988) Innovation as an interactive process: from user-producer interaction to the national system of innovation. In Technical Change and Economic Theory, eds.
7.Piore, M.J. and Sabel, C.F. (1984) The Second Industrial Divide. Basic Books, New York.
8.Amin, A. and Thrift, N. (1992) Neo-Marshallian nodes in glo- bal networks. International Journal Urban & Regional Research 16, 571–587.
9.Dutta, S. and Segev, A. (1999) Business transformation on the Internet. European Management Journal 17, 466–476.
10.Cooke, P., Urange, M.G., Extebarria, E., 1997. Regional innovation systems: institutional and organizational dimensions. Research Policy 4/5, 475–493.
11.Nelson, R. (Ed.), 1993. National Innovation Systems: A Compara- tive Analysis. Oxford Univ. Press, Oxford.
12.Komninos, N. (2006) „The Architecture of Intelligent Cities", Intelligent Environments 06, Institution of Engineering and Technology, pp. 53-61.
13.Carrillo, F. (2004). Capital cities: A taxonomy of capital accounts for knowledge cities. Journal of Knowledge Management. 8(5): p28-46.
14.Yigitcanlar, T. (2010) "Knowledge-based development of cities: a myth or reality?", Proceedings of Revive MTY forum 2010REMTY, pp. 1.

Keywords: Innovation Systems, Intelligent Cities, Innovation Networks, Knowledge Cites.

Electronic grocery shopping logistics in developing countries, Jordan as a case study: Home delivery reference framework.

Mohammad ALNAWAYSEH [1], Wamadeva BALACHANDRAN [2]
School of Engineering and Design / Brunel University

EXTENDED ABSTRACT

1. Introduction

1.1 General Background

In the era of globalisation, the Internet has been increasingly used to facilitate online business transactions, not only between different business entities, but also between business entities and consumers. One of the Internet business applications that received much attention in the last few years is Online Grocery Shopping [1] [12]. Electronic grocery shopping refers to consumers' ability to order groceries from home electronically (i.e., Internet) and the subsequent delivery of those ordered groceries at home [2] [3] [5]. OGS has many potential benefits to consumers, particularly in terms of better prices, large selection, convenience and time-savings. In addition, the retailers will ultimately reap significant benefits as it will lead to more efficient use of personnel and simplification of building infrastructure [13]. However, groceries are one of the most difficult objects of trade for electronic commerce: material flows are distinct from information flows, the number of frequent customers is large, and a purchase consists of many items. Furthermore, it is more local than global, for example, selling digital products that are easily accessible throughout the world.

1.2. Last mile logistics in e-commerce

The strategic importance of logistics and supply chain management is undoubted in academia and practice [4]. It is therefore not surprising that also in the context of e-commerce logistics plays a key role [6]. When it comes to selling non-digital products to consumers, the big challenge of “last mile logistics” arises. The last mile is the link between an online ordering process and physical product delivery [8] [9]. In contrast to store-based retailing, online shops have to organize product delivery to the consumers’ homes and not just to stores. Home delivery logistics in e-commerce, as it is so-called 'the last mile' of online shopping has been one of the key factors that leading to failures of pioneering dotcoms, also it may affect the customers intention to shop online, so it has received a significant attention and becoming a great challenge facing many e-retailers in many countries . However, there has been some doubt about the relevance of home delivery logistics in e-commerce for developing countries. Moreover, there are still a limited number of studies on the home delivery logistics of e-commerce in developing countries.

Last mile logistics in e-commerce consist of the following measures [10]: delivery time (e.g. duration, possibility to fix delivery date); reliability of delivery (e.g. availability of goods, order handling time); flexibility of delivery (e.g. concerning delivery date, delivery address); quality of delivery (e.g. accurate delivery, condition of delivered goods); and information (e.g. on delivery date, online tracking and tracing). [6] Proposed a computer model framework used to evaluate the last mile logistic strategy that has been chosen Fig. (1). In order to fulfil a certain level of last mile logistics services, an electronic retailer has to decide upon different measures. So an electronic retailer must for example select the geographical area it wants to serve [7] and the mode of delivery for the products (e.g. home delivery, mail dispatch, delivery to a pickup point etc.). Another important issue is outsourcing of last mile logistics as building an own logistics infrastructure is very cost intensive under most circumstances. Important parts of logistics services are also payment handling and management of returns. Finally, key issues of last mile logistics is determination of delivery fees and development of a pricing model for logistic services [9]. This applies not only for product delivery but also for additional services such as express delivery or delivery on Saturdays [11]. Various models of Grocery home delivery operations have been developed and are in use as illustrated in Fig. (2).

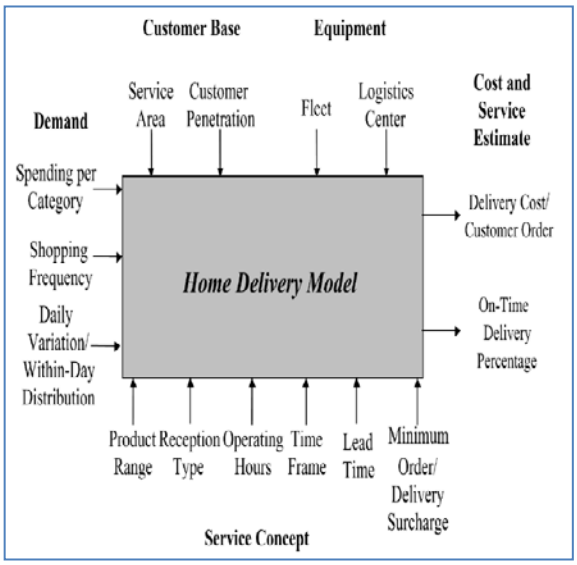

Figure 1. Home Delivery Framework

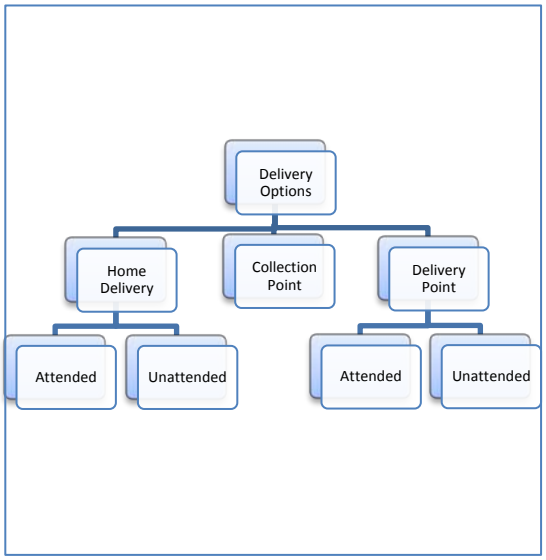

Figure 2. E-grocery Delivery Options

2. Research Methodology

This research will be carried out using many approaches; to identify the Jordanian customers and grocery retailer's perceptions about online grocery shopping as well as their perceptions about the delivery services, we already distribute surveys among them. These surveys were designed after obtaining a general and comprehensive understanding from the literature about online grocery shopping acceptance theories, benefits and barriers to adopt online grocery shopping in developing countries and home delivery service models.

Then to suggest an e-retailing strategy that will be used by the grocery retailers and used as a component for the desired overall home delivery reference framework we will use the obtaining results from the surveys, the statistics that we will collect from governmental and global sources and deep investigation about the Jordanian situation from different angles such as ICT infrastructure and government, retailers capabilities.

Finally, to evaluate the designed framework we will use one of the available scheduling and routing logistical solutions.

3. Conclusion

This research aims to propose a reference framework for home delivery service in Jordan (as an example of the developing countries) by assessing the adoption readiness level of Online Grocery Shopping (one of the e-commerce scenarios) among customers and retailers also by identifying the delivery service models that can operate in Jordan

References

[1]Belsie, L. (1998) A Mouse in the Bakery Aisle? The Christian Science Monitor, http://www.csmonitor.com.

[2]Burke, R.R., 1997. Do you see what I see? The future of virtual shopping. Journal of the Academy of Marketing Science 25, 352,360.

[3]C. Casper, "Online Grocers Rise Again," in Food Logistics, 2006, pp. 18-22.

[4]C. Müller-Lankenau, S. Klein, and K. Wehmeyer, "Developing A Framework for Multi Channel Strategies: An Analysis of Cases from the Grocery Retail Industry," in 17th Bled e-Commerce Conference, Bled, Slovenia, 2004, pp. 1-19.

[5]Ezlika Ghazali et.al, 2006, exploratory study of buying fish online: are Malaysians ready to adopt online grocery shopping?

[6]Hannu YrjoÈla , (2001) , Physical distribution considerations for electronic grocery shopping.

[7]Jan Holmström et.al. (2002), the way to profitable internet grocery retailing –six lessons learned.

[8]K. Boyer and G. T. M. Hult, "Customer Behavioral Intentions for Online Purchases: An Examination of Fulfillment Method and Customer Experience Level," Journal of Operations Management, vol. 24, pp. 124-147, 2006.
[9]K. Boyer, T. Hult, and M. Frohlich, "Ocado: An Alternative Way to Bridge the Last Mile in Grocery Home Delivery," in Case No. 602-057-1: European Case Clearing House, Wharley End, 2002.
[10] M. Punakivi and J. Saranen, "Identifying the success factors in e-grocery home delivery," International Journal of Retail & Distribution Management, vol. 29, pp. 156-163, 2001.
[11]M. Punakivi and K. Tanskanen, "Increasing the cost-efficiency of e-fulfilment using shared reception boxes," International Journal of Retail and Distribution Management, vol. 30, pp. 498-507, 2002.
[12]O'Connor, R., 1998. Europe trails U.S. in web grocery shopping. Chain Store Age 74 (6), 70, 72.
[13]Sherah Kurnia, 2004, Identifying e-Commerce Adoption Driving Forces and Barriers: The Case of the Indonesian Grocery Industry.

Keywords: Last mile logistics, home delivery, electronic commerce, online grocery shopping (OGS).

Key performance indicators within food supply chains- focusing on on-time delivery- How does this affect the supplier relationships?

Rebecca DECOSTER, Yolanda SILVERA*

School of Engineering and Design, Brunel University- Advance Manufacturing and Enterprise Engineering
**r.decoster@brunel.ac.uk*

EXTENDED ABSTRACT

Introduction

The purpose of this research is to develop an analytical model as well as a framework for the measurement of performance within supply chain partnerships. Most existing research on supply chain performance incorporates the use of quantitative analysis, but this has been found to not be entirely appropriate when it comes to the area of supplier relationships and supplier performance management. Most times these quantitative researches are designed by the customer (e.g. major food chains) and its acceptance and application is forced on the suppliers.

There has been the misconception that Supply Chain Management‘s main focus is on software and systems. It has long been thought that all that is required for an effective supply chain is an investment in technology, and allow the technology to operation within their processes. They are required to do nothing as the technology installed will do everything to make their supply chain efficient, and the company will eventually realise its return on its investment. But this way of thinking has been proving to be wrong especially with the advancement of new technologies and the globalisation of the business markets. The leading scholars in the area of supply chain management have also been emphasising this new reality, “when HBR convened a panel of leading thinkers in the field of supply chain management, technology was not top of mind.” People and relationship management were the dominant issues of the day” [1]. Effective Supply Chain Management (SCM) is based upon cooperation and understanding between all parties involved and of utmost importance to the success of this is the flow of information, both up- and down- stream within the supply chain. It is for this reason that effective relationships become absolutely important. This paper emphasises the relevance and importance of performance measurement in supply chains. This paper proposes the use of both quantitative as well as quantitative data analysis so as to allow the usage of this framework/ model to be applied within a wider context of the supply chain allowing for assessment of supplier relationships. The research will focus on the aspect of on time delivery as a performance indicator within supply chains and will also assess how this performance factor affects supplier relationships if not managed properly.

Design/Methodology/Approach

Using a combination of approaches, including the literature review approach as well as using the analytic hierarchy approach (AHP). These approaches are used to facilitate in the analysis of data to allow for future development of a comprehensive model that will allow for the determination of key performance indicators for supply chain and allow for the analysis of the impact of on-time delivery to the supplier relationship. The AHP method is a “hierarchical representation of a system” [2]. The approach also involves the use of questionnaire and the analysis of the results using the AHP method. Based on the analysis a framework/model will be developed to ascertain the important factors for performance management within supply chains and the determination of the importance of the key performance indicator, on time delivery.

Findings/Results

	High Performing Supplier	Average Performing Supplier	Low Performing Supplier	
On Time Deliveries	✓	✓	✓	Does Not Deliver On Time
Appropriate Communication	✗	✓	✗	Non-Communicative
Share Similar Values - e.g. Environmental Issues	✓	✓	✓	Does Not share Similar Values
High Quality Products	✓	✗	✗	Low Quality Products

The table above represents a sample of a repertory grid which was derived from a questionnaire developed to ascertain how both suppliers and their customers viewed the particular areas of focus (on time deliveries, communication etc), and how important were these areas of focus to development of good supplier/ customer relations. From the assessment of the above grid and questionnaires it was found that all paries (both suppliers and retailers) had bought into the importance of delivering items on time.

Conclusion / Discussion

This paper is intended to introduce the use of both qualitative and quantitative methods of research such as the use of the Analytic Hierarchy Process method, as well as the use of the literature review approach to determine performance measurements in supply chains. It has been shown from previous research that "AHP is useful to make more precise business decisions that may help a company to achieve a competitive edge" [3]. It is important to understand the key performance indicators of supply chains and to ensure that the most appropriate performance indicator is selected for focus so as to ensure that effective supplier relationships are developed.

References

[1] N. Burt, William Copacino, Chris Gopal, *et al*, *Harvard Business Review on Supply Chain Management* 2006; pp. 65.

[2, 3] Eddie W.L Cheng, Heng Li, *Measuring Business Excellence* 5,3 2001, pp 30-36

Douglas M. Lambert, A. Michael Knemeyer, John T.Gardner: *Building High Performance Business Relationships.* SCMI: Florida, 2010; pp 10.

Keywords: Analytical Hierarchy Approach (AHP), supply chain management, performance indicators, supplier relationships

Energy efficient routing using multiple heterogeneous-radios in mobile ad-hoc networks

Hadi Noureddine[*], Shahbaz Khan[+], Hamed Al-Raweshidy[*]

[*]Department of Electronic and Computer Engineering, Brunel University, London, UK
[+] University of Engineering & Technology, Peshawar, Mardan Campus, Pakistan

EXTENDED ABSTRACT

Abstract—the objective of this work is to reduce the energy consumed by the wireless nodes during the dissemination process of the routing information in highly dense Mobile Ad-hoc Networks. We propose a Heterogeneous Multi-Radio (HMR) routing scheme. The key concept behind HMR is to split the data and routing control traffic over two different radio interfaces.

Introduction

Mobile ad hoc networks (MANETs) consist of a collection of wireless hosts spread across a geographical area, connected to each other via wireless links in the absence of any sort of infrastructure. Each wireless host can directly communicate with all the hosts located within its transmission range. When the destination is beyond the source node coverage, multi-hop communication takes place to successfully relay the data traffic through the intermediate hosts to the destination. The mobility feature of MANET causes link breakage that overload the network with update messages to maintain the end-to-end routes. The high control traffic required for maintaining routing information degrades the protocol performance and increases the utilization of the network resources. Since MANET devices are generally power and memory constraint, route discovery and maintenance operations can impose serious limitations on the protocol performance, especially when link breakage occurs very frequently. Exploiting multiple radios for improving the performance [1, 2] of routing protocols is not a new idea. The usage of multiple radios is scenario specific and several techniques have been proposed – each focusing on optimization in a specific scenario. However, most of the proposed techniques use homogeneous multiple radios. There are a few papers which proposed the idea of using multiple heterogeneous radios [2- 4]. Our work is most relevant to the solution proposed in [3], wherein the concept of multiple heterogeneous radios of IEEE 802.11 standard is used. In normal operation, a primary IEEE 802.11a radio is used in combination with a reactive routing protocol. In case of link failures the system resorts to a secondary optional route which is maintained using IEEE 802.11b interface and which relies on a proactive routing protocol. The secondary route is used for control and management purposes. The secondary radio operates at lowest transmission rates and thus longer transmission ranges. However, this approach does not exactly exploit the benefits associated with the idea of using heterogeneous radios. From energy efficiency perspective, both the radios use the same transmission power and thus would impose considerable overhead for route maintenance using a proactive routing protocol. There are various research challenges associated with routing using heterogeneous radios [2], [4] and [5].

HeterogeneousMulti-radio Routing

Assumption: let us consider G (V, E) is the graph representing the network when the edges V and E are 802.11 connection-based. We assume that by switching all nodes to the low power radio interface (e.g.802.15), the corresponding graph G’ (V, E’) of the network will still include all the nodes. In other words, $\forall$ n$\in$V,$\exists$ an edge e $\in$E’ , where n is a part of link.

The assumption above allows the flooding scheme employed by the routing protocol to propagate routing control traffic to reach all the nodes in the network through both interfaces. Routing information that is transmitted in the entire network is stored in the routing table, on which the node relies to determine the end-to-end route..

The proposed scheme aims to improve the resource utilization and more specifically the energy consumption of the wireless node by reducing the power consumed during the dissemination process of the routing control traffic. The platform can be applied to any routing protocol especially the proactive type that periodically injects control traffic in the network. The routing scheme consists of a Cross-layer Interface Module (CIM) connected to the MAC layers of both radio interfaces, as illustrated in Figure 1.

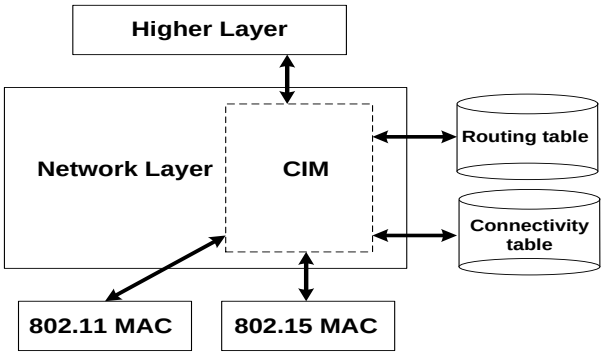

Figure 1: The CIM module

CIM controls the ingoing and outgoing traffic for both interfaces. The CIM associated corresponding traffic (whether is a data or a routing traffic) to the specific interface. Data traffic coming from the application layer will be directed to the 802.11 MAC, while the 802.15 MAC handles the routing traffic directed by the module.

Analysis

In this section we analytically evaluate the proposed Heterogeneous Multi-Radio (HMR) Routing scheme to verify its performance against the Single Radio (SR) Routing scheme. Considering $\boldsymbol{E_{UWB}}$, $\boldsymbol{E_{WLAN}}$ as the energies consumed by a wireless node to forward an update packet over UWB and WLAN radio interfaces respectively. The energies required for an update message to be propagated in the entire network over UWB and WLAN interfaces are expressed by $\boldsymbol{N * E_{UWB}}$ and $\boldsymbol{N * E_{WLAN}}$ respectively**.** Consequently, the energies consumed by all the nodes in the network to update their information over the interfaces UWB and WLAN are $\boldsymbol{N^2 * E_{UWB}}$ and $\boldsymbol{N^2 * E_{WLAN}}$ respectively. Where $\boldsymbol{N}$ is the number of the wireless nodes in the network.

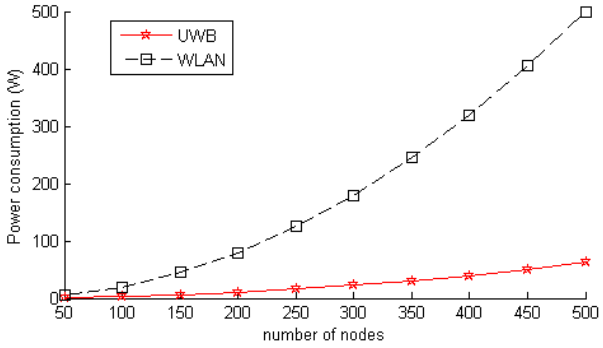

Figure 2: The transmitted power consumption in (W) of the WLAN and UWB interfaces vs. the number of nodes.

$$\boldsymbol{P_{HMR} = P_{WLAN} + P_{UWB}}$$
$$\boldsymbol{P_{SR} = P_{WLAN} = T^*(P_{TW}C_{TW} + P_{RW}C_{RW} + P_{IW}C_{IW})}$$

Where

$$\boldsymbol{P_{WLAN} = T^*(P_{TW}C_{TW} + P_{RW}C_{RW} + P_{IW}C_{IW})}$$
$$\boldsymbol{P_{UWB} = T^*(\alpha P_{TX} + \beta P_{RX} + \gamma P_{Idle}) = P_{WLAN} + T^*(\alpha\ (P_{SYN} + E_p R_p) + \beta\ (P_{COR} + P_{ADC} + P_{LNA} + P_{VGA} + P_{GEN} + P_{SYN}) + \gamma P_{idle})}$$

Where C_{TW}, C_{RW}, C_{IW} and C_{SW} represent the power consumption in TRANSMIT, RECEIVE, IDLE and SLEEP states respectively, while P_{TW}, P_{TW}, P_{RW}, P_{IW} and P_{SW} are the probabilities that the WLAN card is in any of the respective communication state. P_{TX}, P_{RX} and P_{Idle} are the power consumptions of the

UWB transceiver in transmit, receive and idle state respectively, while α, β and γ are the probabilities that the UWB interface is in any of the respective communication state. Let the probabilities that both the WLAN and UWB interfaces are in any of the three states mentioned earlier, to be as follows: $P_{TW} = 0.4$ (0.1 for control traffic and 0.3 for data), $P_{RW} = 0.4$ (0.1 for control traffic and 0.3 for data), $P_{IW} = 0.2$. Therefore, $\alpha = 0.1$, $\beta = 0.1$ *and* $\gamma = 0.8$.

Table 1: power consumptions parameters of WLAN interface [6]

State	Power (w)
Transmit	2
Receive	0.9
Idle	0.8

Table 2: Power Consumption parameters of the UWB interface [9, 10]

Component	P_{SYN}	P_{ADC}	P_{GEN}	P_{VGA}	P_{LNA}	P_{COR}
Power(mW)	30.6	2.2	2.8	22	9.4	10.08

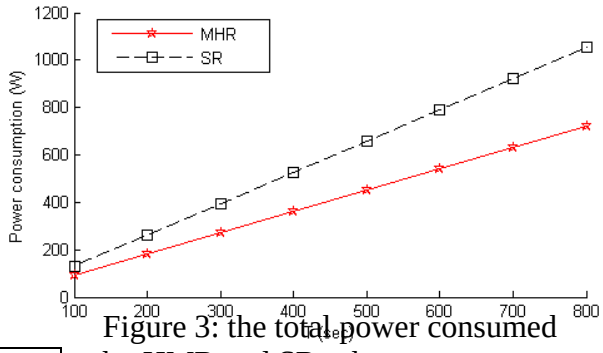

Figure 3: the total power consumed by HMR and SR schemes

Figure 3 illustrates the total power consumption of the single and multi radios routing schemes for different time durations T, showing a significant power saving of the MHR scheme as compared to the single radio routing.

Conclusion

In this letter, we have proposed a novel routing platform for highly dense mobile ad-hoc networks using heterogeneous multi-radio routing scheme. The proposed scheme is demonstrated to be a green radio routing solution that can significantly reduce the power consumption of the wireless nodes, increasing therefore the network and the nodes' battery lifetime.

References

[1]A.Farag´o and S.Basagni, "The effect of multi-radio nodes on network connectivity—a graph theoretic analysis". In: IEEE International Workshop on Wireless Distributed Networks (WDM). IEEE, Los Alamitos (2008).

[2]R. Draves, J. Padhye, B. Zill, Routing in multi-radio, multi-hop wireless mesh networks, in: ACM Annual International Conference on Mobile Computing and Networking (MOBICOM), 2004, pp. 114–128.

[3]W. Yoon, and N. Vaidya, "Routing exploiting multiple heterogeneous wireless interfaces: A tcp performance study". Computer Communications, vol 33, no 1, 2009.

[4]Vartika Bhandaria, Nitin Vaidya, Heterogeneous Multi-Channel Wireless Networks: Routing and Link Layer Protocols, Mobile Computing and Communications Review, Volume 12, Number 1.

[5]P. Bahl, A. Adya, J. Padhye, and A. Wolman, "Reconsidering Wireless Systems with Multiple Radios". ACM CCR, Jul 2004.

[6]Atheros Communications, "Power consumption and Energy Efficiency Comparisons of WLAN products,"
www.atheros.com/media/resource/resource_15_file2.pdf

[7]T. Wang; W.Heinzelman, A.Seyedi, "IEEE International Conference onCommunications, 2009. ICC '09", p.p 1-5, 2009.

[8]G. Lampropoulos, et. al. "A power consumption analysis of tight-coupled WLAN/UMTS networks", In Proceeding of IEEE PIMRC 2007. IEEE 18th International Symposium, pp. 1-5, 2007.

[9]B. Verbruggen, J. Craninckx, M. Kuijk, P. Wambacq, and G. Van der Plas, "A 2.2 mW 5b 1.75 GS/s folding flash ADC in 90 nm digital CMOS," Proc. ISSCC, 2007.

[10] A. Medi and W. Namgoong, "A high data-rate energy-efficient interference-tolerant fully integrated CMOS frequency channelized UWB transceiver for impulse radio," *Proc. JSSC*, 2008.

Estimation Primary User Localization using Cognitive Radio Networks

Nazar RADHI*, H.S.AL-RAWESHIDY

School of Engineering and Design, Brunel University, Uxbridge, Middlesex, UK

EXTENDED ABSTRACT

Abstract—The position awareness of the primary user is one of the necessary features of cognitive radios. The Location information of the primary user in cognitive radio can be exploited to help the communication between secondary users outside the transmission coverage area of primary transmitter or to track the primary users. A cognitive radio network based localization scheme is considered in this paper employs received signal strength (RSS) method to estimate the location and effective isotropic radiated powers of the transmitter source emitting this signal. In our study the simulation result for RSS-based localization show the impacts of number of sampling, nodes, sigma variable in the shadowing channel form on mean square error for position estimation and average power estimation error were demonstrated.

I. INTRODUCTION

Cognitive radio is a promising concept for the realization of smart and advanced wireless technology. One of the main characteristics of cognitive radio is to consolidate context awareness such as waveform, spectrum environment, location and power. A cognitive radio is a smart radio that knows what services are available and interested, and how to find these interested services [1]. On of the main cognitive radio objectives are to detect and reuse the uncopied primary user spectrum bands exploit spectrum more efficiently.

The Cognitive Radio in communication system is defined as a radio that is aware of their environment and based on the information they can make decision about their radio operating [2]. The location information may or may not contain of the environmental information. Additionally, information of the location related to communication systems is considered as definition of cognitive radio. Meanwhile, the position information of the primary users can be helpful for communication between cognitive radios [3]. Also, position information can be used to track the primary users, the reason of that to allocate the secondary users at distance where the detect the exist of the primary transmission signal well out side the primary users transmission coverage area to avoid harmful interference [4].

In this paper we propose RSS-based localization in cognitive radio network to determine the position of primary transmitters. The number of cognitive nodes and primary transmitter are deployed and there is one cognitive node uses as decision maker which is collected the averaged RSS values from the cognitive nodes and the location of the nodes and, then applies the RSS-based localization method.

Furthermore, some of the location estimation techniques require knowledge of the effective isotropic radiated powers of the transmitter emitting the primary signal. Because of effective isotropic radiated powers of the primary signal source is unknown that can be lead to limitation in using this technique for system. This explains the idea behind using the RSS-based localization in the proposed cognitive radio network based location estimation scheme. This localization scheme dose not requires the effective isotropic radiated powers of the transmitter emitting the primary signal [5]. In our study the position and average power estimation are investigated using RSS-based localization method in the proposed cognitive radio networks, which were implemented in using radio frequency sensor networks [6].

The paper been organized as follow: section II introduces related work about location estimation schemes. The proposed model to be used in this investigation is discussed in section III. Section IV reports on simulated implementations and analyses of the proposed scheme's results. In Section V, concluding remarks and recommendation for future work.

II. INTRODUCTION

In a cognitive radio system, there are two types of users, user has priority to access the spectrum is called the primary user and the user has opportunity to use uncopied bands that not used by primary users is called secondary user. Meanwhile, to determine these uncopied spectrum bands, the secondary users nodes apply spectrum sensing techniques to use this band for communication. Figure 1 shows the network configuration proposed in [5],[6]. In this configuration of network, it is assumed that the patterns of radiation of the transmitter antennas omni-diraction of azimuthally. In this method there are at least four cognitive radio nodes, their positions are known, the RSS from primary transmitter signal source must be measured. Since every cognitive radio node sends its position information and its RSS measurement value to all other cognitive radio nodes, location procedure can be applied on any node.

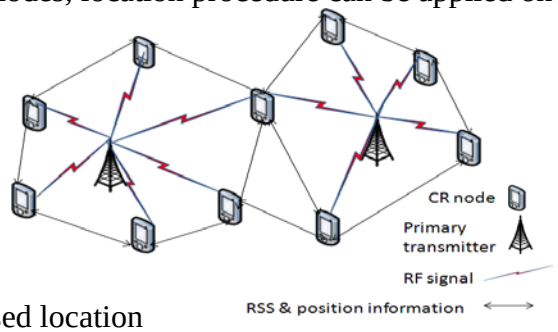

Fig. 1. A Network Configuration for RSS-based location

From [5],[6] the ideal value at the i^{th} cognitive radio node is equal to the ideal received power $P_{r,i}^{ideal}$.

$$P_{r,i}^{ideal} = C_i \frac{P_t}{d_i^{\beta}}, \qquad i = 1,2,\ldots..N\ldots \quad (1)$$

The least squared method can be used to solve this equation. The solution of equation (3) is provided the position of the primary transmitter and its isotropic radiated power. Subsequently, the $(P_t)^{2/\beta}$ value is found. The obtained x, y and P_t quantities are termed as x_{est}, y_{est} and P_{est} respectively. The shadowing effect is using the log-normal path loss model. Given as;

$$P_{r,i} = C_i \frac{P_t}{d_i^{\beta} S_i} \qquad i = 1,2,\ldots N \qquad \ldots. \qquad (4)$$

When $S_i = 10^{0.1X_i}$ is a long-normal random variable and variable of a Gaussian random is X_i.

With mean is zero and variance σ^2 and the other parameters are as mention earlier in equation 3. To reduce the unwanted effect of shadowing, RSS value which is $P_{r,i}$ values are averaged as;

$$P_{r,i}^{ideal} \approx \frac{1}{M} \sum_{j=1}^{M} P_{r,ij} \qquad \ldots. \qquad (5)$$

The total number of samples is M and $P_{r,ij}$ is the j^{th} sample RSS value at the i^{th} cognitive radio node in dBm.

III. SIMULATION MODEL AND RESULT

Figure 2 shows the scenario of the cognitive radio nodes and primary transmitter are deployed randomly over interest area. In additional, the location and effective isotropic radiated powers of the primary transmitter's signals are estimated. The assumptions of the simulation scenario are; The position of the nodes is calculated and a node is determined as decision maker, RSS values at each cognitive radio node due to the transmitters are measured and The distances between the nodes are more than the half of the wavelength of the primary transmitter signal.

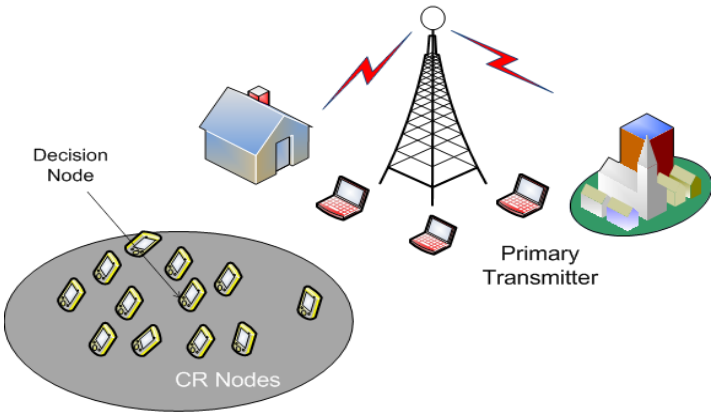

Fig. 2. Isotropic radiated power and position estimation of RSS-based location method

The simulation model as shown in figure 2 is created in MATLAB, the calculation of node position and RSS measurement are assumed to be given. In this model RSS values are averaged to reduce the unwanted shadowing effect.
The RSS-based location method is implemented by using equation (3). In particularly, assumed that values of C_i = 1 for all cognitive radio nodes, path loss β = 2, and the configuration of the simulation deploys the cognitive radio nodes in location system as (700, 200)m, (800, 150)m, (100, 200)m, (300, 250)m, (200, 400)m, (1000, 500)m, (600, 400)m (700, 400)m, (150, 550)m, (400, 700)m, (150, 50)m, (800, 150)m, (500, 250)m, (100, 300)m, (150, 150)m, from node 1 to 15 respectively.

To evaluate the performance of the RSS-based location method, mean square error (MSE) and average power estimation error (APE) are used. In particular, we investigate the performance over various cases of the number of cognitive radio nodes, number of samples and σ (standard deviation of the Gaussian random variable used in the shadowing model).
Simulation of location is implemented to isotropic radiated power and estimate the position of primary transmitter which are assumed that power of primary transmitter is 1 W and position is (1400m, 1000m). All results are obtained by 10000 times of simulation running and averaging the result.

A. Number of cognitive radio nodes effects

The number of cognitive radio nodes is investigated in proposal model and figure 3 shows the relation between the position estimation MSE versus number of cognitive radio nodes for different values of samples number when σ =3. In figure 4, the plots are shown the number of cognitive radio nodes effect on average power estimation error APE for different value of σ where the samples number is 300. In both figures, it shows that when the number of cognitive radio nodes configuration in the location process increases, the error positions and average power estimation error are decreases.

B. Standard deviation Sigma effects

In investigate the shading effects the RSS values measured, figure 5 shows the position estimation MSE versus standard deviation σ for the number of samples of different values when there are four cognitive radio nodes configuration in the location process. In figure 8, shows the effects of changing the standard deviation (σ) on the averaged power estimation error APE for different numbers of cognitive radios when the samples number is 300. Meanwhile, both figures show that when standard deviation σ increases, the position estimation error and average power estimation error increases because the effect of shadowing becomes strict.

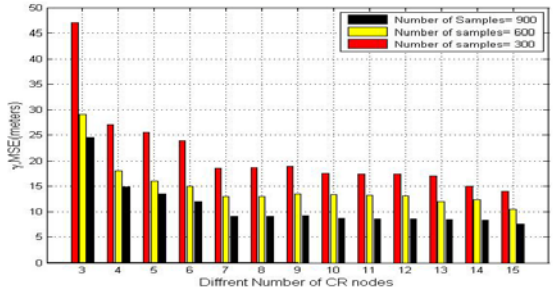

Fig. 3. Results of simulation for MSE versus Number of CR nodes (Different Number of Samples & Sigma=3)

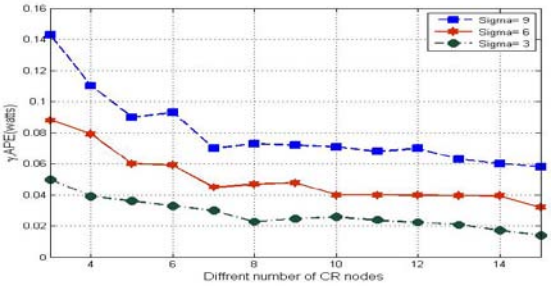

Fig. 4. Results of Sumilation for APE versus Number of nodes(Numbers of sigma & Samples Number=300)

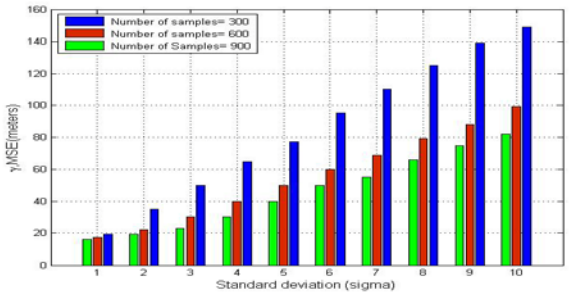

Fig. 4. Results of Simulation for MSE versus Sigma (Different Number of Samples & CR nodes=4)

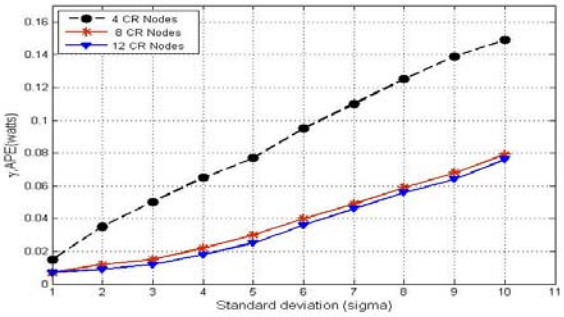

Fig. 6. Results of Simulation for APE versus Sigma (Different Number of CR nodes & Samples Number=300)

IV. CONCLUSIONS

Our study is proposed for location scheme to estimate the position and isotropic radiated powers effective of the imitation transmission from primary transmitters. Different number of cognitive radio nodes, number of samples and stander deviation of the Gaussian variable in the shadowing model were simulated to study the effects on the performance of the location method. In the proposed technique, the simulation result showed that performance of average power estimation error and the position estimation error can be affected in a similar manner by the number of cognitive radio nodes, samples and stander deviation. For future study, a range-free location scheme could be used to conclude the position of CR nodes. Received signal strength measurements could be determined using a received signal strength indicator circuit.

REFERENCES

[1]J. Mitola and G. Q. Maguire, “Cognitive Radio: Making Software Radios more personal,” IEEE Pers. Commum, vol. 6, no. 4, pp. 13-18, Aug. 1999.
[2]J. Grosspietsch, D. Maldonado, K. Nolan and J Poson,”SDR for Cognitive radio Definitions and Nomenclature” report document SDRF, 10/09/2008.
[3]D. Gong, Z Ma. Y. Li, W. Ches, and Z. Cao, “High geometric range free localization in opportunistic cognitive sensor network,”IEEE International Pers Commun, pp. 139-143, 2008.
[4] J. MA, G. Ye Li, and B. Juang, “Signal processing in Cognitive Radio,” IEEE Pers, vol. 97, no. 5, pp. 805-823, 2009.
[5] S. Kim, H. Jeon and J. Ma, “Robust transmission Power and position in Cognitive Radio,” IEEE Pers Commun, pp. 1-6, 2008.
[6]L. Liu, Z. Li and C. Zhou, ”Back propagation-Based Cooperative Localization of Primary User for Avoiding Hidden-Node problem in Cognitive Networks,” IEEE Journal of digital Multimedia Broadcasting, Vol. 2010, pp. 1-9, April 2010.

A novel efficient flooding algorithm based on node position for mobile ad hoc network.

Sofian HAMAD*, Hamed Al-Raweshidy

Department of Electronic and Computer Engineering

EXTENDED ABSTRACT

Abstract- Flooding is widely used by the routing protocols as the operation to propagate update packets in the network. The basic flooding is shown to cause high retransmissions, packet collisions and media congestion that can significantly degrades the network performance. Knowing the geographical position of the mobile nodes can assist the protocol to reduce the number of retransmissions, enhancing therefore, the protocol performance. In this paper, we propose an Efficient Flooding Algorithm that makes use of the nodes' position to rebroadcast the packets and efficiently disseminate the control traffic in the network. The proposed algorithm is applied on the route discovery process of Ad-hoc On Demand Distance Vector (AODV) protocol to reduce the number of propagating Route Request (RREQ) messages. The simulation results shows that our scheme reduces the routing overhead of AODV protocol by up to 36%.

I. Introduction

There has been a growing research activity on wireless Mobile Ad-hoc Networks (MANETs) over the past years due to their potential effectiveness in civilian and military applications. MANETs are formed dynamically by an autonomous system of mobile nodes that are connected via wireless links without using an existing fixed network infrastructure or centralized administration [1]. The nodes are free to move randomly and organize themselves arbitrarily; thus, the network's wireless topology may change rapidly and unpredictably. Nodes in MANETs act as end points as well as relay routers to forward packets for other nodes in a wireless multi-hop environment. One of the fundamental challenges in MANETs and especially in a multi-hop scenario is the design of dynamic routing protocol that can efficiently establish routes to deliver data packets between mobile nodes with minimum communication overhead while ensuring high throughput and low end-to-end delay.

Many routing protocols have been proposed for MANETs over the past few years [2-7]. In general, the routing protocols for MANETs fall into two categories [8] i-e proactive and reactive routing protocol. Proactive routing protocols, such as DSDV [5] and OLSR [9], attempt to maintain consistent and up-to-date routing information tables on each node to every possible destination in the network by periodically exchanging routing table information. On the other hand, in on-demand routing protocols, such as AODV [2] and DSR [3]; routes are only discovered when needed. Each node maintains a route for a destination without periodic routing table exchanges or full network topological view. Additionally, there are hybrid protocols that combine the best features of both proactive and on-demand protocols. In such protocols, each node maintains routing information about its zone using proactive routing, but uses on-demand routing outside the zone [7]. The periodic routing information updates due broken links are inherent in proactive routing protocols can lead to a heavy control overhead during high mobility. Hence, these protocols surfer from excessive routing control overhead and therefore are not scalable in MANETs, which have limited bandwidth and whose topologies are highly dynamic.

In conventional on-demand routing protocols [2-4], a node discovers routes to a particular destination, by broadcasting a Route Request packet (RREQ). Upon receiving the RREQ, the node checks whether or not the packet has been previously received. In case of packet has been received previously the node will drop the packet, otherwise the node will checks whether it has a route to the destination, if yes, the node will send back Route Reply (RREP) to the source node; otherwise the node will rebroadcast the RREQ to its immediate neighbors until the destination is found. This method of route discovery is referred as blind flooding. Every mobile node rebroadcasts one copy of received RREQ, so the maximum number of rebroadcasts is equal to N – 2, where N is the number of nodes in the network.

This can potentially lead to excessive redundant retransmissions therefore high channel contention and causing excessive packet collisions in dense networks. Such a phenomenon is refried to as broadcast storm problem [10], which significantly increases network communication overhead and end-to-end delay [10, 11]. To reduce the impact of blind flooding, a number of broadcasting techniques have been suggested in [10-12].

II. **Proposed Method**

The aim of this work is to design an efficient flooding algorithm for mobile ad hoc network to improve the network performance by eliminating the redundant retransmission, therefore reducing the chances of contention and collision among the neighboring nodes. This can be achieved by involving a specific set of nodes in the dissemination process of the RREQ. The key concept of the proposed algorithm is to partition the radio transmission range of the mobile node into four zones. Then, one node per zone is selected to forward the RREQ. The selection process is performed by determining the closest node to the edge of the zone as shown in Figure1 to provide more coverage area. The sender attaches the address of the Candidate Neighbor to Rebroadcast the RREQ (CNRR) into the RREQ field. Any neighbors when received the RREQ it will check if the sender select it as forwarder node or not, if so, it will partition its transmission range and select a new set forwarder nodes and attach them into the RREQ and rebroadcast the RREQ, otherwise it will drop the RREQ. We assume in this work that every node is able to obtain its geographical position. Besides that, every node shares its position information with its direct neighbor through the HELLO message mechanism.

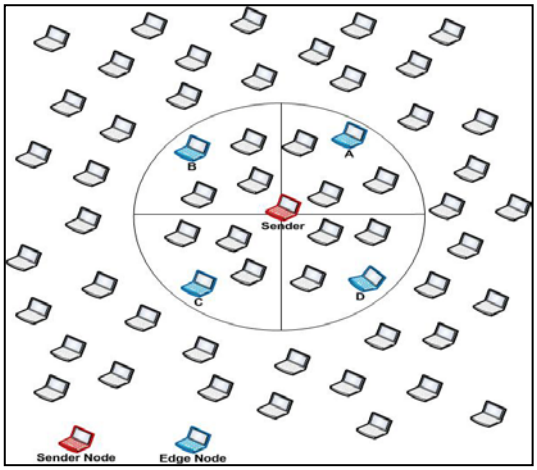

Figure 1: Divide the transmission range and locate new RREQ packet each neighbor in the right Zone. side.

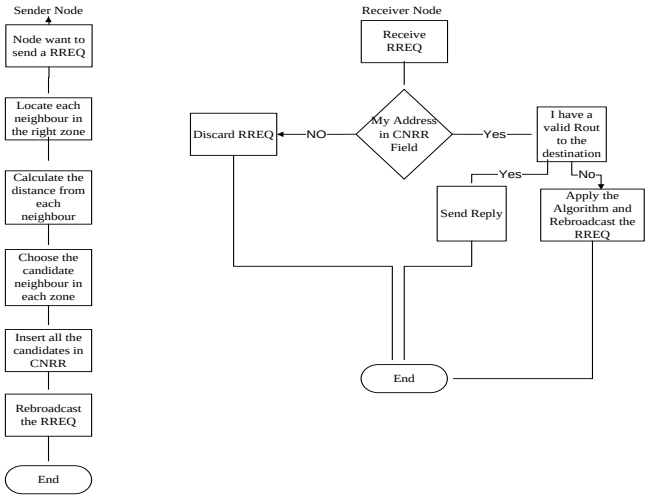

Figure 2: Flowchart of processing a on the Sender side and Receiver

For instance, Figure. 1 illustrates an example of how to partition the transmission range into four zones. To locate each neighbor in the right zone we follow the bellow equation:

S = Sender Node

If: $S_x \leq A_x$ *and* $S_y \leq A_y$ *)* (1) Then we can locate node A inside Zone1 of node S.

Else if: $S_x > B_x$ *and* $S_y \leq B_y$ (2) Then we can locate node B inside Zone 2 of node S.

Else if: $S_x \geq C_x$ *and* $S_y > C_y$ (3) Then we can say node C inside Zone 3 of node S.

Else: $S_x < D_x$ *and* $S_y < D_y$ (4) Then we can say node D inside Zone 4 of node S.

After locate each neighbor in the right zone, and then calculate the distance from the sender node to each neighbor according to bellow equation:

$$Distance\ (S, N) = \sqrt{(S_x - N_x)^2 + (S_y - N_y)^2} \quad (5)$$

According to equation 5, node S will be able to know the distance from each neighbor.
So now node S locates each neighbor in the right zone from its perspective in addition the distance from each neighbor. To choose the candidate neighbor in each zone, node S will choose the farther node in each zone. The final step is to insert the four candidates neighbors into CNRR (Candidate Neighbor to Rebroadcast RREQ) inside the RREQ field which has been modified.
At the end, node S will send the RREQ which now contains four candidates' neighbors (A, B, C and D).
On the reception of RREQ, each node checks CNRR field inside RREQ and the decision of rebroadcast is taken based on the inclusion of its network address in the list. If the node finds its address inside this field that means rebroadcast the RREQ otherwise discard it.
Nodes A,B,C and D when receive the RREQ, they check CNRR field and since they find themselves inside the RREQ therefore they do the same as node S and rebrodcast the RREQ.
We noticed that in MANETs all the nodes move randomly with high mobility, the farthest neighbours may move out the communication range with a high probability. Also, due to the collisions, interference and decrease of the channel capacity with high distance between the sender and receiver; some farthest neighbours in the candidates list may fail to receive the broadcast RREQ successfully. We deal with these problems by mechanisms in which the candidate nodes are selected based on their distance from the source node. A source node can select only a candidate node among the neighbours if the distance between them is less than 80% of the source transmission range.

III. **Performance Evaluation**

In order to evaluate the performance of our EF-AODV protocol, we simulate the proposed mechanisms using NS2 Simulator [14].

A. Simulation Environment

In our simulations, the MAC layer runs on the IEEE 802.11 Distributed Coordination Function (DCF). The bandwidth set to 2 Mbps and the transmission range is set to 250 m. The evaluations are conducted with a total of 150 nodes that are randomly distributed in an area of 700m x 700m. We use Random Waypoint to model node mobility. In Random Waypoint model, each node starts to move from its location to a random location with a randomly chosen speed from minimum speed equal to 5 and maximum speed equal to 30. In each test, the simulation lasts for 600 seconds. The size of each Constant Bit Rate (CBR) packet is 1000 bytes and packets are generated at the fixed interval rate of 4 packets per second. 10 flows were configured to choose a random source and destination during the simulation.

B. Performance Metrics

Four metrics were used to evaluate our EF-AODV and AODV protocol:

- Packet Delivery Ratio: The ratio of the data packets succeed to deliver at the destinations to those generated by the CBR sources.
- Total End-to-End Delay: This includes all possible delays caused by buffering during route discovery and link recovery phase, queuing at the interface queue, retransmission delays at the MAC, and propagation and transfer time.

C. Results and Discussion

Here we examine five performances of EF-AODV and compare it with AODV protocol. The results of simulation experiments demonstrate that EF-AODV indeed has more advantages and improves the performances of classic AODV.

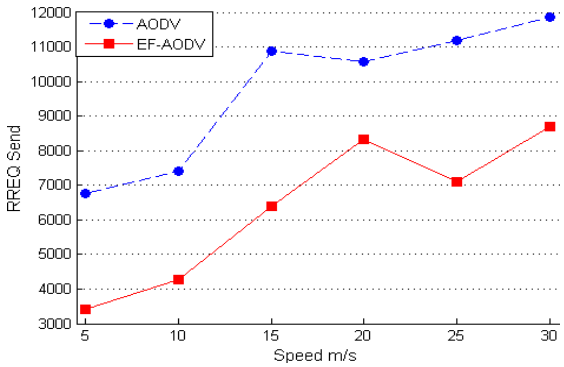

Figure 4(a): number of Rebroadcast RREQs vs Speed

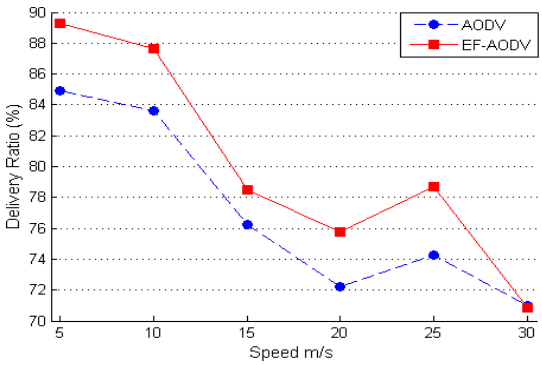

Figure 4(b): Packet Delivery Ratio vs Speed

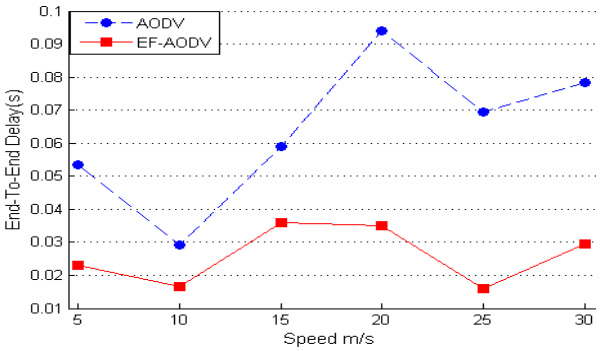

Figure 4(c): Total End-To-End Delay vs Speed

Rebroadcast:

In AODV, a mobile node rebroadcasts all the RREQ that are received for the first time if it doesn't have a valid route to the destination. Therefore, there are N-1 possible rebroadcasts, where N is the total number of nodes. In EF-AODV, each node decides to rebroadcast or not according to our algorithm also we care and maintain the same level of reachability. Fig. 4(a) show when mobility increase, more route requests are generated and some of them may be unsuccessful to reach their destinations. Such failures cause another round of transmission of route request packets.

Packet Delivery Ratio:

Fig. 4(b) represents the comparison of Packet Delivery Ratio and we can see that EF-AODV outperforms AODV. The reason is that with high mobility EF-AODV updates the position of the nodes by exchanging of HELLO messages that lead to update the candidate node in the field of CNRR, in contrast AODV creates route without knowing the position of its neighbours that lead to more redundant messages which affect the performance for all network in term of packet delivery ratio, throughput, delay and overhead.

Delay:

In fig. 4(c), we record the start time of a packets as well as the time when the packets reach the destination. The difference between these two values is used as the End-To-End delay. The effect of sending rebroadcast RREQ leads to collisions and contention for channel which leads to the packet delay until the channel is free and no collision occurs. The number of total packets transmitted in the channel has a important impact on the End-To-End delay. If the number of packets is high, then the number of collisions is also high and more retransmissions are needed. As a result, fewer packets lead to lower delays.

V. **Conclusion**

We proposed a new algorithm that candidate four nodes to rebroadcast the RREQ while prevent some anther nodes from rebroadcasting RREQs, which results in better bandwidth usage and reduced channel contention. EF-AODV achieves significant improvements comparatively based on network overhead, End-To-End delay and Packet Delivery Ratio.

References

[1] "Mobile Ad-hoc Networks (manet)," http://www3.ietf.org/proceedings/02mar/179.htm.

[2] C. E. Perkins, E. M. Belding-Royer, and S. R. Das, "Ad hoc On-Demand Distance Vector (AODV) Routing," IETF Mobile Ad Hoc Networking Working Group INTERNET DRAFT, 19 January 2002.

[3] D. B. Johnson, D. A. Maltz, and Y.-C. Hu, "The Dynamic Source Routing Protocol for Mobile Ad Hoc Networks (DSR)," IETF MANET Working Group INTERNET-DRAFT, 19 July 2004.

[4] V. Park and S. Corson, "Temporally-Ordered Routing Algorithm (TORA) Version 1," http://www.ietf.org/internet-drafts/draft-ietf-manettora- spec-02.txt, IETF, Work in Progress, July 2001.

[5] C. E. Perkins and P. Bhagwat, "Highly dynamic destination-sequenced distance vector routing (DSDV) for mobile computers," Proceedings of ACM SIGCOMM'94, pp. 234-244, September 1994.

[6] Y.-B. Ko and N. H. Vaidya, "Location-aided routing (LAR) in mobile ad hoc networks," Proceedings of the 4th annual ACM/IEEE international conference on Mobile computing and networking (Mobicom '98), pp. 66-75, October 25-30,1998.

[7] Z. J. Haas, M. R. Pearlman, and P. Samar, "The zone routing protocol (ZRP) for ad hoc networks," IETF Internet Draft, draft-ietf-manet-zonezrp- 04.txt., July 2002.

[8] C. K. Toh, Ad-hoc Mobile Wireless Networks: Protocols and Systems: Prentice Hall, Inc., 2002.

[9] Thomas, Philippe " www.ietf.org/rfc/rfc3626.txt".

[10] S.-Y. Ni, Y.-C. Tseng, Y.-S. Chen, and J.-P. Sheu, "The broadcast storm problem in a mobile ad hoc networks," Proceedings of the Fifth Annual ACM/IEEE International Conference on Mobile Computing and Networking, pp. 152-162, August 1999.

[11] Y.-C. Tseng, S.-Y. Ni, and E.-Y. Shih, "Adaptive approaches to relieving broadcast storms in a wireless multihop mobile ad hoc networks," Proceedings of IEEE Transactions on Computers, vol. 52, pp. 545--557, May 2003.

[12] B. Williams and T. Camp, "Comparison of broadcasting techniques for mobile ad hoc networks," Proceedings. of the 3rd ACM international symposium on Mobile ad hoc networking & computing, MOBIHOC, pp. 194 - 205, June 2002.

An integrated transportation system for baseband data, digital and analogue radio signals over fibre network

S. R. ABDOLLAHI,* H.S. Al-RAWESHIDY, R. NILAVALAN

WNCC Group, School of Engineering and Design
E-mail: seyedreza.abdollahi@brunel.ac.uk

EXTENDED ABSTRACT

I. INTRODUCTION

RoF is the technique of modulating the radio frequency (RF) sub-carrier onto an optical carrier for distribution over a fibre network. RoF technique has been considered a cost-effective and reliable solution for the distribution of the future wireless access networks by using optical fibre with vast transmission bandwidth capacity. RoF link is used in remote antenna applications to distribute signals for Microcell or Picocell base station (BS). The downlink RF signals are distributed from a central station (CS) to many BS known as a Radio Access Point (RAP) through the fibres. The uplink signals received at RAPs are sent back to the CS for any signal processing. RoF has the following main features: (1) it is transparent to bandwidth or modulation techniques. (2) Needs simple and small BSs. (3) Centralized operation is possible. (4) Support multiple wired and wireless standards, simultaneously. (5) Low power consumption.

II. DIGITAL RADIO OVER FIBRE

Digital signal processing has revolutionized modern communication systems by offering unprecedented performance and adaptivity. Since, digital systems are flexible and more conveniently interface with other systems, and are more reliable and robust against additive noises of devices and channel, and achieve better dynamic range than analogue systems. In a DRoF system, firstly, an electrical RF signal is digitized by using an EADC by the Nyqiust or bandpass sampling theorem. Secondly, the generated digital data modulated with a continuous coherent optical carrier wave either using direct modulation technique or by using an external electro-optical modulator. Then, the modulated optical carrier is transmitted through the fibre. After that, at the base station, after detecting the optical signal by a photo diode, a digital detected data converts back to analogue domain by using an EDAC. Finally, the analogue electrical signal fed to an antenna [1-3].

III. ALL-PHOTONIC DIGITAL RADIO OVER FIBRE

In this section a novel all-photonic DRoF architecture is proposed. This architecture only used an electro-optical modulator, which is simultaneously performing an optical sampling and modulating operation at the CS. A photonic ADC (PADC) by using a mode-locked laser (MLL) and electro-optical modulator is able to scale the timing jitter of the laser sources to the femtosecond level, which is allow designers to push the resolution bandwidth by many orders of magnitude beyond what electronic sampling systems can achieve currently.

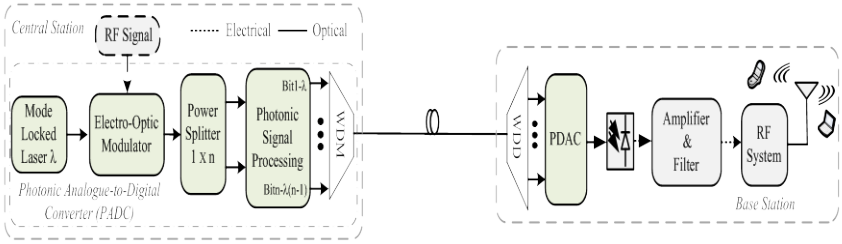

Figure 1: Proposed all-photonic DRoF architecture.

In Fig. 1, at the CS, the RF signal is sampled and modulated by optical train pulses. The optical power of sampled pulses is split into n levels by using a symmetrical optical splitter, as n denotes the number of quantization bits. Finally, the split signals are fed to a photonic signal processing block for quantization and wavelength conversion operations. At the BS, first the received signal is demultiplexed by wavelength division demultiplexer (WDD) and fed to the Photonic-DAC (PDAC).

In the PDAC block, the received digital optical signals on different wavelengths are converted back to their original wavelength at □. The proposed network architecture thatintegrates the photonic system with RF transceiver at RAP, for transporting the ARoF, DRoF, and BoF traffics by using the common infrastructure with wavelength division multiplexing technique. Therefore, this proposed system has the following features: ability to support a broad range of services, presenting competition by flexibility, protection of previous and future investments, reliability and low maintenance costs, seamless upgrade of existing access network. By realizing this scheme, it is possible to use free spectrum capacity of metro and access networks for transporting the broadband wireless and wired data traffic. This technique more centralizes the signal processing, system management, and monitoring processes. Therefore, wireless networks can be integrated with existing optical networks to reduce the future super-broadband access network system implementation and service cost overheads for the wired, wireless and mobile end-users.

IV. SIMULATION RESULTS

Investigation on system performance is shown in Fig.2. In this figure, the comparison of BER and spurious-free dynamic range (SFDR) of DRoF and ARoF links are illustrated. Therefore, the ARoF link strongly suffers with fibre link's impairment and its performance, seriously dependents on the laser source power, fibre length and the interference of other channels. However, DRoF are more independent on fibre lengths, and the proposed all-photonic DRoF system, by using optical low phase noise sampling pulse can support high bandwidth RF signals. Consequently, in addition of using present digital optical communication infrastructures the number of CSs will decrease and as a result, the service provider and operators cost overhead per bit will be reduced.

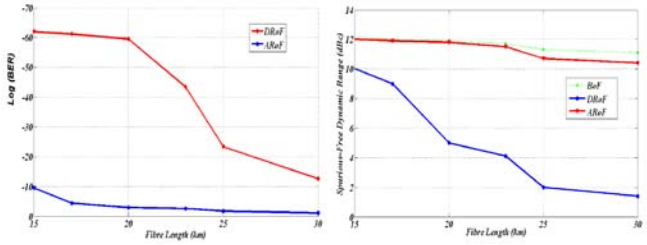

(a) (b)

Figure 2: BER and SFDR comparison of DRoF with ARoF for 1 Gbps ASK modulated signal with 5 GHz carrier over 30 km single-mode fibre length: (a) Bit Error Rate (b) Spurious-Free Dynamic Range (SFDR).

V. CONCLUSIONS

The problems for digitizing the future super-broad band analogue radio frequency (RF) wireless signal by using proposed all-photonic signal conversion technique is overcome. In this architecture, by using the proposed PADC, a 5 GHz, ASK modulated RF signal with 1 Gbps bandwidth is sampled with 15 Gigasample/s MLL pulse.

REFERENCES

[1] P. A. Gamage, A. Nirmalathas, C. Lim, D. Novak and R. Waterhouse, "Design And Analysis Of Digitized Rf-Over-Fiber Links", Journal Of Lightwave Technology, Vol. 27, No. 12, Pp. 2052-2061, 2009.

[2] C. Lim, A. Nirmalathas, M. Bakaul, P. Gamage, K. L. Lee, Y. Yang, D. Novak and R. Waterhouse, "Fiber-Wireless Networks And Subsystem Technologies", Journal Of Lightwave Technology, Vol. 28, No. 4, Pp. 390-405, 2010.

[3] G. C. Valley, "Photonic Analog-To-Digital Converters", Optics Express, Vol. 15, No. 5, Pp. 1955-1982, 2007.

Keywords: wireless communication, optical communication, radio over fibre, and Analgo-to-Digital Conversion (ADC).

Improving the detection of latent fingerprints using phosphor nanopowders

Alexander REIP*, Jack SILVER, Robert WITHNALL
Wolfson Centre for Materials Processing, Brunel University, Uxbridge UB8 3PH, Middlesex, UK
alexander.reip@brunel.ac.uk

EXTENDED ABSTRACT

Introduction

Nanotechnology has been increasingly employed in forensic science for the detection of latent fingerprints, using multiple techniques from new aluminium nanomaterials for dusting to quantum dot dispersions, to try to increase and enhance areas where prints are likely to be found at scenes of crime. Different substrates use a diverse range of methods to develop prints when they are found and each method has its own drawbacks. It is not viable to use many of these in conditions other than in a lab due to the harmful effects they can cause over long term use. With this in mind a new easier to use technique that can be used on any substrate from wood to glass to paper was looked into.
Past research has shown the success of using europium doped yttria for increasing the detection of fingerprints and that work has been built upon to improve the powders ability to adhere to the fingerprint by modifying the surface of the phosphor while making sure the modifications do not hinder the fluorescent ability of the phosphor [1].

Methodology/Approach

The europium doped yttria was used as well as a terbium doped yttria due to both having an high intensity when excited at 254 nm but each having a different emission (europium at 612 nm and terbium at 543 nm.) (See fig 1) Having synthesised two different phosphors modifications can be examined to see whether these give better adherence or resolution.

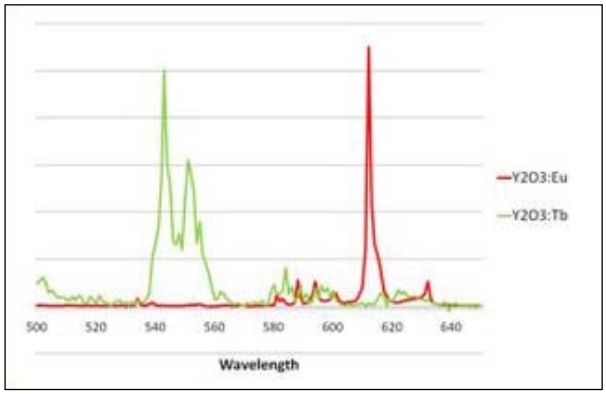

Fig 1 – Emission spectra of Y_2O_3:Eu and Y_2O_3:Tb using an exciting wavelength of 254 nm

Y2O3:RE (RE = Eu, Tb) was synthesized using the homogeneous precipitation method. Molar ratios of Y(NO3)3 and RE(NO3)3 were mixed, diluted with distilled water to 500mL and the resulting solution heated to 90oC whilst stirred. Once at temperature urea (35g) was added and the solution left at temperature for 2 hours. After this time the precursor was filtered and dried at 50oC. This was then coated with silica using a modified version of the Stöber method [2]. 1g of the precursor was dispersed in 400mL of ethanol to which 20mL distilled water and 25mL tetraethoxyorthosilane was added. This solution was stirred and 8mL ammonia added. The solution was left stirring for 1 hour and then the coated precursor was separated by centrifuge and washed with ethanol. This was then dried at 60oC in an oven followed by sintering in a furnace at 1000oC for 6 hours. 1g of one of the silica coated phosphors was dispersed in 100mL ethanol. The solution was stirred and 20mL tetraethyloctylsilane was added. This was left stirring for 48 hours before being separated by centrifuge, washed with ethanol and dried.
To ensure consistency in the results the fingerprints were taken from one donor. The finger was washed with ethanol and allowed to dry in air for ten minutes without contact. These eccrine prints were then placed on cleaned glass slides. To create sebaceous prints the same method was used except after the drying period the finger was rubbed on the back of the neck and then between the fingers before being placed onto the glass slide. To observe the differences in the ageing of fingerprints some

samples were left for two weeks in the dark in a slide tray. A depletion series was made using three fingers cleaned as before and set down fifteen times in a row on a sheet of glass to test how far along each of the powders could detect. The particle sizes and morphology were determined by SEM using an Oxford Supra 35 and TEM using a JEOL JEM 2000 FX. Fluorescence spectra were taken on a Bentham Spectrometer and infrared spectroscopy was taken using a Perkin Elmer Spectrum One FTIR Spectrometer with an ATR attachment.

Results and Discussion

The silica coated Y2O3:Tb was modified with a trimethoxy(octyl)silane to give the coated phosphor a long chained hydrocarbon tail which was found to increase the adherence to the more oil based sebaceous fingerprints. The silica coated Y2O3:Eu was found to have a high attachment to the more aqueous based eccrine fingerprints and so this was used without modification. The particles were found to be approx 200nm when imaged with a SEM (fig 2.) and after coating and modification the size was 300nm seen using a TEM (See fig 3.)

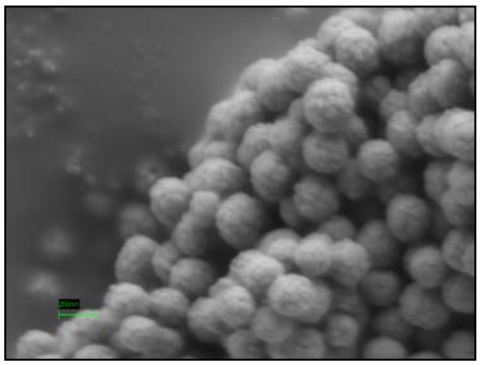

Fig 2 – SEM of Y_2O_3:Eu

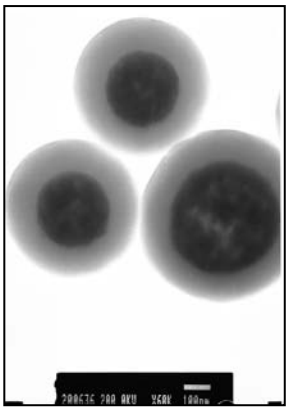

Fig 3 – TEM of Y_2O_3:Tb particles coated with silica and modified with TMOS

Using infra red spectroscopy the modification was found to have attached to the surface of the silica and when tested on two week old and newly created fingerprints the purely silica coated phosphors adhered primarily to newer prints whereas the TMOS modified phosphor adhered to the more aged prints due to the lack of decomposition and lack of evaporation of the oils. The newer prints contained more aqueous salts and sweat so were a much better surface for the silica coated phosphors (see fig 4.)

Fig 4 – TMOS coated then modified Y_2O_3:Tb dusted print (left) and Y_2O_3:Eu coated with silica dusted print (right)

Conclusion

The phosphor powders show great promise in enhancing the detection of latent fingerprints compared to traditional powders. The next work that will be carried out is to see whether more information can be developed from the fingerprint. These tests include modifying coated phosphors with drug antibodies so areas can be dusted for fingerprints that could have traces of drugs on them and also looking at the treated print using Raman spectroscopy to see whether other compounds can be detected such as explosive residues.

References

[1] Mi Jung Choi et al (2008). “Metal-containing nanoparticles and nano-structured particles in fingermark detection.” Forensic Science International 179 (2-3): 87-97

[2] Stöber. W, Fink. A and Bohn E (1968) “Controlled growth of monodisperse silica spheres in the micron size range.” J. Colloid Interf. Sci. 26: 62-69

Keywords: fingerprint, detection, phosphor, nanoparticle and forensic

Copper based materials for a new generation of displays.

Inmaculada ANDRÉS-TOMÉ*, Paolo COPPO.

Wolfson Centre for Materials Processing, Brunel University, Uxbridge UB8 3PH, Middlesex, UK

Inmaculada.Andres@brunel.ac.uk

EXTENDED ABSTRACT

INTRODUCTION

During the last 30 years there has been a high significant development and interesting research in the field of displays. The technology of these displays has evolved from the heavy construction of the cathode ray tube (CRD), to the increasingly lighter liquid crystal display (LCD) and light emitting diode (LED) display. This has now leaded to a new generation of display type, based on organic light emitting diodes (OLEDs). Their properties, such as optical and electrical confer them potential applications as low cost or lightweight devices. These characteristic have revolutionized the market [1] and they have been commercialized by Philips, TDK, Nippon Seiki, Sanyo and Pioneer [2]. However, they have a high price because the OLED technology has been manufactured with expensive materials.

OLED technology converts electricity into light by using organic material sandwiched between cathode and anode electrodes [4]. The structure consists of a number of thin layers, where aluminium is used as cathode and glass coated with indium tin oxide (ITO) is used as anode. These layers are deposited by solution processing or vacuum-deposition; the structure is showed in the figure 1. The process of light emission consists in the injection of electron and holes at the electrode-semiconductor interface, where they recombine and excited states are created, which decay by emission of photons, in other words by emission of light.

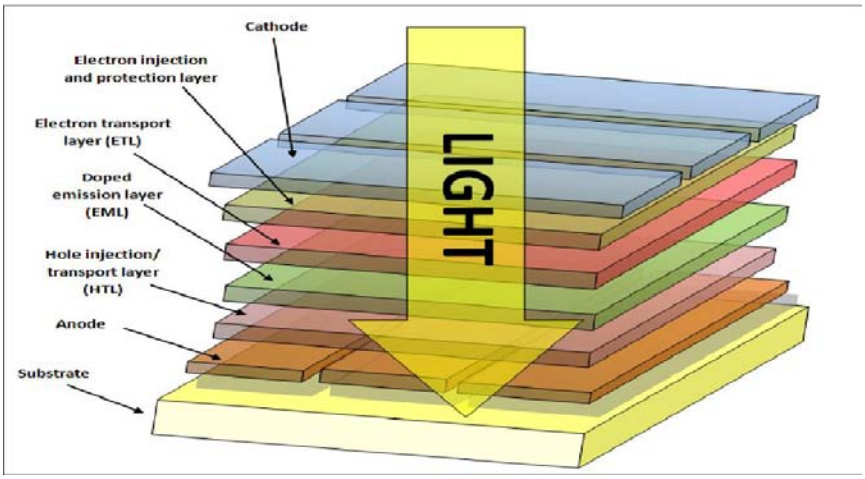

Figure 1. Multilayer design of an OLED

Each layer consists of an organic semiconducting material doped with a light emitting molecule, which is the main point of our research. We have focused on phosphorescent organic molecules which have a range of emission between sky blue to deep red in the visible spectrum. Some essential requirements have to be met by the material used in OLEDs, such as photochemical and thermal stability.

When a species absorbs energy by electromagnetic radiation UV or vis, it travels to an excited state by absorption of the energy. This excess of energy could be lost by different ways such as vibrational relaxation or internal conversion, or it could be by radioactive ways such as the called fluorescence and phosphorescence, figure 2 [4]. The main difference between both emissive processes is the timescale of the process; the fluorescence takes 10-9s whilst the phosphorescence takes 10-6s. Current OLED technology prefers phosphorescent molecules because they emit from a triplet excited states. When excited states are produced by electricity, 75% of triplets are generated, as opposed to only 25% singlets. All the emissive processes are influenced by different parameters like the surrounding environment, the presence of oxygen, the temperature and the structure of the species.

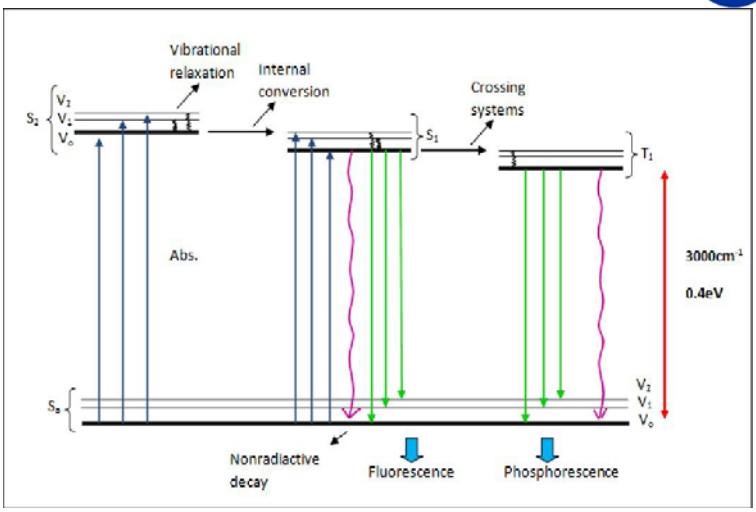

Figure 2. Molecular energy level diagram.

METHODOLOGY

Our research is focused on the synthesis of new luminescent metal complexes, the study of their luminescent properties and the understanding of the underlying spectroscopic origins of their luminescent behaviour. During the last twenty years, there have been considerable advances in this field and most of them are based on the use of iridium (III) complexes as active material [5]. However, iridium (III) based materials are expensive and not sustainable, which in turn leads to a high price of the final product. An alternative is the use of copper (I) complexes [6], which are by far more accessible for mass market applications. We have prepared two groups of copper (I) complexes, which show promising photophysical properties. In the first group we prepared trinuclear copper (I) complexes carrying alkynyl ligands, by careful tailoring of these conjugated ligands with appropriate substituents on the aromatic ring [7], while in the second group we prepared mononuclear copper (I) complexes with the ligands 2-phenylpyridine and 2-bipyridyl [8], figure 3. The complexes were characterized with a range of techniques, such as absorption and emission spectroscopy, nuclear magnetic resonance (NMR), thermogravimetric analysis (TGA), differential scanning calorimetric (DSC) and cyclic voltammetry (CV).

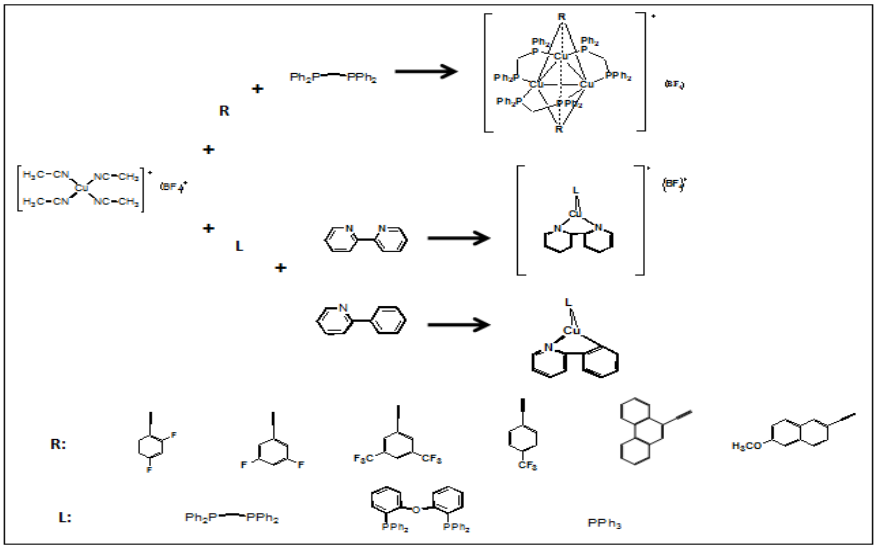

Figure 3. Synthetic procedure for the preparation of trinuclear and mononuclear copper (I) complexes.

CONCLUSION

Both groups of copper (I) complexes exhibit a very broad and tuneable emission colour and lifetime range. For the first group, they range from 30μs to 1ms and the second group from 10μs to 33μs. Such wide range can cover applications stretching from OLEDs to luminescent labels for biological applications. The quantum yields we have obtained are comparable to those reported for Iridium (III) cyclometallated complexes [9]. These complexes exhibit excellent solubility in organic solvents and can be processed as amorphous films or they can be incorporated in solution processed polymer films.

REFERENCES

[1] P.E. Burrows, S.R. Forrest, M.E. Thompson. “Prospects and applications for organic light-emitting devices”. Optical and magnetic materials, vol.2, 2, pp. 236-243, 1997.
[2] B.W. D’Andrade, S.R. Forrest. “White organic light-emitting devices for solid-state lighting”. Advanced Materials, vol.16, 18, pp. 1585-1595, 2004.
[3] P. Coppo. “The day lighting became organic”, SPR Photochemistry, vol. 37, pp. 393-406 .
[4] J.W. Lichtman, J-A. Conchello. “Fluorescence microscopy”. Nature Methods, Vol.2, 2, pp. 910-919, 2005.
[5] P. Coppo, E.A. Plummer, L. De Cola. “Tuning iridium (III) phenylpyridine complexes in the “almost blue” region”. Chemical Communications, pp. 1774-1775,2004.
[6] A. Barbieri, G. Accorsi, N. Armaroli. “Luminescent complexes beyond the platinum group: the d10 avenue”. Chemical Communications, 19, pp. 2185-21932008.
[7] I. Andrés-Tomé, C.J. Winscom, P. Coppo. “Copper (I) trinuclear phosphorescent complexes with tuneable optical and photophysical properties”. European Journal of Inorganic Chemistry, 23, pp. 3567-3570, 2010.
[8] J. Min, Q. Zhang, W. Sun, Y. Cheng, L. Wang. “Neutral copper(I) phosphorescent complexes from their ionic counterparts with 2-(2′-quinolyl)benzimidazole and phosphine mixed ligands”. Daltons Transactions, 40, pp. 686-693, 2011.
[9] E. Orselli, G.S. Kottas, A.E. Konradsson, P. Coppo, R. Frohlich, L. De Cola, A. Van Dijken, M. Duckel, H. Borner. “Blue-Emitting Iridium Complexes with Substituted 1,2,4-Triazole Ligands: Synthesis, Photophysics, and Devices”. American Chemical Society, Inorganic Chemistry, Vol. 46, No. 26, pp. 11082-11093, 2007.

Keywords: OLED’s, luminescence, mononuclear and trinuclear copper (I) complexes

Face recognition with weightless neural networks using the MIT database

K. KHAKI*, J. STONHAM
Department of Engineering, Brunel University, UK

EXTENDED ABSTRACT

Introduction

In the recent years, many algorithms have been proposed to tackle the problem of face recognition and detection [1]. However, these solutions have unacceptable prerequisites - the images require computationally intensive pre-processing, or the images used have to be manually selected, the recognition algorithm cannot operate in real time due to computational overheads, and they only produce optimal, but not perfect results if the images are normalised in terms of lighting and background. The solution presented in this paper overcomes these constraints and produces significantly better results than those previously published.

The methodology has been tested on various public domain databases, and exceptional results have been achieved. The reason the MIT database has been chosen for this abstract is because it is the most challenging. Apart from the person in the image being the same, the lighting, clothing and background changes within each set, and differ from all other sets of images. The database was first used by MIT, however they did not perform any recognition on the images themselves, rather converted each image set into a 3D computer image, which was then used, and an overall recognition percentage of 88% was achieved [2]. It should be noted that the training and testing is carried out on the 'test' folder of the MIT database. Sample images from the MIT database are displayed in Figure 1.

.

Figure 1
Two sample images per person that were trained or tested on

Methodology

The 'test' folder consists of 10 image sets, each containing 200 images of an individual. Since the images are a variety of sizes ranging from 100x100 to 115x115, image resizing is done initially to bring all the images to a constant 100x100. This resizing is done using subsample normalization,

which does not change the values of any of the pixels in an image; rather it deletes rows and columns of pixels to reduce the overall size of the image. Then, each image set is divided into two; the first 100 images are for training, and the other for testing.

The algorithm developed and used in this work is a random n-tuple mapping on grayscale images, where each image is divided into 200 sets of 5 pixels groups. An n-tuple state is then obtained by using a ranking transform which eliminates the requirement for pixel thresholding operation. The digital neuron then correlates the recurring states obtained from the training phase with the current input from the test pattern.

Results

The training set and testing set consisted of 10 individuals, each with 100 unique images. The algorithm had a training and testing rate of 10 images per second, and produced a recognition accuracy of 99.9% overall, with a 0% False Rejection Rate (FRR) and 0.1% False Acceptance Rate (FAR). This compares with the 88% accuracy published by MIT [2] and it also shows significant savings in processing time. Additionally it should be noted that the memory requirements for a single neuron is 128 bits, and as 2000 neurons are used per net, the system has an efficient hardware implementation capability with a total storage requirement of 250kB; this is independent of the size of the data set being processed. Figure 2 shows the overall recognition results of the method presented in this paper.

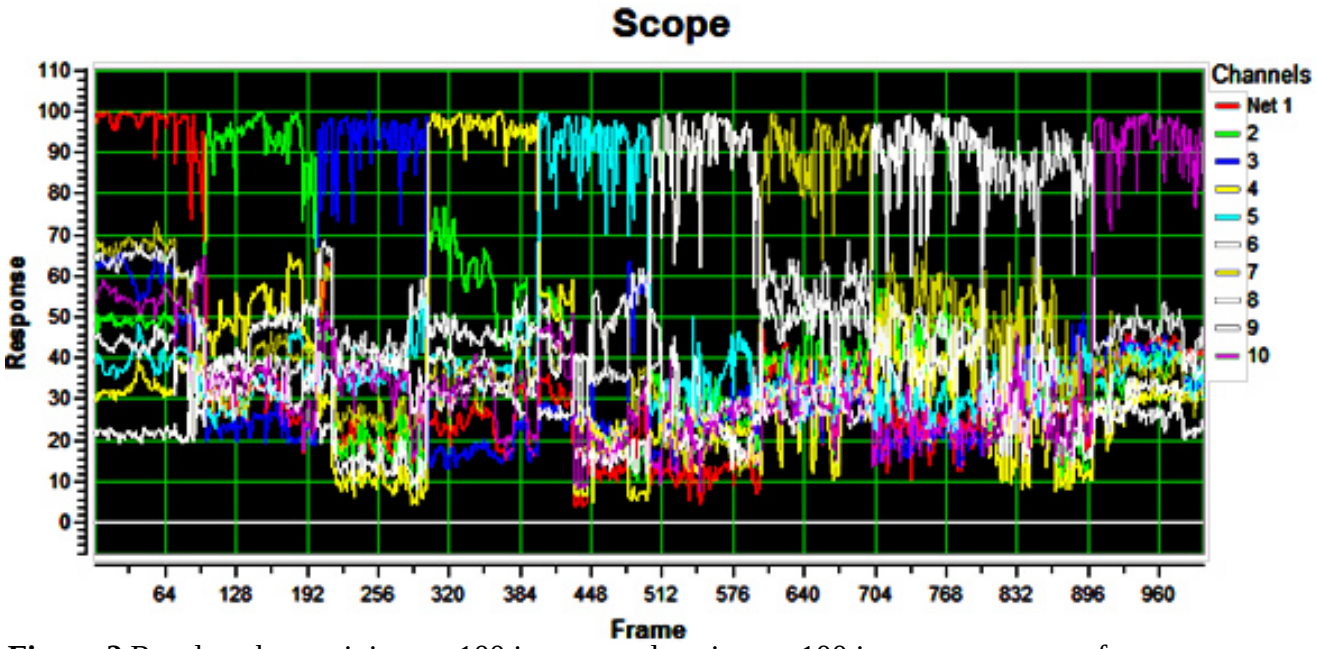

Figure 2 Results when training on 100 images and testing on 100 images per person for ten individuals.

Summary

The system has provided 100% accuracy on the AT&T and Yale databases. The 99.9% accuracy with the MIT database has resulted in one error in 1000 images. It should be noted that these results have been obtained from an un-optimised system. The training and feature sampling strategies have been randomly specified. It is therefore expected that robust error free performance can be achieved in an optimised system.

References

[1] M. Samer Charifa, A. Suliman and M. Bikdash. “Face Recognition Using a Hybrid General Backpropagation Neural Network”. 2007 IEEE International Conference on Granular Computing
[2] B.Weyrauch, J.Huang, B.Heisle and V. Blanz. “Component-based Face Recognition with 3D Morphable Models”. 2004

Keywords: Net, Pixel Operator, Neuron, FAR, FRR

Novel grain refiner for Al-Si alloys

Magdalena NOWAK*, Hari Babu NADENDLA

Brunel Centre for Advanced Solidification Technology

EXTENDED ABSTRACT

Introduction

Over the centuries the grain refinement has been an important technique for improving the properties of aluminium products. Aluminium castings with large grain structure have poor castability and mechanical properties compared to fine grain structure [1, 2]. The grain refinement practice using chemical addition is well established for wrought alloys, however in the case of casting alloys, the practice of adding grain refiners and the impact on castability is not well established. The addition of well known Al-5Ti-B grain refiner to casting alloys with silicon (Si) content above 3 wt.% is not effective [3] due to chemical reaction between Ti and Si. The current research is to find an alternative, but effective, chemical phase which can refine Al-Si alloy grains.

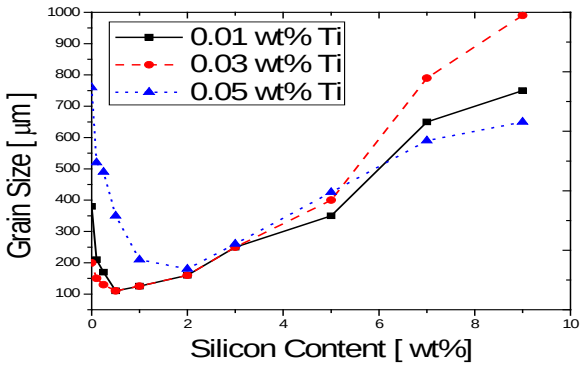

Figure 1 Grain size of Al-Si alloys with three different levels of Ti addition. When Si >3 wt%, grain size increases due to consumption of Ti by Si to form Ti-Si phases.

Methodology

Investigation of phase diagrams was undertaken to find the potential grain refiner for foundry alloys. Titanium is the well known grain refiner for Aluminium, however from Al-Ti and Al-Nb equilibrium phase diagrams it can be seen that both systems present a peritectic reaction between liquid aluminium and solid particles (X= Ti and Nb). The crystals structure of Al3Ti and Al3Nb are both tetragonal with eight atoms per cell and with unit cell parameters of a = 3.85 Å, c = 8.61Å and a = 3.84 Å, c = 8.58 Å respectively [4]. These similarities indicate that niobium could act as grain refiner as efficiently as titanium.

Experiments & results:

To confirm this theory, various Al-Si binary and a commercial sourced cast alloy (Al-10Si-Mg) were cast by adding Nb based grain refiner. The Fig 2a shows that the Nb based grain refiner is effective for wide range of Si levels. It is the first time such fine grain structures (inset to Fig.2a) were achieved. Effectiveness of grain refiner under various cooling rate conditions (Fig 2b) has also been investigated to simulate various practical casting conditions. As a result of finer grains the elongation and strength are improved (Fig. 2c). TEM study reveals that Al3Nb are coherent within Al matrix, suggesting that they are responsible for enhancing heterogeneous nuclei.

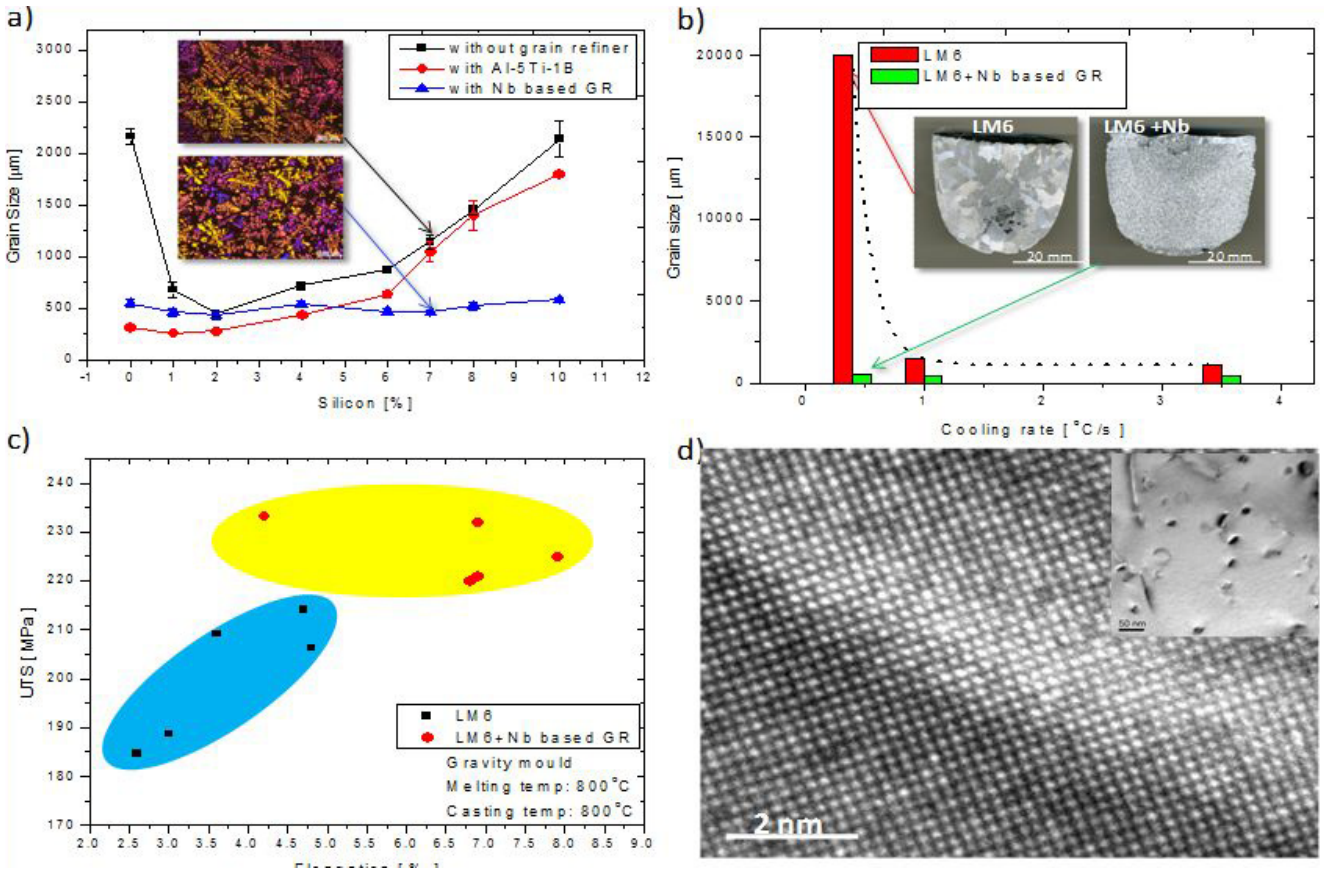

Figure 2 a) Grain size as a function of Silicon addition to Al. Data for with and without Ti and Nb based grain refiners. Inset shows microstructures for Al-7Si alloys. b) The cooling rate versus grain size. The notable improvements in the grain size were achieved for very slow cooling rates as well. c) The improvements in elongation and strength for a LM6 alloy. d) The transmission electron microscopy (TEM) image of Al_3Nb particle within Al matrix.

Conclusion:

We developed an effective grain refiner for Al-Si alloys. For the first time, much needed fine grain structure for Al-Si casting alloys is achieved.Grain size is less sensitive to cooling rate. Complex shaped castings with reduced defects, fine grain structure and improved mechanical properties are now possible.

References:

[1] McCartney D.G. Int.Mater: Review 34 (1989): 247-60.
[2] Easton M., StJhonson D.Metalurgical and Materials transactions 30A (1999): 1613.
[3] Jhonsson M., Backerud I., Sigworth G.KMetal.l Trans. A) 24A (1993).
[4] Mondolfo F. Aluminium Alloys: Structure and properties. Boston: Butterworths, 1976.

Keywords: grain refinement, casting alloys.

Positron Emission Tomography volume analysis based on ANN

Mhd Saeed SHARIF,* Maysam ABBOD
Electronic and Computer Engineering,School of Engineering and Design
Brunel University, Uxbridge, Middlesex, UK
* mhd.sharif@brunel.ac.uk

EXTENDED ABSTRACT

Introduction

Tumour classification and quantification in positron emission tomography (PET) imaging at an early stage of illness are important for radiotherapy planning, tumour diagnosis, and fast recovery. Medical images can be acquired using different medical modalities such as positron emission tomography (PET), computed tomography (CT), magnetic resonance imaging (MRI), and ultrasound. PET is a tomographic technique which is used to measure physiology and function rather than anatomy by imaging elements such as carbon, oxygen and nitrogen which have a high abundance within human body. PET plays a central role in the management of tumour beside the other main components as diagnosis, staging, treatment, prognosis, and follow-up. Due to its high sensitivity and ability to model function, it is effective in targeting specific functional or metabolic signatures that may be associated with various types of diseases [1], [2], [3], [4].

There are many techniques for segmenting medical volumes, in which some of the approaches have poor accuracy and require a lot of time for analyzing large medical volumes. Artificial intelligence (AI) technologies can provide better accuracy and save decent amount of time. Artificial neural network (ANN), as one of the best AI technologies, has the capability to classify, measure the region of interest precisely, and model the clinical evaluation. ANN is a mathematical model which emulates the activity of biological neural networks in the human brain. It consists of two or several layers each one has many interconnected group of neurons. The main aim of this research is to evaluate the capability of ANN to detect and classify the region of interest (ROI), tumour, in PET volumes. Thresholding, clustering and multiresolution analysis (MRA) approaches have been used also to segment the ROI, and they are used as truth ground to compare the outputs of the artificial neural network. Promising results have been achieved utilizing phantom and clinical PET volumes.

Methodology

The 3D PET volume acquired from the scanner goes through the preprocessing block, where thresholding, and median filter are utilised to remove external artefacts and enhance smoothly the quality of slices features. The optimal class number is determined by plotting Bayesian information criterion (BIC) values against different values of number of classes K. K values are between 2-8 and is not further increased, as in this medical application, any additional separation is unnecessary based on expert consultation and comments. This number is fed to ANN which classifies each processed slice into the corresponding number of classes. Where each voxel is classified into its corresponding class. The classification performance is evaluated then using confusion matrix (CM) and receiver operating characteristic (ROC) curve. The outputs are finally selected and displayed.

Results and discussion

Different PET data sets have been used in this study to evaluate the performance of the proposed system based on ANN. One of these data sets is the Zubal PET phantom data set which has simulated tumours with different sizes. The optimal class number obtained from BIC plot is 5 classes. The ANN output for tumour 1 is illustrated in Fig. 1.b. The fraction of samples misclassified in total using CM is 4.068348E-04, and the area under the ROC curve (AUC) is 0.9998, which indicates a good ANN performance for classifying this data set.

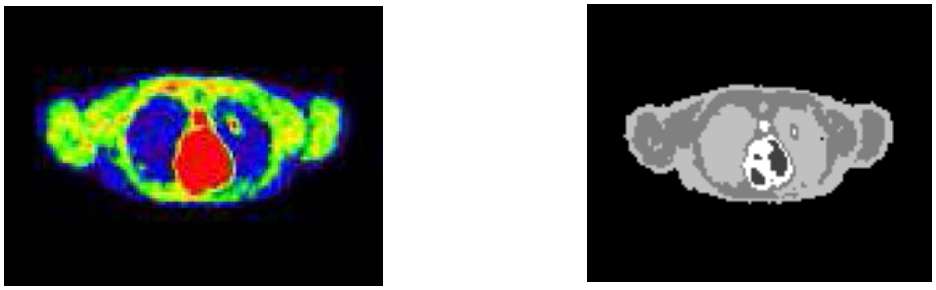

(a) (b)

Fig 1: PET Phantom: (a) Original PET slice (128x128), (b) Reconstructed classified slice from ANN (128x128)

Conclusion

An artificial intelligent approach based on ANN and BIC has been proposed for 3D oncological PET volume classification. A detailed evaluation has been carried out on the system outputs, which has shown promising results. The performance evaluation has been carried out using CM and AUC of ROC curve. The ROI is precisely classified in all phantom and clinical data sets. The application of different clinical data sets has also shown promising results in detecting and classifying patient lesion.

References

[1] D. A. Mankoff, M. Muzi, and H. Zaidi, ”Quantitative analysis in nuclear oncologic imaging”, in Quantitative Analysis of Nuclear Medicine Images. edited by H. Zaidi, Springer, New York, pp. 494-536, 2006.

[2] D. Montgomery, A. Amira and H. Zaidi, ”Oncological PET Volume Segmentation Using a Combined Multiscale and Statistical Model”, Medical Physics (The American Association), 34 (2), February 2007.

[3] P. Dendy, B. Heaton, ”Physics for Diagnostic Radiology” , Institute of Physics, 2002.

[4] A. Webb, ”Introduction to Biomedical Imaging”, IEEE Press Series in Biomedical Engineering, 2003.

Keywords: Artificial Neural Network, Medical Image Analysis, Positron Emission Tomography, Tumour.

Computational design and tuning of graphene bilayer grown on the 4H-SiC substrate

Nikolai Issakov

Advanced Manufacturing & Enterprise Engineering

EXTENDED ABSTRACT

Introduction

Computational design for stepwise graphene bilayer (BL) growth on the 4H-SiC substrate at different external conditions was undertaken since the novel materials made with graphene layers stacked one on the top of another that each is electronic independent attract the special interest for theory and practice [1-10]. Two layers jointed together reveal the freestanding graphene quality, whereas the every subsequent layer adds the novel features. The layered systems supported and interacted with another condensed matter are nowadays a subject of special interest because they enable to be inserted as a ready building block into desired devices.

Methodology

The results of systematic study and simulation of epitaxial graphene BL grown on the 4H-SiC substrate are performed. The CASTEP code worked out on the DFT first principles was used for the computational design, total energy calculation, geometry optimization, band structures and DOS [11, 12]. The results were used to elucidate the evolving electronic states while the designed BL progress. The simulation was intended as a stepwise process involving substrate decomposition, Si atoms removal and residual C atoms self-organization by means of chemical surface conversion [13-17]. The electronic properties of consistent layers including the substrate grown by the interfacial monolayer (ML) and terminating BL plane were studied and interpreted for the different combinations of alternating substrate unit cells, surface terminations, commensuration between constituting layers, etc.

Results

The great difference was revealed since the substrate choice. The initial $(\sqrt{3}\times\sqrt{3})R30°$ and (3×3) reconstructions were tasted. The alternation determined by substrate unit cell was further enforced by the difference of Si-face and C-face terminations. For the both reconstructions of Si-face termination the transition half-filled band splitting into two narrow sub-bands separated by the Fermi level proved to be likewise the n-type structure. For the C-face termination the Fermi level is stretched towards the top of valence band as it takes place for the p-type structure. Due to substrate – C layer interaction the interface was adapted to supporting structure given a rise to the difference of subsequent layers. A gradual complication of gap states as two polar rows are formed commenced from the initial differences of SiC substrate. This is why the substrate proper choice is of crucial importance for the interface and BL as a whole. The coordinates for interfacial layers were calculated at the distance admissible for covalent bonds. The calculations while arranging the second C layer at the distance from the first one acceptable for the Van der Waals forces proved to be poorly operated by the DFT. Therefore the calculations were clarified by the monitoring for variable distances between C layers. The electronic evolution was gradually traced by the band structure monitoring given the special attention for gap states in vicinity of the Fermi level and tuning of the gap sizes. As a result for the BL on (0001) - $(\sqrt{3}\times\sqrt{3})R30°$ substrate the tendency for valence and conduction band meeting in K and M points and divergence in Γ point take place that is appropriate for the freestanding graphene.

Conclusion

Three consistent layers simulating the graphene BL on the 4H-SiC substrate were studied on the basis of DFT first principles with the object of building block construction. The electronic structure evolution was examined by analogy with the fingerprints to reveal a novelty introduced by the alternating substrate grown with the successive carbon layers in commensurable stacking order. Crucial role of proper substrate choice, especially as for the unit cell reconstructions and top-level termination, pre-determines the interface quality and growth of subsequent layer. The variability and dynamics of gap states are controlled by combination of constituent layers, coherency of C-planes, distances and stacking order of layers.

References

[1] Berger C et al 2006 Science 312 1191-96

[2] Aoki M and Amawashi H 2007 Solid State Communications 142 3 123-127

[3] Wang S. et al. 2008.Physical Review B78 (20), , p.201408

[4] Zhou S Y, Siegel D A, Fedorov A V and Laurare A 2008 Phys. Rev. Lett. 101 086402

[5] Starke U and Riedel C. 2009 J. Phys. Condens. Matter 21 134016

[6] Magaud L, Hiebel F, Varchon F, Mallet P, Veuillen J.-Y. 2009, Physical Review B79

[7] Neek-Amal M, Asgari R, M R Tabar Nanotechnology20 (13), 2009, p.135602

[8] Wang Q and Hersam M. 2009. Nature Chemistry 1 (3), p.206

[9] Chen Y P and Yu Q 2010 Nature Technology 5 8 559-560

[10] Kuroda M, Nistor R and Martina G 2010 Bull. APS 55 2 T21.009

[11] Payne M C, Teter M P, Allan D C, Arias T A and Joannopoulus J D 1992 Rev. Mod. Phys. 64 1945

[12] Segall M, Lindan P, Probert M, Pickard C, Hasnip P, Clark S and Payne M. 2002 J. Phys. Condens. Matter 14 2717-44

[13] Muehlhoff L, Bozack M J, Choyke W J and Yates J T Jr 1986 J. Appl. Phys. 60 7

[14] Forbeaux I, Themlin J-M and Debever J-M 1999 Surf. Sci. 442 9

[15] Hass J, E. Millán-Otoya J E, First P N, and Conrad E H 2008 Phys. Rev. B 78,

[16] Rutter G, Guisinger N, Crain J, Jarvis E, Stiles M, Li T, First P and Stroscio J. 2007 Phys. Rev. B 76 235416

[17] Hiebel F, Mallet P, Varchon F, Magaud L and Veuillen J-Y, 2008, Phys. Rev. B 78

Key words: graphene, monolayer, bilayer, interface, band structure, DOS, unit cell, termination, reconstruction.

Initial results of a CAD import into G4MICE

M.D. LITTLEFIELD

School of Engineering and Design

Centre for Sensors and Instrumentation

Matthew.Littlefield@brunel.ac.uk

EXTENDED ABSTRACT

This paper describes the initial investigation into translating a Computer Aided Design (CAD) model into a form suitable for the G4MICE physics simulator. G4MICE is an application which provides simulation capabilities to the MICE project. These capabilities allow users to model the MICE experiment and simulate the movements and effects of particles propagating through the experiment. G4MICE produces Monte Carlo data from the simulation which can be analysed. The Muon Ionisation Cooling Experiment (MICE) is a project which will design and build a set of cooling channels which will reduce the emmittance of a beam of muons.

Introduction

Modern large scale accelerator physics experiments use simulation tools in order to theoretically model the experiment and the behaviour of the propagating particles and thus the beam itself. This is to allow us to quickly and cost effectively test theories and analysis techniques and also to confirm and test data which has been produced. Having a simulation which models the experiment accurately is paramount, because any minor changes within the beam line may affect the beam and thus the results either experimental or theoretical. Currently the G4MICE simulator has geometries within it which are inaccurate. An investigation on the possibilities of incorporating a CAD import into G4MICE has been carried out and if successful will be implemented as the method of creating geometries in G4MICE.

Approach

Initial research into the subject found that there was already functionality included into Geant4 (G4), which is the base simulator for G4MICE, which allows a CAD model to be translated into a Geometry Description Markup Language (GDML) and can then be read into G4 where the geometry is built ready for simulation and analysis. G4MICE did not have this capability since the way information was input into the simulator is different to G4 and thus an extra step was needed. These steps were to translate a GDML of the test case, which in this case was a basic CAD model of a cooling channel, into MICE Modules and then add extra functionality to G4MICE which enables G4MICE to create geometries from this information. Firstly the GDML file was translated into a .dat text file which contained the information about the geometry in a manner which G4MICE could read in the information. This was done using Extensible Stylesheet Language Transformation (XSLT) which picks specified information from the GDML file and re writes it according to the style sheet. Once the GDML was written in a format which G4MICE could read the translation was complete. The images below shows the CAD model and the G4MICE model which went through this transformation.

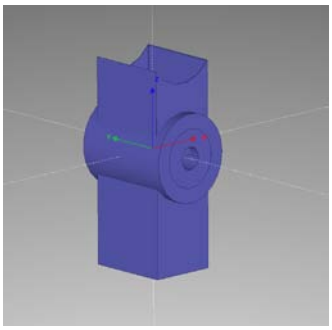

Figure 1: CAD Model of Test Case

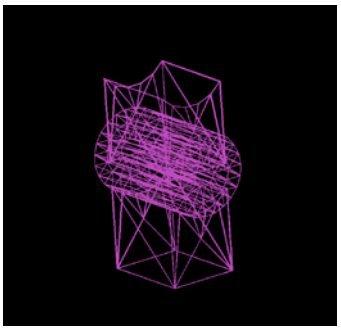

Figure 2: G4MICE Model of Test Case

Conclusion

It is clear from the images that the transformation was a success. Now that the principle of importing CAD models into G4MICE has been proved the structure of the way in which users access these translated models for simulation and analysis needs to be created. This structure is a little more complex than simple geometrical translations as there are other pieces of information needed for the simulations. Within the beam line there are magnetic fields and the information about these fields are needed for the G4 component of G4MICE to compute these fields. This information comes from default MICE Modules already currently in use. This information can be combined with the geometrical information of each beam line element using XSLT. There are also different settings, such as magnet currents, which change for each run of the experiment and a system called the Configuration DataBase (ConfigDB) has been created which submits these settings to a database for future reference. This also needs to be added to the structure of how users will access the information. After some discussions and some planning sessions the structure below is the proposed structure for the data management.

Figure 3: Diagram of Proposed Data Management Structure

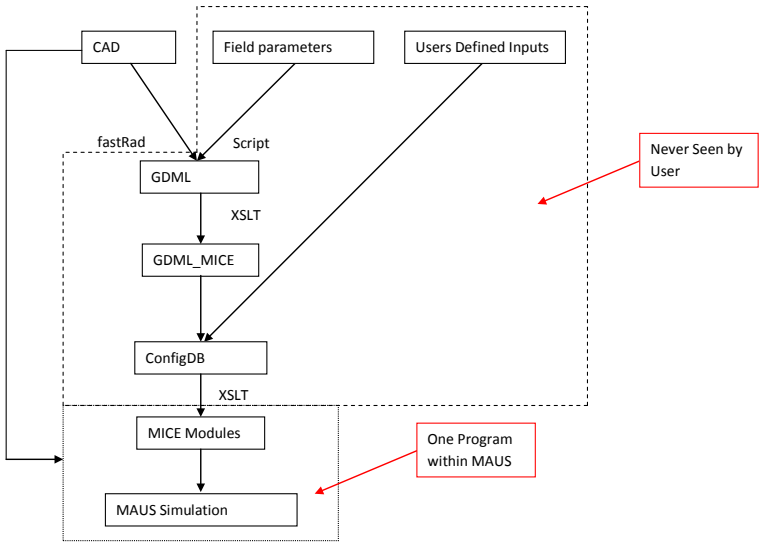

One thing to note from this diagram is the G4MICE program itself is being re written and has also been rebranded as MAUS. This is to reduce the complexity of the program and to increase its usability. Although simpler the new system introduces a structure which accounts for change in the geometry. This system will be updated every time a major change in the geometry occurs and will note any minor changes. The ConfigDB will store all the information required and can be accessed by users who will be allowed to obtain any geometry they require either current or previous steps of the experiment. Work has now begun on implementing this system into the new simulator MAUS.

References

1. [Online], *http://geant4.web.cern.ch/geant4/*, Accessed 25/03/11.
2. [Online], *http://gdml1.web.cern.ch/gdml1/*, Accessed 25/03/11.
3. [Online], *http://www.w3.org/TR/xslt*, Accessed 25/03/11.

Keywords: CAD, G4MICE, MAUS, geometry transfer.

Measurement of the top-antitop quark production cross section at CMS with 36 pb-1 of data in the electron+jets channel with b-tagging

William P MARTIN on behalf of the CMS Collaboration

Centre for Sensors & Instrumentation, School of Engineering & Design

william.martin@brunel.ac.uk

EXTENDED ABSTRACT

Introduction

The top quark was first observed in proton-antiproton collisions at $\sqrt{s} = 1.8\,TeV$ at the Tevatron collider at Fermilab [1, 2]. Since then its properties have been studied by the Tevatron experiments and found to be in agreement with the Standard Model of particle physics [3]. With the turn-on of the Large Hadron Collider (LHC) at CERN [4], top-quark pair production can be studied in great numbers in proton-proton collisions but also at energies almost four times greater. This allows for extended studies of the top quark properties and the determination of the production cross section (equivalent to rate) in an energy region where Standard Model top quark production is an important background for new physics. The Compact Muon Solenoid (CMS) is one of the large particle detector experiments at the LHC, designed to detect a wide range of particles and phenomena.

In the Standard Model the top quark decays almost 100% of the time via the weak process to a *W* boson and bottom quark, $t \rightarrow Wb$. This analysis focused on decays in which one of the two *W* bosons decays to a quark-antiquark pair and the other to a lepton and neutrino, giving a nominal final state containing a charged lepton, a neutrino and 4 jets (a narrow cone of hadrons and other particles), two of which are from b-quarks. This abstract will focus only on the result determined for decays where the lepton is an electron, using a technique for identifying jets originating from b-quarks, known as b-tagging, to improve the measurement purity.

Methodology

The measurement is produced using 36 pb^{-1} of CMS data taken from March to November 2010. Electron candidates are required to have a transverse momentum of at least 30 GeV and are then only accepted if well-contained within the Electromagnetic Calorimeter (ECAL). Any collision, or 'event', that contains a second electron or a muon is rejected as the presence of two leptons indicates a dileptonic $t\bar{t}$ decay. The remaining major selection requirement of this analysis is to count events that have ≥ 3 jets. B-quarks can travel a relatively long distance in the detector before they hadronise into jets and can be detected; Thus jets formed from b-quarks, when reconstructed, do not originate from the primary interaction point. A simple algorithm that exploits this behavior is used to identify b-quark jets, which has been tuned to give a high identification efficiency for the amount of data being studied.

To calculate the $t\bar{t}$ cross section a binned Poisson likelihood fit is performed to the secondary vertex mass (SVM) distribution in the selected data. The SVM is the sum of the four-vectors of the particle tracks associated with the secondary vertex. The fit minimises the negative log likelihood, summing over the SVM, number of jets and number of b-tagged jets in each event. Simulated data is used to produce 'templates' for the expected behaviour of the signal and background processes. These are summed and included in the fit, to simultaneously produce both the cross section measurement and the magnitude of each background contribution.

In this analysis the dominant background to the measurement comes from events with two hadronic jets in the final state involving other particles produced via the strong-interaction (QCD background). These can mimic the signal process when they contain one narrow jet and an energy deposit in the ECAL. True $t\bar{t}$ events have a sizeable transverse energy imbalance in the detector, due to an unmeasurable neutrino from the leptonic W-decay which the QCD background does not have. This signature is used as a tool to suppress this background by requiring each reconstructed event have greater than 20 GeV of missing transverse energy.

Results

The electron+jets channel fit gives a $t\bar{t}$ cross section measurement, with uncertainties, of

$$\sigma_{t\bar{t}} = 158 \pm 14(stat) \pm 19(syst) \pm 6(lumi)pb$$

"Lumi" stands for Luminosity, which is equivalent to the amount of data taken by the detector. A simultaneous analysis was conducted in the muon+jets channel to produce another cross section measurement. This was combined with the above to produce a joint lepton+jets cross section measurement (labeled CMS l+jets+btag in *fig.1*). The other results are from an identical experiment without b-tagging and a dilepton analysis that required events with two leptons, at least two jets, and missing transverse energy. The top most result is a combination of the three analysis measurements. The inner thick error bars of the data points correspond to the statistical uncertainty and the outer capped bars to the combined statistical and systematic uncertainties summed in quadrature. The grey vertical areas represent the Standard Model estimates of the cross section, with the dark grey (NNLO) being the more precise.

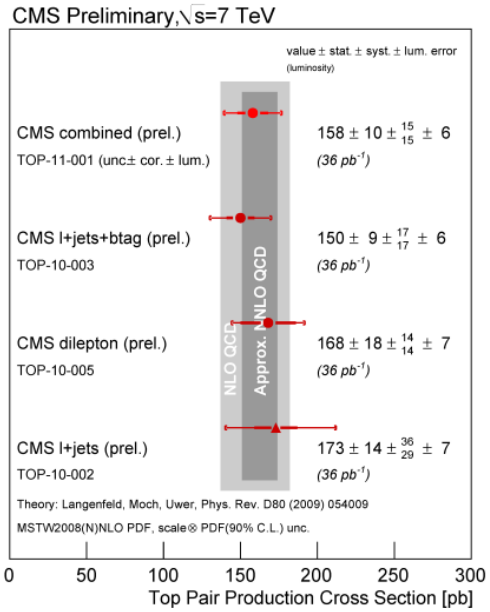

Figure 1: Summary of various inclusive top pair production cross section measurements made in 7 TeV proton-proton collisions by CMS [6].

Conclusion

An analysis of the $t\bar{t}$ production cross section at $\sqrt{s} = 7\ TeV$ was carried out using data recorded by the CMS detector at the LHC during 2010. Using 36 pb^{-1} of lepton+jets data and implementing b-tagging to suppress the backgrounds, a combined measured cross section of

$$\sigma_{t\bar{t}} = 150 \pm 9(stat) \pm 17(syst) \pm 6(lumi)pb$$

was obtained. This result is found to be consistent with the Standard Model and is in good agreement with the measurements from other current CMS analyses.

References

[1] CDF Collaboration, "Observation of top quark production in pp collisions", Phys. Rev. Lett. 74 (1995) 2626

[2] D0 Collaboration, "Observation of the top quark", Phys. Rev. Lett. 74 (1995) 263

[3] J. R. Incandela et al., "Status and Prospects of Top-Quark Physics", Prog. Part. Nucl. Phys. 63 (2009) 239

[4] L. Evans and P. Bryant (editors), "LHC Machine", JINST 3 (2008) S08001

[5] The CMS Collaboration "Measurement of the tt Pair Production Cross Section at √s = 7 TeV using b-quark Jet Identification Techniques in Lepton + Jet Events" CMS TOP-10-003,

[6] The CMS Collaboration "Combination of top pair production cross sections in pp collisions at √s = 7 TeV and comparisons with theory" CMS PAS TOP-11-001, http://cdsweb.cern.ch/record/1336491/

Keywords: particle physics, CMS, top quark, cross section, b-tagging

Liveness in fingerprint images by active pore detection technique

Shahzad MEMON*, Nadarajah MANIVANNAN, Wamadeva BALACHANDRAN

Centre for Electronics System Research (CESR)
Electronics and Computer Engineering, School of Engineering and Design
Brunel University, London

EXTENDED ABSTRACT

Introduction

Fingerprint biometric identification systems are widely in use for forensic applications, Government applications (immigration border control, building access and ID cards) and commercial applications (credit cards and mobile telephones). The fingerprint capturing is carried out by fingerprint sensors such as optical, TFT, capacitive and RF sensors [1]. The identification process consists of five stages: fingerprint capturing, image enhancement, feature extraction, feature matching and decision making in which the fingerprint image is accepted or rejected. Despite many advantages, fingerprint biometric sensor technology has been deceived by fake finger stamps prepared from silicon or gelatine (see figure.1). Many people believe that fingerprint biometric systems can detect liveness in biometric samples, however; artificial fingerprints created today are close to the original real finger, and it has been proved that about 80%-85% of these systems are easily fooled by different kinds of fake fingers with stamped patterns [2-4]. It showed that that the scarcity of distinguishing between fake and real finger in existing fingerprint sensing systems. In this paper, we present a novel advanced image processing algorithm to establish liveness of fingertip. This image processing technique detects sweat pore activities of the fingertip to establish liveness of the fingerprint

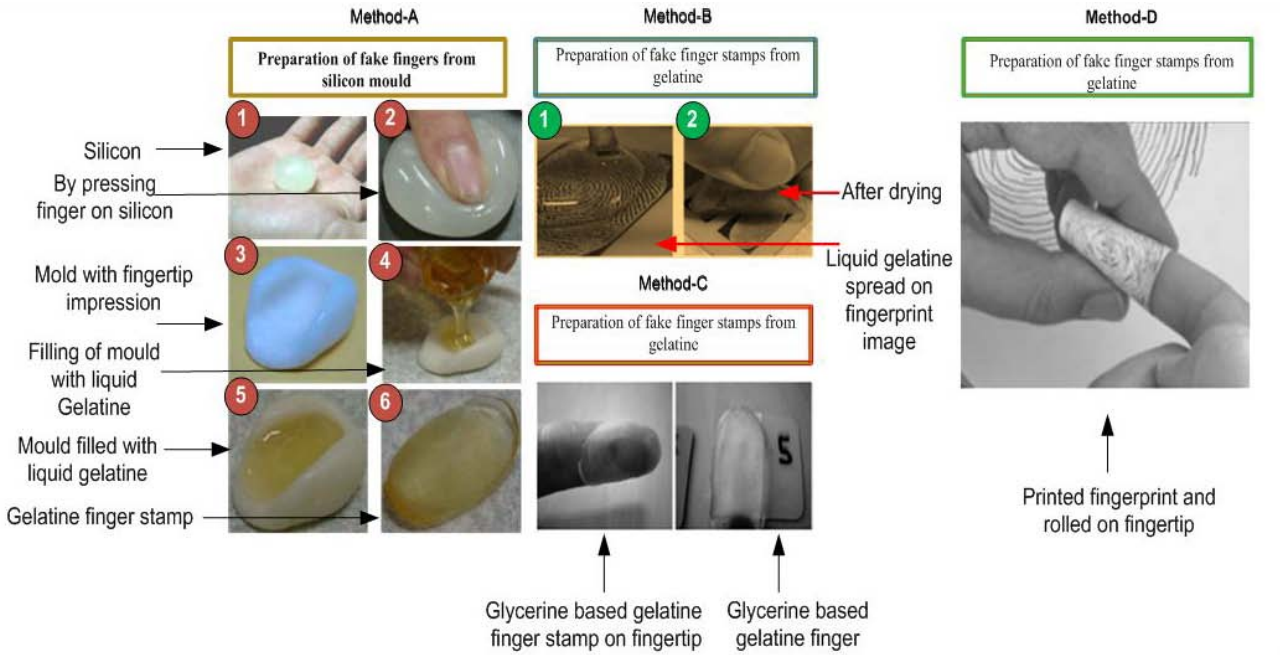

Figure.1 Methods A-D for preparing of fake fingerprint stamps [2-4]

Methodology

These are many sweat glands available on the skin of human body. Specifically, the glands under fingertip skin are known as eccrine glands. These glands discharge sweat fluid drops as thermoregulation process via pores on ridges of fingertip (see Figure.2). Sweat pores are very small (80–200 μm) circular-like structures on the ridges of the fingerprint [5]. The opening and closing of these sweat pores have traits which can be used for liveness detection from fingertip images. High resolution imaging makes it possible to reliably extract the active and passive pores on fingertips. High-resolution fingerprint images (~1000 ppi) were obtained using a microscopic camera (See figure 2 and 4 a).

Figure.2 Active Sweat Pores on fingertip ridges

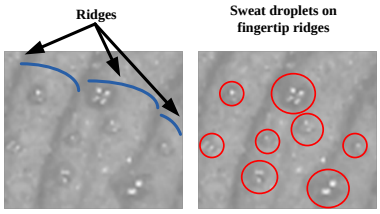

Although there has been work done on pore matching by extracting pores [6], but this is the first time the active (open) sweat pores are detected and distinguished from passive (closed) pores for liveness detection. A novel image processing algorithm (figure 3) is developed to detect the active pores by using high pass and correlation filtering technique. This algorithm not only detects the presence of active sweat pores but also locate their positions.

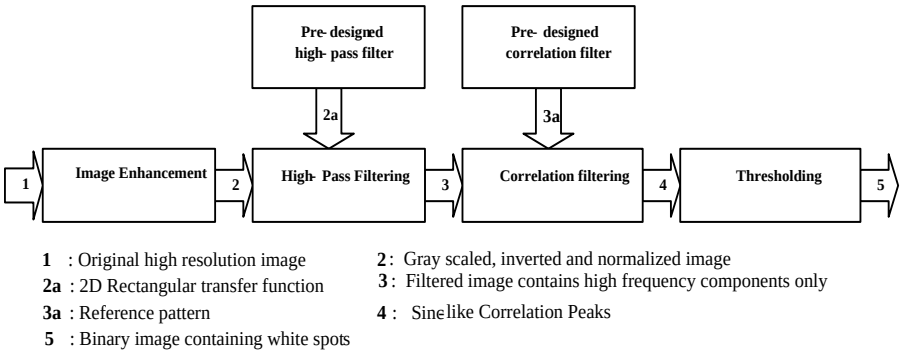

Figure.3 Image processing algorithm (HCFA) to detect Active pores from HR finger tip Images

Results

Figure 4 shows a typical set of results as a typical fingertip image is passed through the HCFA. The detected pores are represented by their correlation peaks (see Fig.4e) and active pores are differentiated from passive pores and background using hard thresholding operation. Final detected active pores are shown in Fig.4f.

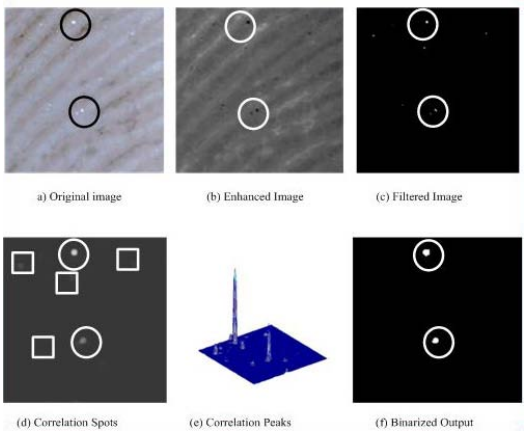

Figure.3 Image processing algorithm

Whilst other image processing techniques are performed in the space domain to identify the pores, our method is based on frequency spectrum filtering and therefore it is more robust to background noise. The results obtained shows very distinguishable correlation peaks at the outputs, which correspond to active sweat pores on fingertip ridges. This automated technique will make it possible to study the distribution of active sweat pores for liveness detection in fingerprint recognition.

Conclusion

Liveness detection can be performed by detecting active sweat pores which discharge sweat liquid to keep the thermal balance of the finger. A new advanced image processing algorithm (HCFA) is proposed for the detection of active sweat pores as a sign of liveness. The active pores are only visible on real fingers and it's difficult to replicate same phenomena in fake fingertip stamps.

References

[1] S. Memon, M. Sepasian and W. Balachandran, "Review of finger print sensing technologies," in Multi-topic Conference, INMIC,IEEE International, 2008, pp. 226-231.
[2] T. Matsumoto, "Gummy and Conductive Silicone Rubber Fingers Importance of Vulnerability Analysis, “Advances in Cryptology— ASIACRYPT 2002, pp. 59-65, 2002
[3] C. Barral and A. Tria, "Fake Fingers in Fingerprint Recognition: Glycerine Supersedes Gelatine," Formal to Practical Security, pp. 57- 69,2009
[4] M. Tistarelli, S. Z. Li and R. Chellappa, "Handbook of Remote Biometrics: for Surveillance and Security," Advances in Pattern Recognition, pp. 382, 2009.
[5] H. Choi, R. Kang, K. Choi and J. Kim, "Aliveness detection of fingerprints using multiple static features," World Academy of Science,Engineering and Technology, 2007 .
[6] Anil Jain, Yi Chen and Meltem Demirikus. Pores and ridges: Fingerprint matching using level 3 features. IEEE Transactions on Pattern Analysis and Machine Intelligence, pp.15-27, 2007.

Keywords: Fingerprint, Liveness, Active Pores

Wavelet-Based Finite Element Method for Static and Vibration Analysis

Mutinda MUSUVA*, Cristinel MARES
Mechanical Engineering Department, School of Engineering and Design, Brunel University.
Mutinda.Musuva@brunel.ac.uk, Cristinel.Mares@brunel.ac.uk

EXTENDED ABSTRACT

Introduction

The conventional finite element method (FEM) has been used as a numerical analysis technique to solve various engineering problems by obtaining their approximate solutions on complex geometries and material composition via the use of polynomial interpolating functions [1]. However, the implementation of the method for problems with regions of the solution domain where the gradient of the field variables are expected to vary suddenly or fast, bring on difficulties in the analysis of a system and sometimes lead to inaccurate results or higher computational. Moreover, the resolution of the elements can only be analysed at a specific scale once the order of the governing polynomial functions have been selected. Subsequently, there has been growing concern over the ability of the method with respect to its efficiency, accuracy and reliability, to analyse complex problems with high gradients as well as strong nonlinearities. For this reason, work has been carried out exploring the fusion of conventional FEM and wavelet analysis to obtain an approximate solution for various engineering problems [2,3], widely referred to nowadays as the Wavelet Finite Element Method (WFEM). Initially used mainly by mathematicians as a decomposition tool for data functions and operators, wavelet analysis is proving to be an effective tool due to its key properties such as multiresolution analysis (MRA), “two-scale” relation and compact support [4]. An investigation of the characteristics of the wavelet finite elements formulations is carried out by comparing different wavelet families for the Euler Bernoulli finite element beam in dynamics applications to highlight the efficiency and general properties of such formulations.

Methodology and Approach

From conventional FEM, for a beam element with two degrees of freedom (DOF) per node, the physical DOFs given by the vector *w* can be represented by the polynomial shape functions, *S*. However for the WFEM, the scaling functions of the various wavelet families are used to represent the shape functions of the beam elements. For instance in the Daubechies wavelet case, the wavelet scaling functions are given as:

$$\phi(x) = \sum_{k=0}^{N-1} p(k)\phi(2x-k) \quad (1)$$

Where $p(k)$ are the wavelet filter coefficients which are constructed using polynomials. As in conventional FEM, using the variational principle of the minimum total potential energy, π, for a static analysis [1]:

$$\pi = \int_0^{L_e} \frac{EI}{2} \left(\frac{d^2w}{dx^2}\right)^2 dx - \int_0^{L_e} q(x)w\,dx \quad (2)$$

Where E is the Young’s Modulus of the beam, *I* is the moment of inertia and $q(x)$ is the function of the external load applied across the element. One obtains the equation:#

$$Kw = R \quad (3)$$

In the case of dynamic analysis, one can apply the Hamilton Principle and obtain the equation of equilibrium as:

$$M\ddot{w} + Kw = R \quad (4)$$

Where in equations (3) and (4), $\ddot{w}$ and *w* are the beams acceleration and displacement vectors respectively, *M* is the mass matrix, *K* is the stiffness matrix and *R* represents the force vector. The

elemental stiffness and mass matrices as well as the force vector in wavelet space, $\widetilde{K}_e$, $\widetilde{M}_e$ and $\tilde{R}_e$, are given as:

$$\widetilde{K}_e = \int_0^1 \phi''(\xi - i)\phi''(\xi - j)\, d\zeta \quad (5)$$

$$\widetilde{M}_e = \int_0^1 \phi(\xi - i)\phi(\xi - j)\, d\zeta \quad (6)$$

$$\tilde{R}_e = \int_0^1 q(x)\, \phi(\xi - i)\, d\zeta \quad (7)$$

Using the scaling function from (1), the displacement *w* can be approximated as:

$$w = \sum_{k=-(N-2)}^{0} \alpha_k \phi(\xi - k) \quad (8)$$

The matrices and vectors in wavelet space are converted into physical space using a transformation matrix *T*. The assembly of the elements to make up the system are then carried out to ensure for the correct implementation of boundary conditions and nodal connectivity.

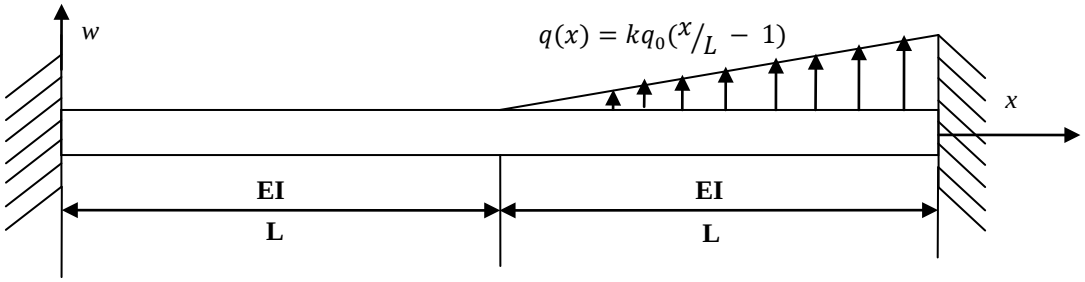

A fixed-fixed beam of length 2*L* with a varying distributed load *q*(*x*) running from lengths *L* to 2*L* as shown in the figure above, is taken into consideration to verify and highlight the efficiency as well as general properties of the given formulations. The beam is considered to have an equal cross sectional area, *A*, running from length 0 to 2*L*, and flexural rigidity, *EI*, obtained from the modulus of elasticity *E* and moment of inertia *I*.

Results

Numerical examples for static and dynamic analysis of beam finite element formulations will be carried out, compared with results from exact solutions and discussed in detail.

Summary

In this paper, different theoretical formulations for the WFEM have been developed and analysed through numerical simulations. The application of wavelets for structural analysis shows vast potential especially with features such as multiresolution and compact support which make these formulations attractive. These properties show potential for various applications in complex problems such as structures with strong nonlinear behaviour, presenting high gradient variations of stress and strain in operational conditions, advanced composite materials and nano-structures.

References

[1]Roa, S. S., "The Finite Element Method in Engineering", Butterworth-Heinemann, 1999.
[2]Ma, J., Xue, J., Yang, S. and He, Z., "A Study of the Construction and Application of a Daubechies Wavelet Based Beam Element", Finite Elements in Analysis and Design, Vol. 39(10), 2003, pp. 965-975.
[3]Chen, X., Yang, S., Ma, J. and He, Z., "The Construction of Wavelet Finite Element and Its Application", Finite Elements in Analysis and Design, Vol. 40(5-6), 2004, pp. 541-554.
[4]Strang, G. And Nguyen, T., *Wavelets and Filter Banks*, Wellesley-Cambridge Press, Massachusetts, 1997.

Keywords: Wavelets, Connection Coefficients, Wavelet Finite Element Method, Vibration Analysis.

Direct Numerical Simulation of Oxygen Transfer at the Air-Water Interface in a Convective Flow Environment and Comparison to Experiments

Boris KUBRAK[1], Dr Jan WISSINK[1] and Dr HERLINA[2]
1 Brunel University; 2 KIT Karlsruhe, Germany

EXTENDED ABSTRACT

Introduction

Gas transfer through the air-water interface plays an important role in environmental and chemical engineering. One typical process is the absorption of oxygen into natural water bodies such as lakes and oceans. It is vital to sustain aquatic life. This process is controlled by interaction of molecular diffusion and turbulent transport. In nature the flow conditions are usually turbulent. It is well known that the level of turbulence plays an important role in the the gas transfer process and is the dominant driving mechanism.

Natural sources of turbulence can be classified into three major types which are surface-shear-induced turbulence (e.g. wind shear on open waters), bottom-shear-induced turbulence (e.g. in rivers) and buoyant-convective turbulence (e.g. in lakes due to surface cooling). Fig 1 shows a schematic illustration of the turbulence sources and their [1]. This work investigates the case A.

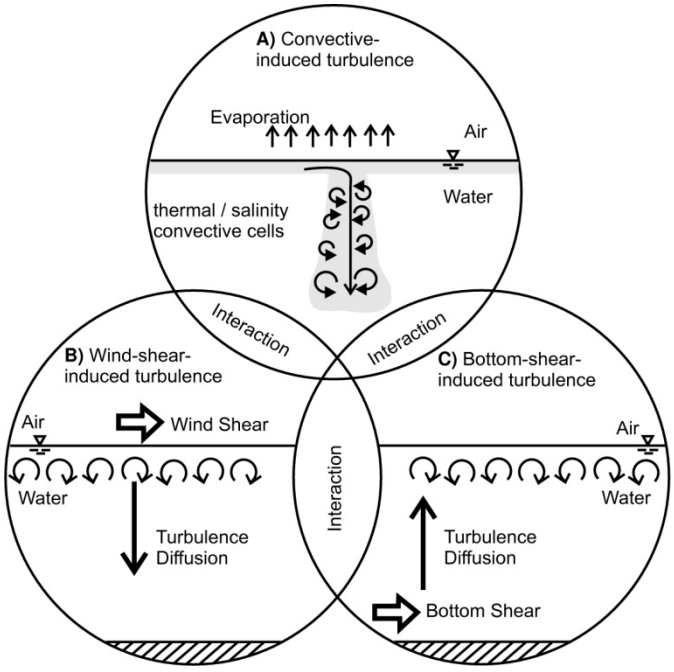

Fig 1: Schematic illustration of turbulence sources driving gas transfer in natural water

Numerical Method

The numerical scheme for scalar transport implemented here is a fourth-order WENO (weighted essentially non-oscillatory) finite difference scheme as described by Liu, Osher and Chan [2]. WENO schemes were initially developed to capture discontinuities in the solution such as shock waves without resulting in oscillation. In a convection-diffusion problem like the gas transfer on an interface there is no discontinuity expected but high gradients may occur near the interface. The velocity field is solved by a poisson-solver using a fourth-order Adams-Bashworth method.

Results

The results presented here are from 2D simulations that are carried out in order to perform parameter studies. A quadratic 2D domain was choosen with edge length of 10 cm. The gridsize is nx = 800 and nx = 300 whereas the mesh was refined near the top where the concentration boundary layer will form. A mesh refinement study where the mesh was refined by factor 1.5 and 2 found no higher resolution in gas concentration and flow structures. There where periodic boundary conditions on the sides and a free slip condition on the bottom. After t = 10s random disturbances of 1% were added to the

temperature field. This is in order to avoid the triggering of the instability to depend on the mesh size or numerical round off error. The same random field was used for all simulations. The oxygen concentration field was measured in experiments at KIT by a Laser Induced Fluorescence (LIF) method [3]. The experiments were performed in a tank where the surface temperature was 3 ºC lower than the bulk temperature of the water.

Fig. 2 shows a comparison of 2D-LIF images to our 2D DNS results. Note that the DNS results show the top section of the domain that have the same dimension as the LIF-maps. The whole domain was much larger so the sides and bottom in these plots can be considered as open boundaries. For reasons of better comparison the timescale was set to t = 0s from the moment when the instability began. There is a very good qualitative agreement with the experiment. Especially between t = 16s and t = 28s the spatial distance between high concetration plumes and the size of the eddies is very similar in the experiment and the simulation.

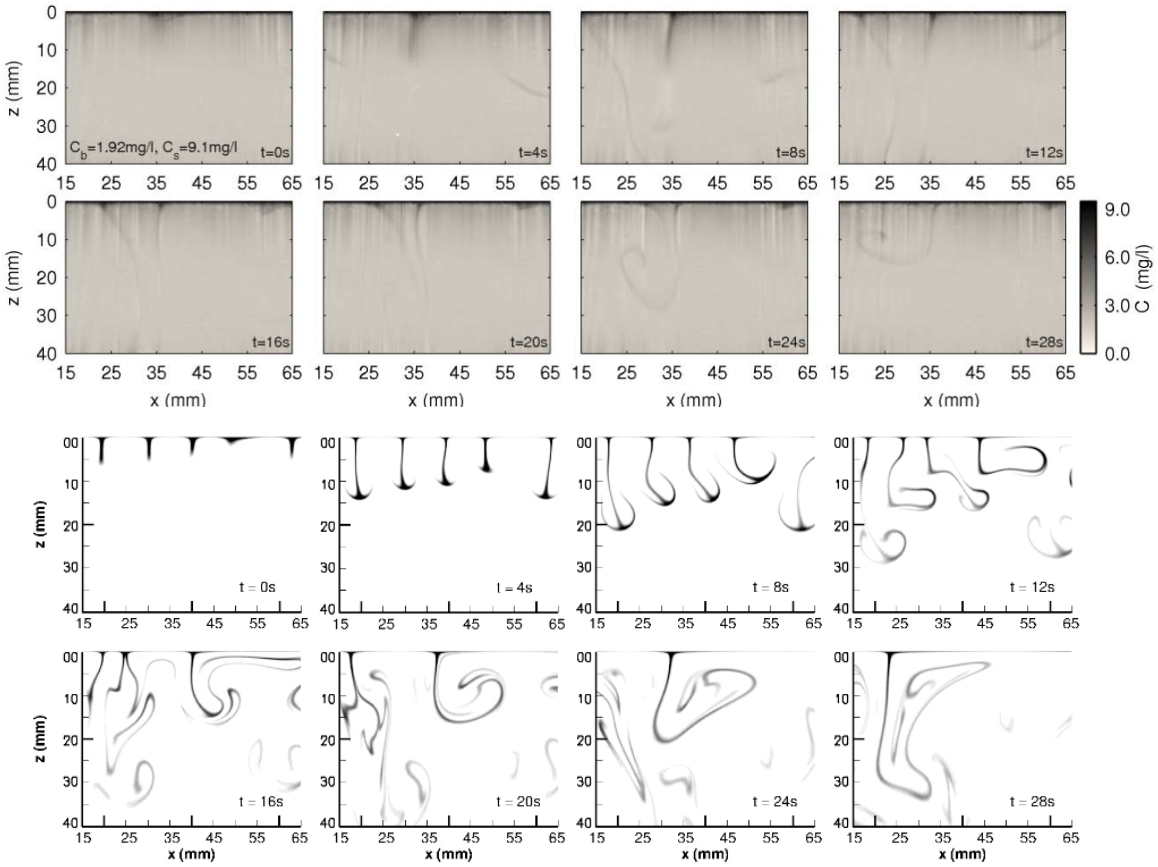

Fig 2: Comparison of sequences of LIF images (top) and Simulation results (bottom). High oxygen concentration plumes show similar spatial distance and eddy size

Conclusion

The DNS results show similar flow structures and eddy size as seen in the experiment. The WENO scheme proved to be a successful method to resolve a scalar transport problem with a low diffusivity (and therefore high gradient) such as the oxygen concentration in water. Very fine plumes of high oxygen concentration were found to penetrate the deeper regions and there structure was well maintained. The work sheds light on this microscale process in previously unknown detail.

References

[1]Herlina, Gas Transfer at the Air-Water Interface in a Turbulent Flow Environment, University Karlsruhe, ISBN 3-937300-74-0, 2005.

[2]X. Liu, S. Osher and T. Chan, Weighted Essentially Non-oscillatory Schemes, Journal of Computational Physics 115, 200-212, 1994.

[3]T. Muensterer and B. Jaehne, LIF measurement of concentration profiles in the aqueous mass boundary layer, Experiments in Fluids 25, 190-196, 1998.

Plasma assisted pyrolysis of gaseous hydrocarbons to produce COx free hydrogen

I. ALEKNAVICIUTE*, T. G. KARAYIANNIS, M. W. COLLINS

School of Engineering and Design, Brunel University, Uxbridge, Middlesex, UK
* irma.aleknaviciute@brunel.ac.uk

EXTENDED ABSTRACT

Introduction

Hydrogen plays an important role in many industrial processes and hydrogen production is considered to play a key role in the future energy security and the conservation of the environment [1, 2]. Conventional hydrogen production methods, such as steam reforming, are well developed; however, the use of catalyst in the system presents a major disadvantage of catalyst deactivation [3]. Plasma assisted hydrogen production from hydrocarbons has been successfully investigated for different types of plasmas, mainly non-thermal discharges [4]. Non-thermal plasma systems can provide extremely high concentrations of energetic and chemically active species, keeping bulk temperatures as low as room temperature [5]. A corona discharge reactor operating under atmospheric pressure has been developed and a series of experiments have been carried out to investigate COx free hydrogen production from propane.

Experimental facility and methodology

Propane is subjected to corona discharge in a pin-to-plate electrode configuration with argon as a working gas and the products are characterised by Gas Chromatography Mass Spectrometer (GC-MS). The plasma chamber consists of two 316 stainless steel disks, a stainless steel pin electrode, borosilicate glass cylinder, C103 copper disk with integrated cartridge heater, in house built PID temperature control system, high voltage power supply, vacuum pump, pressure gauge and data logging system for temperature and pressure; see figure 1. The amount of propane and argon entering the system is measured by volume, using a pressure gauge. High voltage DC power is supplied to the pin electrode initiating electrical break down of the argon gas and hence generating active plasma species such as electrons and ions.

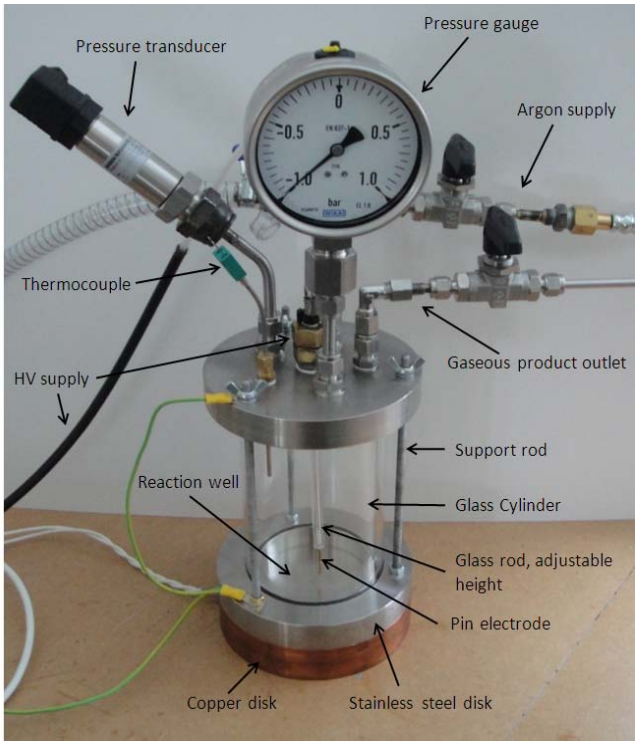

Figure 1: Plasma chamber design, showing all relevant components.

Cracking of hydrocarbon molecules is achieved by plasma ionization of the hydrocarbon molecules by an impact of an energetic electron and photo-ionic decomposition. Gaseous and liquid samples are be collected after each experiment and characterized by the GC-MS instrument comprised of a Hewlet Packard series 5890 Gas Chromatography instrument and a Trio-1 Mass Spectrometer. Solid carbon is classified by Scanning Electron Microscope (SEM) and X-ray Photoelectron Spectroscopy (XPS).

Results and discussion

Experiments were performed to record preliminary observational results for propane reformation using corona discharge. Observations include carbon black deposition and pressure change in the system, whist the parameters such as the polarity, inter-electrode distance and residence time were varied. At atmospheric pressure, 10mm inter-electrode gap distance and 1 minute residence time for negative corona discharge, a rapid carbon deposition and pressure increase has been observed. Carbon deposition indicates that propane molecules have decomposed to carbon and hydrogen; this is also confirmed by pressure increase. Increasing the residence time results in additional yellow liquid film formation and the pressure build up is not as rapid. This indicates that longer residence time might favor the recombination of carbon and hydrogen atoms to form higher hydrocarbons; yellow color indicates the formation of double carbon to carbon bonds.

Conclusions

Non-thermal plasma reforming unit operating at atmospheric pressure has been developed for converting gaseous hydrocarbons to COx free hydrogen. A series of experiments have been performed, and the preliminary observations for propane pyrolysis have been recorded under different conditions:

1. Pressure increase and carbon black deposition have been observed under all condition investigated, indicating successful cracking of propane molecules;

2. Longer residence time results in a possible higher hydrocarbon formation;

3. Higher pressure increase rate has been observed for positive corona discharge, indicating a better potential for propane pyrolysis, when compared to negative corona discharge.

The future work includes an accurate parametric study to investigate the effects of (i) inter-electrode distance, (ii) residence time, (ii) power input, and (iii) corona polarity on hydrogen production.

References

[1]Balat, M. (2008). Potential importance of hydrogen as a future solution to environmental and transportation problems. Int. J. Hydrogen Energy, vol. 33, p. 4013.

[2]Ahmed, S., Krumpelt, M. (2001). Hydrogen from hydrocarbon fuels for fuel cells. Int. J. Hydrogen Energy, vol. 26, p. 291.

[3]Luche, J., Aubury, O., Khacef, A., Cormier, J-M. (2009). Syngas production from methane oxidation using a non-thermal plasma: Experiments and kinetic modelling. Chemical Engineering Journal, vol. 149, p. 35.

[4]Deminsky, M., Jivotov, V., Potapkin, B., Rusanov, Y. (2002). Plasma Assisted Production of hydrogen from hydrocarbons. Pure Appl. Chem., vol. 74 p. 413.

[5]Fridman, A. (2008). Plasma Chemistry. Cambridge: Cambridge University Press.

Keywords: propane pyrolysis, hydrogen production, non-thermla plasma

In-cylinder gas temperature measurement with two-line planar laser induced fluorescence

Mohammadreza ANBARI ATTAR*, Hua ZHAO
Centre for Advanced Powertrain and Fuels Research (CAPF), Brunel University, London, UK.
m.a.attar@brunel.ac.uk

EXTENDED ABSTRACT

1. Introduction

Increasing concerns over Internal Combustion (IC) engines pollution and fuel price have forced automotive industry to approach new technologies and combustion strategies to reduce the emission and improve the efficiency of the IC engines. Therefore quantitative measurement techniques that characterize the combustion phenomena are crucial for development and commercialization of new technologies and combustion strategies. Among measurement techniques, laser base techniques such as Planar Laser Induced Florescence (PLIF) have proven their advantages over the old methods which have been traditionally employed. PLIF is a diagnostic potentially capable of measuring temperature distribution and composition with high precision and accuracy.

2. Methodology

2.1 BACKGROUND THEORY

Two-line PLIF involves capturing images from two excitation pulses usually applied in rapid succession [1,2]. The PLIF signal in the linear excitation limit is given by

$$S_f = \frac{E}{hc\nu}\, dV_c \left[\frac{\chi_{tr} P}{kT}\right] \sigma(T)\phi(T,P,\chi_i)\frac{\Omega}{4\pi}\,\eta_{opt}$$

where S_f is the number of photons incident per pixel at the detector [photons/pixel], E is the local laser fluence [J/cm^2], h is Planck's constant [J s], c is the speed of light in vacuum [cm/s], ν is the frequency of the incident laser radiation [cm^{-1}], dVc is the excited volume [cm^3], χ_{tr} is the tracer mole fraction, P is the total pressure [MPa], k is the Boltzmann constant [J/K], T is the temperature [K], σ is the absorption cross section [cm^2], φ is the fluorescence quantum yield (FQY), Ω is the collection solid angle of the optics used for imaging the fluorescence, and η_{opt} is the optical transmission efficiency of optics and filters. For temperature measurements we take the ratio of fluorescence signals from two excitation wavelengths.

$$\frac{S_{f2}}{S_{f1}} = C_{cal}\frac{E_2}{E_1}\,\frac{\sigma_2(T)\phi_2(T,P,\chi_i)}{\sigma_1(T)\phi_1(T,P,\chi_i)}$$

where the constant C_{cal} is determined by making PLIF calibration measurements at a known uniform temperature.

2.2 EXPREMENTAL SETUP

2.2.1 Excitation Wavelengths and Tracer

Two optimal wavelengths of 277 nm and 308 nm were selected based on the results of a full uncertainty analysis [3]. This combination can be used for in-cylinder measurements of temperature and composition under both motored and fired operations. 3-pentanone was chosen as a tracer for imaging of temperature since:

- Its fluorescence is only modestly affected by oxygen quenching.
- Its absorption spectrum is easily accessible with high pulse energy lasers.
- Its boiling point and transport properties closely match typical model fuels.
- It has a high LIF signal intensity.

Tracer seeding was provided by a premixed seeding system. Tracer was injected into the intake port with a Bosch multipoint port fuel injector. A 3kW electric heater was installed on the intake port before the port fuel injector assuring rapid steady evaporation of the injected tracer.

2.2.2 Optical Engine

A single-cylinder optical engine was used for the engine measurements. The in-cylinder geometry consists of a pent-roof head and a flat piston. The head is a prototype with four valves, a centrally located injector, and a spark plug. Figure 1 shows the relative locations of the injector and valves. The piston is outfitted with a 55 mm diameter window. Optical access for the laser sheets is provided by a fused silica ring, while imaging access is through the piston window. The relevant engine specifications are summarized in Table 1.

Bore	80 mm
Stroke	89 mm
Swept volume	450 cc
Compression ratio	9:1
Intake Valve Opening	90 ATDC
Exhaust Valve Closing	80 BTDC
Engine speed	1200 rpm

Table 1: Engine specifications

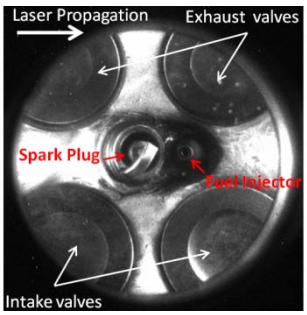

FIG. 1: relative locations of the injector, the spark plug and the valves

2.2.3 PLIF System

The PLIF system consists of two excimer lasers, a Raman convertor, a single ICCD camera, and the ancillary optics. A XeCl laser was used to generate the 308 nm laser pulses. The 277 nm wavelength was generated via Raman shifting of a 248 nm KrF excimer laser to the first Stokes wavelength in H_2 (purity 99.999%). The output of the Raman convertor was put through an equilateral dispersing prism to separate the pump and shifted wavelengths. The beams output by the two excimer lasers are rectangular with the long axes in the vertical direction. The beams also needed to have their long axes flipped and to be raised to the height of the fused silica ring in the engine. This was accomplished using a vertical lift consisting of two high reflectors. The laser sheets were approximately 60 mm wide and 1 mm thick. Laser energy per pulse was 20 mJ for both lasers. The fluorescence transmitted through the piston window was imaged onto the camera using a 104 mm f/4.5 Nikon lens with a 350 nm long-pass filter. The ICCD camera utilized an interline transfer CCD array. The interline CCD array coupled with the P46 phosphor allowed two images to be acquired with a minimum inter-frame time of 2 μs. For this work the inter-frame time was set to 100 μs and the gate widths for the two images were set to 500 ns. The camera and lasers were synchronized to the engine by a crank-angle degree resolution crankshaft encoder connected to a counter/divider unit and DG535 delay generator.

3. Results and Discussion

Figure 2 shows in-cylinder pressure during engine motoring. The intake and exhaust valves profile as well as PLIF image timing are shown in this figure. The LIF data images were taken at 180CAD, 270CAD and 320CAD. Beside these images, several sets of images are needed to correct and calibrate each set of data images for each excitation wavelength. These image sets include average background images taken at the data and calibration image timings with the lasers firing but without tracer seeded into the intake air, and average calibration images. The average background images are subtracted from the data and calibration images. Temperature is determined by first taking the ratio of each data image with its respective calibration image. Next, the calibration-corrected data images at 308 nm are divided by those at 277 nm. Figure 3 shows LIF data images at selected CADs subtracted by corresponding background images. The lower row frames in this figure were taken when the cylinder was illuminated with 308 nm laser beam. The upper row frames taken 100 μs later when the cylinder was illuminated with 277 nm laser beam. As it was expected the LIF signal

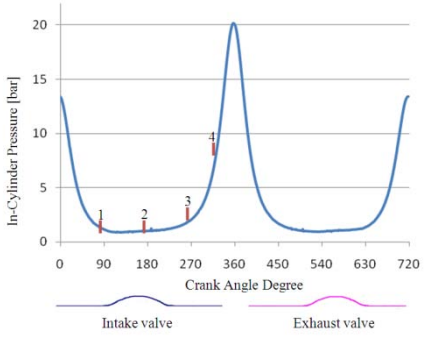

FIG. 2: In-Cylinder motoring pressure, intake/exhaust valves and image timing.

intensity increases as the piston moves to top dead centre (TDC) which corresponds to an increase in temperature during the compression stroke.
For quantitative measurements of temperature it's required to further process the captured images and remove the systematic errors. An appropriate algorithm for correcting systematic errors in the recorded images is given by

$$L_{fl} = \left[L_{pix} - (L_d + L_b)\right]\left(\frac{1}{R_{tot}}\right)\left(\frac{E_0}{E_c}\right)$$

Where L_{fl} is the original fluorescence signal recorded on each pixel, L_{pix} is the total signal on each pixel, L_d and L_b are the dark charge and the background signals respectively. R_{tot} is the total pixel responsivity including responsivity of the detector, amplifier and analogue to digital convertor. And finally E_0/E_c is for the laser sheet correction.

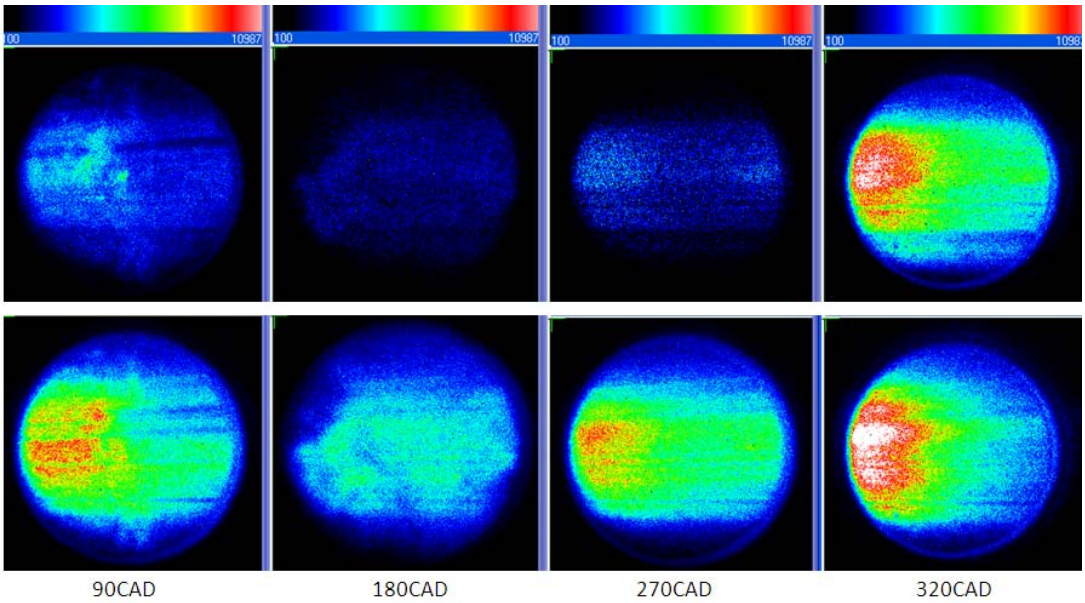

FIG. 3: Two-line PLIF images taken at compression stroke with the background subtraction; Upper frames from 277 nm laser sheet, lower frames from 308 nm laser sheet with 100 μs delay from the first frames

4. Conclusion and Further Work

An optimized diagnostic technique for measurement of temperature based on planar laser induced fluorescence was developed. The optimum wavelengths for two-line excitation and the tracer were carefully chosen. The preliminary tests images show the promising results. Further work in this project include; correcting systematic errors of the images for the quantitative measurements of temperature, tracer mole fraction measurements, motoring temperature measurement with direct fuel injection (DI) as well as investigation of charge cooling effect and effect of hot exhaust in positive valve overlap (PVO) and negative valve overlap (NVO).

References

[1] S. Einecke, C. Schulz, and V. Sick. Measurement of temperature, fuel concentration and equivalence ratio fields using tracer LIF in IC engine combustion. *Applied Physics B-Lasers and Optics*, 71(5):717–723, 2000.
[2] T. Fujikawa, K. Fukui, Y. Hattori, and K. Akihama. 2-D temperature measurements of unburned gas mixture in an engine by two-line excitation LIF technique. *SAE Technical Paper*, 2006-01-3336, 2006.
[3] J. D. Koch. Fuel tracer photophysics for quantitative planar laser-induced fluorescence. PhD thesis, *Stanford University*, 2005.

Keywords: Planar Laser Induced Fluorescence (PLIF), temperature measurements, combustion measurements.